In presenting the dissertation as a partial fulfillment of the requirements for an advanced degree from the Georgia Institute of Technology, I agree that the Library of the Institute shall make it available for inspection and circulation in accordance with its regulations governing materials of this type. I agree that permission to copy from, or to publish from, this dissertation may be granted by the professor under whose direction it was written, or, in his absence, by the Dean of the Graduate Division when such copying or publication is solely for scholarly purposes and does not involve potential financial gain. It is understood that any copying from, or publication of, this dissertation which involves potential financial gain will not be allowed without written permission.

3/17/65
b

THE WET MAGNETIC SEPARATION OF MONTMORILLONITE FROM KAOLINITE

A THESIS

Presented to

The Faculty of the Graduate Division

by

Joe Kennedy Cochran, Jr.

In Partial Fulfillment

of the Requirements for the Degree

Master of Science in Ceramic Engineering

Georgia Institute of Technology

June, 1968

THE WET MAGNETIC SEPARATION OF

MONTMORILLONITE FROM KAOLINITE

Approved:

Chairman

Date approved by Chairman: 5-22-68

ACKNOWLEDGMENTS

I wish to express my appreciation to my wife, whose continuing encouragement and understanding has been an ever constant boost to my morale throughout the course of this work.

I would like to thank Dr. Willis E. Moody, whose constructive criticisms and valuable time spent in conference has been an invaluable assistance in the design and analysis of these experiments.

I would like to thank the J. Hall Carpenter Foundation for the fellowship fund, gift of equipment, as well as other funds and cooperation which made this research possible.

I also thank Dr. Lane Mitchell and Dr. Allen T. Chapman for their cooperation as part of my reading committee.

I wish to thank Mr. Thomas Mackrovitch for his help in the fabrication of the magnetic susceptibility apparatus and Miss Jane Thatcher for typing the rough draft.

TABLE OF CONTENTS

Page

ACKNOWLEDGMENTS ii

LIST OF TABLES v

LIST OF ILLUSTRATIONS vii

SUMMARY ix

Chapter

I. INTRODUCTION 1

II. REVIEW OF LITERATURE 2

Magnetic Separation
Magnetic Susceptibility
Particle Size
Magnetic Susceptibility of Montmorillonite and Kaolinite
Relation of Mineral Susceptibility to Chemical Content
Particle Size and Morphology of Montmorillonite and Kaolinite
Structure of Kaolinite and Montmorillonite
Base Exchange Capacity
Organic Absorption
Metal Acetylacetonates

III. INSTRUMENTATION AND EQUIPMENT 22

Magnet
Magnetic Susceptibility Apparatus
X-ray Diffractometer
X-ray Spectrograph
Miscellaneous Equipment

IV. PROCEDURE 31

Preparation of Suspensions and Magnetic Separations
Measurement of Magnetic Susceptibility
Determination of Per Cent Montmorillonite
Determination of Per Cent Iron

V. DISCUSSION OF RESULTS 44

A. Selection of Clay
B. TSPP, $FeCl_3$, and Calgon Separations
C. Metal Acetylacetonate Separations

TABLE OF CONTENTS (Continued)

VI. CONCLUSIONS AND RECOMMENDATIONS 74

Conclusions
Recommendations

APPENDICES

A. DETERMINATION OF THE FIELD STRENGTH OF A CARPCO LABORATORY MAGNETIC SEPARATOR 77

B. DATA ON AIR FLOATED PIONEER KAOLIN 79

C. CALIBRATION OF HdH/dX FOR MAGNETIC SUSCEPTIBILITY MEASUREMENTS 81

D. STANDARDS FOR DETERMINING PER CENT MONTMORILLONITE IN KAOLINITE 86

E. STANDARDS FOR DETERMINING PER CENT IRON IN KAOLIN 90

F. THE RELATION OF TIME AND PARTICLE SIZE TO THE MAGNETIC SEPARATION OF WEAKLY MAGNETIC PARTICLES IN THE MICRON AND SUBMICRON PARTICLE SIZE RANGE 93

G. PER CENT MONTMORILLONITE DATA 105

H. MAGNETIC SUSCEPTIBILITY DATA 112

I. PER CENT IRON DATA 122

J. WEIGHT ANALYSIS OF MONTMORILLONITE 123

BIBLIOGRAPHY 128

LIST OF TABLES

Table		Page
1.	Defloculation of TSPP Suspension	32
2.	Defloculation of $FeCl_3$ Suspension	34
3.	Defloculation of M(X)A Suspension	38
4.	Metal Acetylacetonate Additions	39
5.	Results of Calgon Separation	60
6.	Magnetic Susceptibility of M(X)A Compounds	69
7.	Summary of Data From M(X)A Separations	71
8.	Magnetic Field Strength for Carpco Laboratory Magnetic Separator	77
9.	Chemical Analysis of Pioneer Kaolin	79
10.	Particle Size Distribution of Pioneer Kaolin	80
11.	Calibration of HdH/dX for Determination of Magnetic Susceptibility of TSPP Separation Fractions	83
12.	Calibration of HdH/dX for Determination of Magnetic Susceptibility of $FeCl_3$ Separation Fractions, Calgon Separation Fractions, Original and Nonmagnetic Fractions of M(X)A Separations, and the Metal Acetylacetonates	84
13.	Calibration of HdH/dX for Determination of Magnetic Susceptibility of Magnetic Fractions of M(X)A Separations	85
14.	X-ray Diffractometer Settings for Montmorillonite-Kaolinite Standards and Separation Samples	87
15.	Peak Areas and Ratios for Kaolinite-Montmorillonite Standards	88
16.	X-ray Spectrograph Settings for Iron Determination	91
17.	Per Cent Montmorillonite in TSPP Separation Fractions	106

LIST OF TABLES (Continued)

		Page
18.	Per Cent Montmorillonite in $FeCl_3$ Separation Fractions . . .	107
19.	Per Cent Montmorillonite in Calgon Separation Fractions . .	108
20.	Per Cent Montmorillonite in M(X)A Separation Fractions . . .	109
21.	Magnetic Susceptibility of TSPP Separation Fractions	113
22.	Magnetic Susceptibility of $FeCl_3$ Separation Fractions . . .	115
23.	Magnetic Susceptibility of Calgon Separation Fractions . . .	116
24.	Magnetic Susceptibilities of Metal Acetylacetonates	117
25.	Magnetic Susceptibilities of M(X)A Separation Fractions . .	118
26.	Per Cent Iron in TSPP, $FeCl_3$, and Calgon Separation Fractions	122
27.	Weight Analysis of Montmorillonite in TSPP Separation . . .	123
28.	Weight Analysis of Montmorillonite in $FeCl_3$ Separation . . .	124
29.	Weight Analysis of Montmorillonite in Calgon and M(X)A Separation	125

LIST OF ILLUSTRATIONS

Figure		Page
1.	Relation Between Diamagnetism, Paramagnetism, and Ferromagnetism	4
2.	Diagrammatic Structure of Kaolinite	10
3.	Diagrammatic Structure of Montmorillonite	12
4.	Schematic Diagram of a Metal Acetylacetonate Chelate Ring	18
5.	A Schematic Diagram of the Structure of $[Co(II)A_2]_4$	19
6.	Structure of $CuA(CH_3O)$ in $CHCl_3$	20
7.	Laboratory Clay Processing Plant Showing the High Intensity Wet Magnetic Separator	23
8.	Arrangement of Spheres in Separation Zone of Magnet During Separations	25
9.	Magnetic Susceptibility Apparatus	27
10.	Electromagnet Used in Magnetic Susceptibility Measurements	28
11.	Schematic Diagram of Calgon Separation	36
12.	Per Cent Montmorillonite vs. Magnetic Separation Time for TSPP and $FeCl_3$ Separations	46
13.	Weight Distribution vs. Separation Time for TSPP and $FeCl_3$ Separations	47
14.	Per Cent Montmorillonite Distribution for TSPP and $FeCl_3$ Separations	48
15.	Efficiency Ratio vs. Time for Magnetic Portion of TSPP and $FeCl_3$ Separation	49
16.	Correlation of Magnetic Susceptibility and Per Cent Montmorillonite for TSPP Separation	52

LIST OF ILLUSTRATIONS (Continued)

Page

17. Correlation of Per Cent Iron and Per Cent Montmorillonite for TSPP Separation 52

18. Correlation of Magnetic Susceptibility and Per Cent Iron for TSPP Separation 55

19. Correlation of Magnetic Susceptibility and Per Cent Montmorillonite for $FeCl_3$ Separations 55

20. Correlation of Per Cent Iron and Per Cent Montmorillonite for $FeCl_3$ Separation 57

21. Correlation of Per Cent Iron and Magnetic Susceptibility for $FeCl_3$ Separation 57

22. Correlation of Magnetic Susceptibility and Per Cent Iron for Combined Data from TSPP, $FeCl_3$, and Calgon Separations 63

23. Standard Curves for Determining Per Cent Montmorillonite in Kaolinite 89

24. Standard for Determining Per Cent Iron 92

25. Diagram of Maximum Path a Magnetic Particle Must Travel to Reach the Point of Maximum Flux Concentration 99

26. Maximum Time of Separation vs. Particle Size 102

SUMMARY

For many years it has been known that montmorillonite impurity in kaolin was a basic cause of high viscosity. In an attempt to remove montmorillonite from kaolinite, wet magnetic separations using a high intensity magnetic separator were made.

Attempts were made to increase the magnetic susceptibility of the montmorillonite by chemical treatment. Eleven different separations were performed at five per cent solids and with additions of (1) tetrasodium pyrophosphate, (2) ferric chloride and sodium hexametaphosphate, (3) sodium hexametaphosphate, and (4) seven different paramagnetic metal acetylacetonate compounds plus a control separation. In order to analyze the various fractions of the separations, the weight, per cent montmorillonite, magnetic susceptibility, and per cent iron were measured for each sample.

The separation made with tetrasodium pyrophosphate addition was the most efficient. Addition of both ferric chloride and sodium hexametaphosphate appeared to have detrimental effects on the separations but a separation or concentration of the montmorillonite in magnetic fractions was still achieved. The additions of plus two valence paramagnetic metal acetylacetonates appeared to have no effect upon the separation. Additions of plus three valence paramagnetic metal acetylacetonates completely stopped any separation or concentration of the montmorillonite in the magnetic fractions. When tetrasodium pyrophosphate was added a relationship was established between per cent montmorillonite and the magnetic susceptibility of the clay that was expressed as

$$\chi = [0.248 \text{ (\% Montmorillonite)} - 0.981] \times 10^{-6}\,\text{gm}^{-1}.$$

The combined data from the separations using tetrasodium pyrophosphate, ferric chloride, and sodium hexametaphosphate established a relationship between per cent iron and magnetic susceptibility that was

$$\chi = [1.992 \text{ (\% Fe)} - 0.598] \times 10^{-12}\,\text{gm}^{-2}.$$

Theoretical calculations were also made that showed the relationship of time of travel to particle size for weakly magnetic particles in a liquid medium. It was determined that the time of travel was inversely proportional to the square of the particle diameter. These calculations showed that for particles in the micron and submicron particle size range time was a controlling factor in the separations. Therefore, separations were made using time as a variable and these separations were most efficient at a separation time of five minutes.

CHAPTER I

INTRODUCTION

More than one-half of the kaolin mined in the United States today according to Cooper (1) is used in the paper industry both as coating and filler material. The clay must be applied to the paper in a water suspension of high solids content to keep the water that must be removed to a minimum but still be within viscosity limitations for coating the paper. There are extensive kaolin deposits that do not meet this viscosity specification and variations in the viscosity may occur in samples taken from the same mine. The variations can be due to the differences in the particle size, particle shape, particle size distribution, and the mineralogical composition of the kaolin.

One mineralogical component that is a basic cause for high viscosity in kaolin is montmorillonite. Work done recently by Iannicelli and Millman (2) indicated that the maximum montmorillonite content permissible for kaolin meeting "preferred" paper-coating viscosity specifications is about three per cent montmorillonite. Many kaolin deposits exceed this three per cent limit.

The purpose of this research was to separate montmorillonite from kaolinite in a water suspension using a high intensity magnetic field. Correlations were also established between the magnetic susceptibility of kaolin clay, per cent iron in the kaolin clay, and per cent montmorillonite in the kaolin clays.

CHAPTER II

REVIEW OF LITERATURE

Magnetic Separation

For many years both wet and dry magnetic separation has been applied to common ferrous ores. Only in recent years have magnetic separatores been developed to separate weakly magnetic materials. Unfortunately, only a limited amount of information has been published on the separation of weakly magnetic materials, and the actual data published is somewhat scanty. A need is most apparent for standardization of the relative magnetic properties of different materials.

There have been established certain variables that directly affect magnetic separations of weakly magnetic materials. These are the field strength of the magnet, the field gradient of the magnet, the magnetic susceptibility of the material to be separated, and the particle size of the material.

Magnetic Susceptibility

If a substance is placed in a magnetic field of strength H, then the magnetic industion is given by B, where:

$$B = H + 4\pi\nu \qquad (1)$$

The quantity ν is the intensity of magnetization, and $\nu/H = K$ is the magnetic susceptibility per unit volume. The magnetic susceptibility per

unit mass is obtained by dividing K by the density of the material. The symbol χ will be used for magnetic susceptibility per gram.

If a substance is placed in a magnetic field, the intensity of magnetization in a substance may be either slightly smaller, or somewhat larger, than that produced in a vacuum by the same field. In the first case, the substance is called diamagnetic; in the second, paramagnetic. There is also the case of ferromagnetism in which the intensity of magnetization may be very much larger than the applied field. Although ferromagnetism is the most commonly known magnetism, it is comparatively rare in nature. It occurs in only a few metals, alloys, and compounds. Paramagnetism is common, especially among the transition group elements. Diamagnetism is a universal property of matter. All substances, even though paramagnetic, have at least an underlying diamagnetism.

In general, the susceptibility of diamagnetic substances is independent of temperature and field strength. The susceptibility of paramagnetic substance is often inversely proportional to the absolute temperature, but independent of field strength. The susceptibility of ferromagnetic substance is dependent both on temperature and on field strength in a rather complicated way. The relationship between several magnetic quantities is shown in Fig. 1. Note that the slope of the curves are directly proportional to magnetic susceptibility.

Any substance placed in a magnetic field will develop an induced moment similar to the induced moment developed by a nonpolar molecule in an electric field. The magnetic moment acquired by the body under these conditions will be proportional to the susceptibility per unit mass times the mass of the body multiplied by the field, $m\chi H$, but the body will

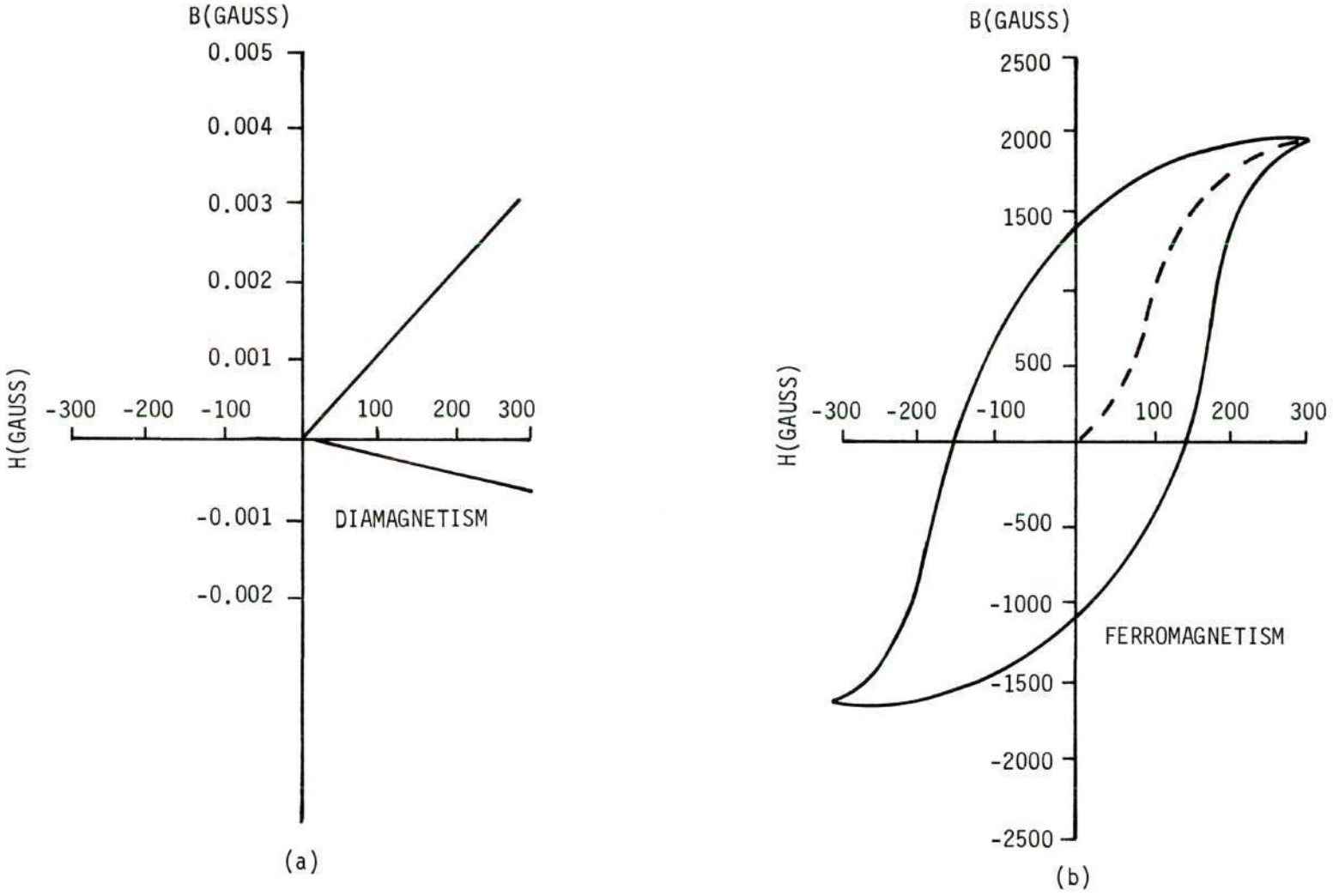

Figure 1. Relation Between Diamagnetism and Paramagnetism (a) and Ferromagnetism (b). Note the change in ordinate scale.

experience no displacing force if the field is uniform. If the field is made non-uniform with a gradient $\frac{dH}{dX}$ in the X direction, the body will be subject to a linear force (3) in the X direction and this will be proportional to the product of the moment and the gradient, as shown by the equation (2):

$$F = m \chi H \frac{dH}{dX} \qquad (2)$$

This equation gives the relationship between the magnetic force that is placed on a particle of a mass, m, and a magnetic susceptibility, χ, when the particle is subject to a field, H, and a field gradient, $\frac{dH}{dX}$, during a magnetic separation.

Particle Size

A small particle size presents many problems to magnetic separation either wet or dry. Stone (4) states in work with dry magnetic separation that:

> The removal of magnetite by conventional low-intensity magnetic separators is no problem until it is attempted on materials of very small particle sizes. The separation of magnetite from asbestos by these methods becomes impossible below particle sizes of 2 or 3 microns.

In the separation of magnetite from wolframite, Spokes and Mitchell (5) ground their samples and discarded the minus 270 mesh fraction, stating:

> The smallest fraction was discarded as being too fine for effective concentration by the magnetic and gravity processes that followed.

When working with the wet magnetic separation of clays, particle size is of primary importance because in most clays the majority of the particles are below two microns. During wet separations, in addition to

the necessity of having clay-water suspension dispersed to allow free migration of the particles to positions of highest field strength, it is also necessary to consider the forces placed on the particle by water. The motion of a particle settling under gravity (6) is expressed by Newton's second law in the equation

$$m \frac{d^2X}{dt^2} = m'g - F_{friction} \tag{3}$$

m and m' are the masses of the particle and fluid displaced by the particle; d^2X/dt^2, the particle's acceleration; g, the acceleration of gravity; and F, the frictional force resisting the particles motion. Assuming the particle is spherical and the resistance is due to friction only, the motion of the particle is given by Stoke's equation,

$$F = 3\pi \mu d \frac{dX}{dt} \tag{4}$$

where μ is the viscosity of the fluid, $\frac{dX}{dt}$ the velocity of the particle, and D is the diameter of the particle. Replacing m and m' by their values in terms of volume and density, $\frac{\pi d^3}{6} \rho$ and $\frac{\pi d^3}{6} (\rho-\rho_o)$, respectively, Equation 3 becomes:

$$\frac{\pi d^3}{6} \rho \frac{d^2X}{dt^2} = \frac{\pi d^3}{6} (\rho-\rho_o)g - 3\pi \mu d \frac{dX}{dt} \tag{5}$$

Magnetic Susceptibility of Montmorillonite and Kaolinite

The magnetic susceptibility of kaolinite and montmorillonite was measured by Reno and Taylor (7). They reported an average value for kaolinite from seven different localities to be 3.2×10^{-6} cm.gm.sec. units with a range of 0.0 to 7.31. However, these values would seem to be high considering that the chemical composition of kaolinite is $Al_2O_3 \cdot 2SiO_2 \cdot 2H_2O$ and that the susceptibilities for Al_2O_3 in cgs. units is -0.098×10^{-6}, SiO_2 is -0.493×10^{-6}, and H_2O is -0.699×10^{-6}. A calculation of the susceptibility of kaolinite from these values, assuming they are additive, gives a value of -0.340×10^{-6} cgs. units. The samples used by Reno and Taylor contained between five and ten per cent impurities and the high values could be attributed to this. They state:

> The large percentage of kaolinite...that did not have a sufficient susceptibility to be measured on the instruments indicates that probably the true susceptibility for these minerals should be close to zero.

Reno and Taylor (7) reported an average magnetic susceptibility for montmorillonite from six localities of 11.3×10^{-6} cgs. units with a range of 6.70 to 23.43.

Relation of Mineral Susceptibility to Chemical Content

Niliakantan (8) in work with biotite micas showed that the average magnetic susceptibility of the micas increased linearly with the per cent iron. The iron in the micas varied from 15 to 23 per cent by weight.

Studies made by Spokes and Mitchell (5) on the wolframite family established that there is a negative correlation between the square of the magnetic susceptibility of wolframite and per cent iron. The correlation that was established was

$$\chi^2 = 1347 - 13.1\ Fe \qquad (6)$$

with a correlation coefficient of -0.762. The explanation for the negative correlation was that manganese in the mineral was having a greater effect on the susceptibility than the iron, and the negative iron correlation indicated a positive manganese correlation.

Spokes and Mitchell also found a correlation between the square of the magnetic susceptibilities of sphalerites and per cent iron. This time the correlation was positive and was represented by

$$\chi^2 = 12.13\ Fe - 5.07 \qquad (7)$$

with a correlation coefficient of 0.9995.

Particle Size and Morphology of Montmorillonite and Kaolinite

Electron micrographs (9) have shown particles of kaolinite with thicknesses from 0.05 to 2 microns and surface dimensions from 0.3 to about 4 microns. Kaolinite occurs as flakes; and in well crystallized varieties, the flakes show well formed six-sided morphology.

Montmorillonite also occurs as flakes, but there is no regular shape to them. Electron micrographs (9) show particles to be about 0.002 microns in thickness and from 0.02 to 0.2 microns across the flake surfaces.

A look into the structures of montmorillonite and kaolinite gives some explanation for the difference in particle size between the two.

Structure of Kaolinite and Montmorillonite

Kaolinite

The chemical formula for kaolinite is $Al_2O_3 \cdot 2SiO_2 \cdot 2H_2O$. The mineral has a triclinic structure with axial relations of $\underline{a} = 5.16\text{Å}$, $\underline{b} = 8.97\text{Å}$, $\underline{c} = 7.38\text{Å}$, $\alpha = 91.8°$, $\beta = 104.5°$, $\gamma = 90°$ according to Brindly (10).

The structure is built up of alternating sheets of silicon tetrahedron and aluminum octahedron as shown in Fig. 2, after Grim (9). The silicon tetrahedra form a ring structure that is continuous in the a and b directions with the tips of the tetrahedra pointing toward the center of the unit comprised of the tetrahedron and octahedron sheets. Each tetrahedron has a solicon ion in the center with oxygen ions at the four corners. The octahedral units have an aluminum ion in the center with hydroxyl radicals at the three corners of the outside layer and two oxygen and a hydroxyl radical at the corners of the center layer common to the octahedron and tetrahedron sheets. The two oxygen ions also form the tips of the silica tetrahedrons pointing toward the center. In order to maintain electrical neutrality only two-thirds of the aluminum sites are occupied and the aluminum sites that are filled form hexagonal rings that are continuous in the a and b directions.

Montmorillonite

The theoretical chemical formula for montmorillonite without considering lattice substitutions is $(OH)_4Si_8Al_4O_{20}nH_2O$.

Due to the extremely small particle size of montmorillonite, single crystal x-ray diffraction data cannot be obtained, so that the structure has had to be determined from x-ray powder data and other better known

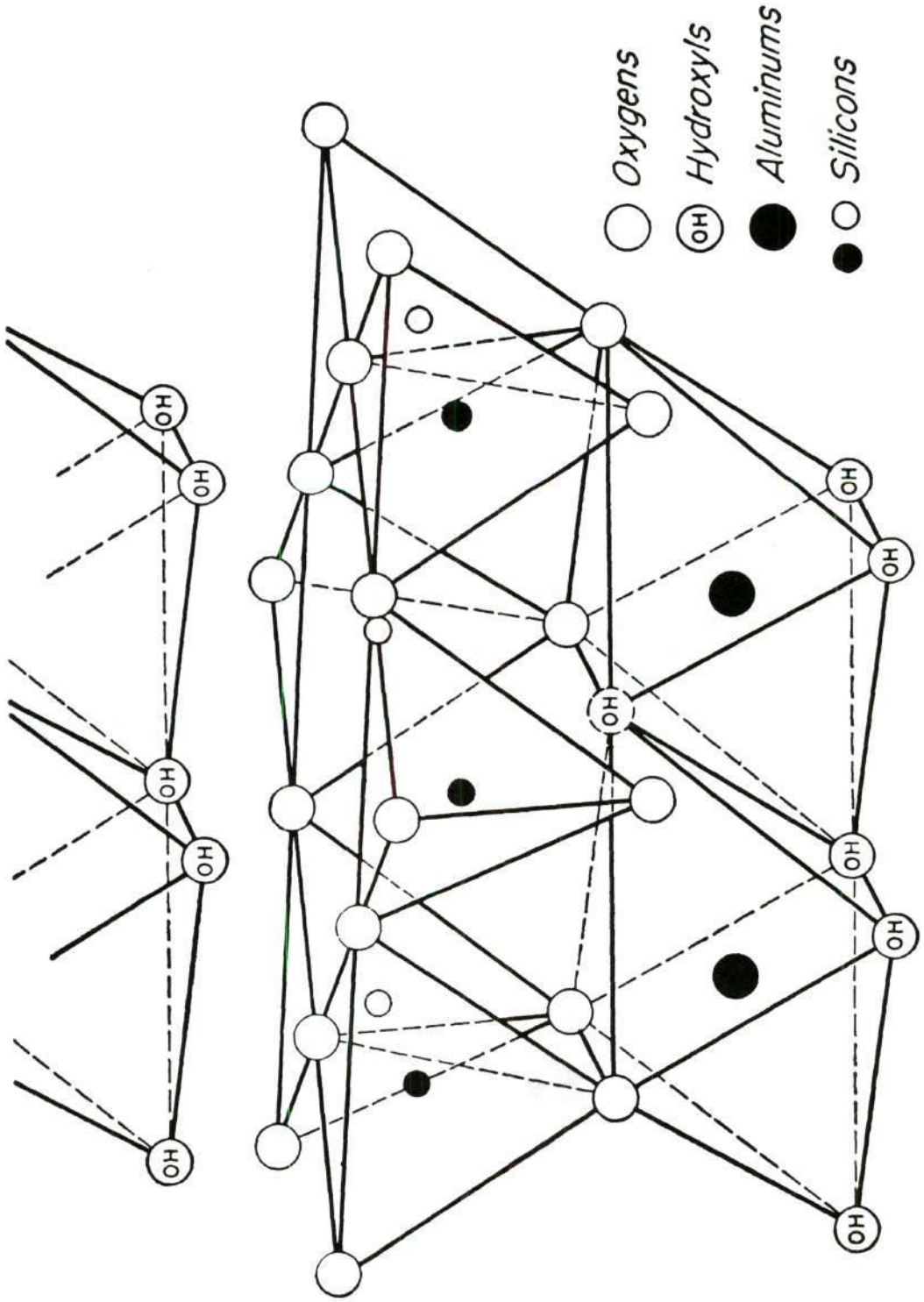

Figure 2. Diagrammatic Structure of Kaolinite after Grim (II).

structures (9). The most accepted structure is one developed by Hofmann, Endell, and Wilm (11), Marshall (12), and Hendricks (13). This structure, as shown in Fig. 3 according to Grim (9), consists of two tetrahedral sheets surrounding a central octahedral sheet. The two tetrahedral sheets form continuous ring structures in the a and b directions with the tips of the tetrahedrons pointing toward the center. There is a silicon ion at the center of each tetrahedron and oxygen ions at the corners. The tips form two-thirds of the ions that comprise the two outside layers of the octahedral sheet. The remaining ions that form these two layers are hydroxyl radicals. An aluminum ion is the center of each octahedron. The three layers are continuous in the a and b direction and stack one on top of the other in the c direction. According to Hendricks and Ross (14), however, as the flakes stack in the c direction, there is only slight orientation in the a and b direction.

In the c direction the flakes are loosely held together, with varying amounts of water between them. With no water between the flakes the c axis is 9.6Å and this varies with different cations between the lattice.

Various cations can make isomorphous substitutions in the montmorillonite lattice. Al^{+++} can replace Si^{++++} in the tetrahedral positions up to approximately 15 per cent. Numerous cations can replace the Al^{+++} in the octahedral positions, among them being Mg^{++}, Fe^{+++}, Zn^{++}, Ca^{++}, Ni^{++}, Li^{+1} (9), with replacement of Mg^{++} and Fe^{+++} being most prevalent. As a result of these lattice substitutions, montmorillonite always varies from the theoretical formula and these substitutions always cause a charge deficiency in montmorillonite (9). Many analysis have shown this charge

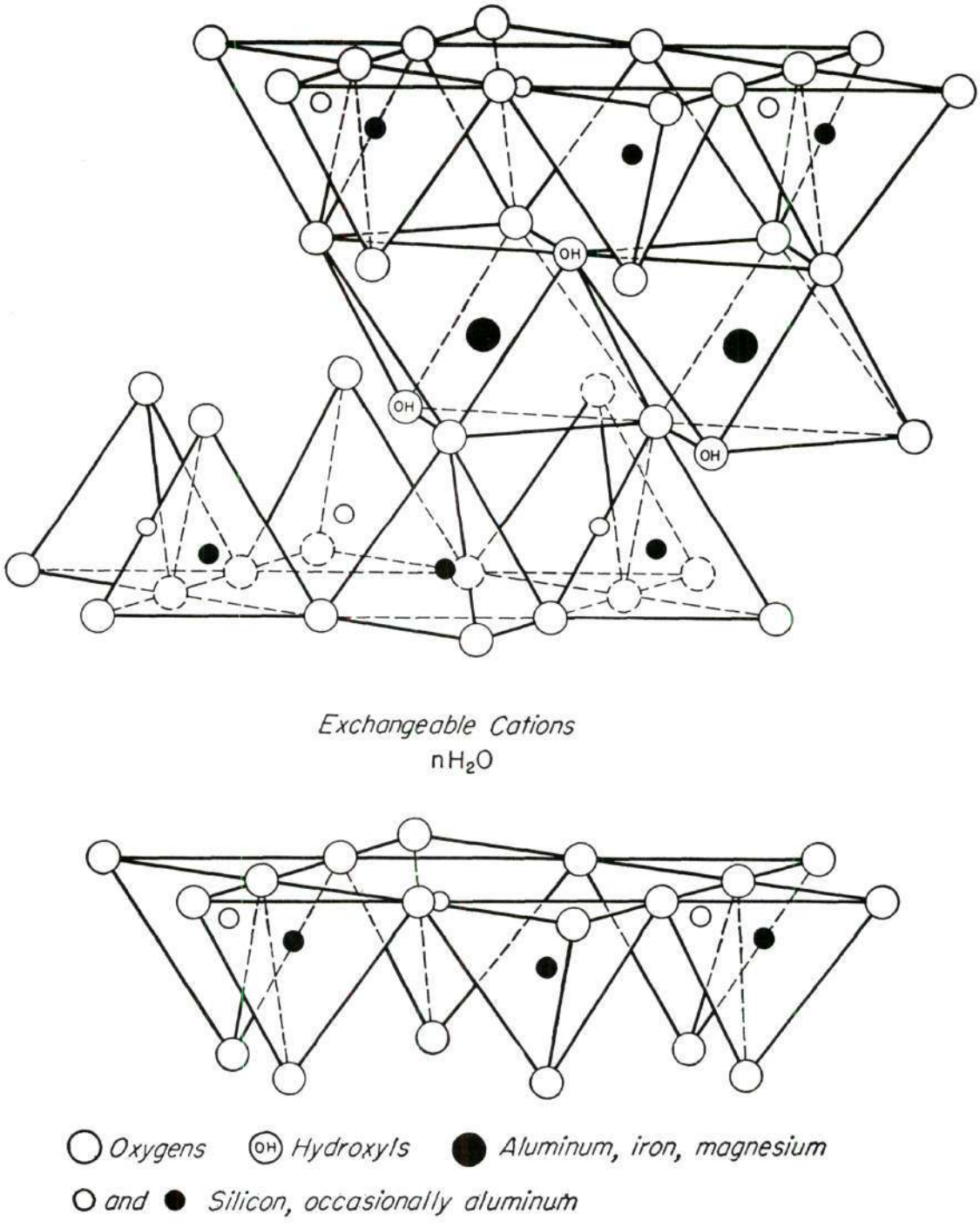

Figure 3. Diagrammatic Sketch of the Structure of Montmorillonite after Grim (II).

to be about -.66 e.v. per unit cell (9). As a result montmorillonite will absorb cations on its surface to neutralize this negative charge. The amount of cations absorbed is said to be the base exchange capacity of montmorillonite.

Base Exchange Capacity

Base exchange is the property of clay minerals of adsorbing various cations on its surface. The base exchange capacity of a clay mineral is the amount of cations of a particular kind that a particular clay will adsorb. This is measured in milliequivalents per 100 grams of clay.

The base exchange capacity of kaolinite is 3-15 meq/100 grams and that of montmorillonite is 50-150 meq/100 grams. This shows that the base exchange capacity for montmorillonite is from 5 to 50 times greater than that for kaolinite and in general the ratio varies from 20-30.

The generally low base exchange capacity for kaolinite is explained from the view point that there is very little replacement within the lattice and only a small charge deficiency results. Because of this, the major contributing factor to the base exchange of kaolinite is broken oxygen bonds at the edge of flakes and replacement of hydrogen ions on the octahedral surfaces. This would cause the base exchange capacity to increase with decreasing particle size since more broken edges would be exposed. This has been reported by a number of different authors.

The large base exchange capacity of montmorillonite is due mainly to the large charge deficiency developed by lattice replacement and the replacement of hydrogen from the octahedral surfaces. A minor portion is due to broken bonds on the edge of the flakes. As a result about 80 per cent of base exchange capacity for montmorrillonite occurs on the surfaces

of the flakes and the remainder occurs on the edges (9). From this one would conclude that the base exchange capacity of montmorillonite would increase, but only very slightly, with decreasing particle size. It has been generally considered that the base exchange capacity of montmorillonite does not increase substantially with decreasing particle size (9). However, it should be pointed out the particle size of montmorillonite is, in all known cases, very small, less than 0.25 microns. This indicates that base exchange occurs between the montmorillonite layers as well as on the surface.

The replaceability of one cation for another on the surface of clays has been given much study, and, in general, other things being equal, a higher valence cation will replace a lower valence ion and an ion of a higher atomic number will replace an ion of a lower atomic number, if the cations are of equal valence (9).

In studies on the adsorption of Fe^{+++} by montmorillonite, Thomas and Coleman (15) showed that the amount of iron adsorbed exceeded the base exchange capacity of montmorillonite by 10 to 15 per cent. Lutz (16) in repeated addition of $FeCl_3$ to electrodialyzed montmorillonite found that the Fe^{+++} ion was adsorbed to an extent of more than twice the base exchange capacity of the clay.

The rate of exchange reaction varies for different clays. The reaction for kaolinite is usually almost instantaneous, whereas it is slower for montmorillonite. It is thought that the reaction for kaolinite is rapid because the exchange takes place on the surface of the clay, and for montmorillonite, penetration between the sheets requires more time (9).

Organic Absorption

As stated earlier, montmorillonite platelets are loosely held together in the c direction, and various amounts of water can exist between each layer. Thus, montmorillonite is said to have an expanding lattice. The amount of expansion or the amount of water that can be absorbed between each montmorillonite layer is related to the type of cation attached to the mineral. In general, Li^{+} and Na^{+} promote large expansion, but Ca^{++}, Mg^{++}, Al^{+++}, H^{+}, Fe^{+++}, and K^{+} tend to reduce expansion (17). With the montmorillonite lattice completely collapsed, the c-axis has a dimension of 9.6Å; but with water absorbed, values as high as 30Å have been reported (17).

Besides absorbing water, montmorillonite can also absorb many polar organic molecules. Among the most common of the organic compounds used in work with montmorillonite are ethylene glycol and glycerol. Expansion of the c-axis to 17.0Å by ethylene glycol and 17.8Å by glycerol is generally accepted as positive identification of montmorillonite in complex clay mixtures. Besides ethylene glycol and glycerol, primary alcohols (18), polyvinyl alcohols (19), fatty acids (20), amines (21), phenol (22), and other organics too numerous to mention here have been used to expand the montmorillonite lattice.

For some organics it is necessary only to expose dry montmorillonite to the organic vapor to expand the lattice, and for others the method by which the organic is introduced into the lattice is most important and complex. Brunton (23) showed that the montmorillonite lattice becomes fully expanded in one hour by exposing the clay to a vapor bath of ethylene glycol at 60°C. Brindley and Satyabrata (18), in work with primary

alcohols, found that the calcium-montmorillonite lattice would be expanded by ethanol simply by exposing the dry mineral to the vapor of the organic, but higher primary alcohols could be "induced" into the lattice only be first expanding with a lower alcohol and then exposing the clay to the liquid of the higher alcohol. Ethanol expanded the calcium-montmorillonite lattice to 13.2 ± 0.2Å when there was a single layer of ethanol present in the lattice and 16.6 ± 0.1Å with a double layer (18). Brindley and Moll (20), in work with fatty acid-calcium-montmorillonite complexes, refer to a "propping open" of the lattice with n-hexagonal or n-octanol before introducing the acid. They state that "...the complexes are very sensitive to the mode of formation and negative results easily arise if great care is not exercised."

Greenland (19) expanded the montmorillonite lattice with polyvinyl alcohols. He stated that polymer molecules of the alcohols as large as 200-600Å for the major axes and 20Å for the minor axes had been absorbed by the montmorillonite. Greenland measured basal spacings of 30Å for sodium montmorillonite that had adsorbed more than 0.70 grams of polymer per gram of clay. The polyvinyl alcohols were adsorbed from an aqueous solution. The alcohols were dissolved in water and then shaken with the clay. For sodium-montmorillonite the adsorption was complete within 24 hours.

Street and White (24) found the phenol would be adsorbed by amine derivatives of montmorillonite from an aqueous solution. The ratio of carbon to nitrogen in the system was believed to be the controlling factor for the quantity of phenol that was adsorbed. An interesting point that was presented was that the phenol adsorption in all cases was between 76 and 120 meq/100 grams of montmorillonite. This indicates that the

montmorillonite was adsorbing the phenol in about the same equivalent amounts as it adsorbs inorganic cations.

Just as Li^+ and Na^+ tend to promote large expansion of the montmorillonite lattice in the presence of water, Greenland (19) and McAtee (21) showed that Na^+ promoted a greater adsorption of polyvinyl alcohols and amines respectively, than did Ca^+, Ca^{++}, or Mg^{++}.

Metal Acetylacetonates

Metal acetylacetonates comprise a group of metalic-organic compounds that are the metal derivatives of acetylacetone, ($C_5H_8O_2$; 2, 4-pentanedionato). Metal derivatives of acetylacetone have been formed with most of the alkale and alkaline earth elements and many of the transition elements. Many of the metal acetylacetonates are common and easily accessible complexes and the preparation of many have been presented explicitly in literature (25). Many of the transition-element acetylacetonates are paramagnetic.

The complexes of metal ions with acetylacetone have been the subject of a wide variety of studies for many years, but there is still relatively little that can be said with certainty about their molecular structure.

Structure

In the formation of metal acetylacetone complexes, the metal ion, represented by M in Fig. 4, replaces a hydrogen ion to form a six-membered chelate ring. R_1 and R_3 in Fig. 4 are normally $-CH_3$ groups and R_2 is normally -H, but these groups may be replaced by other organic groups (26).

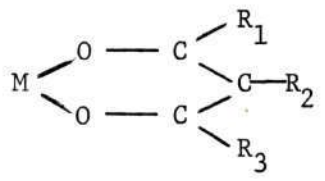

Figure 4. Schematic Diagram of a Metal Acetylacetonate Chelate Ring

Single crystal x-ray work (27) has shown that the structure of anhydrous, cobalt II acetylacetonate, $Co(II)A_2$, is in reality that of a tetramer, $[Co(II)A_2]_4$, as shown in Fig. 5. There are three distinct types of rings: (1) those in which both oxygens are bonded to a single cobalt ion. (2) those in which one oxygen forms a bridging bond between two cobalt ions, and (3) those in which both oxygens form bridging bonds between two cobalt ions. The triclinic unit cell was reported to have the dimensions: $a = 8.61\text{Å}$, $b = 10.38\text{Å}$, $c = 13.72\text{Å}$; $\alpha = 93°50'$, $\beta = 90°25'$, $\gamma = 98°35'$; there are four $Co(II)A_2$ groups in the unit cell.

In noncoordinating solvents such as benzene and carbon tetrachloride, cobalt (II) acetylacetonate, $Co(II)A_2$, units combine form dimers, trimers, and still higher oligomers, with a special stability noted for dimers (28). At high concentrations an apparent leveling off of association number at two was shown in carbon tetrachloride at 77°, which may represent a genuine stability of the dimetric unit, $[Co(II)A_2]_2$, or it may indicate the presence of impurity coordinating molecules such as alcohols, ether, H_2O, etc., which tend to split the tetramer into dimers (27). Cotton and Soderberg (28) using molecular weight studies, showed that cobalt (II) acetylacetonate in CCl_4 completely dissociates to the monomer at concentrations of approximately 0.03M at 25°C, and in CH_2Cl_2 conversion

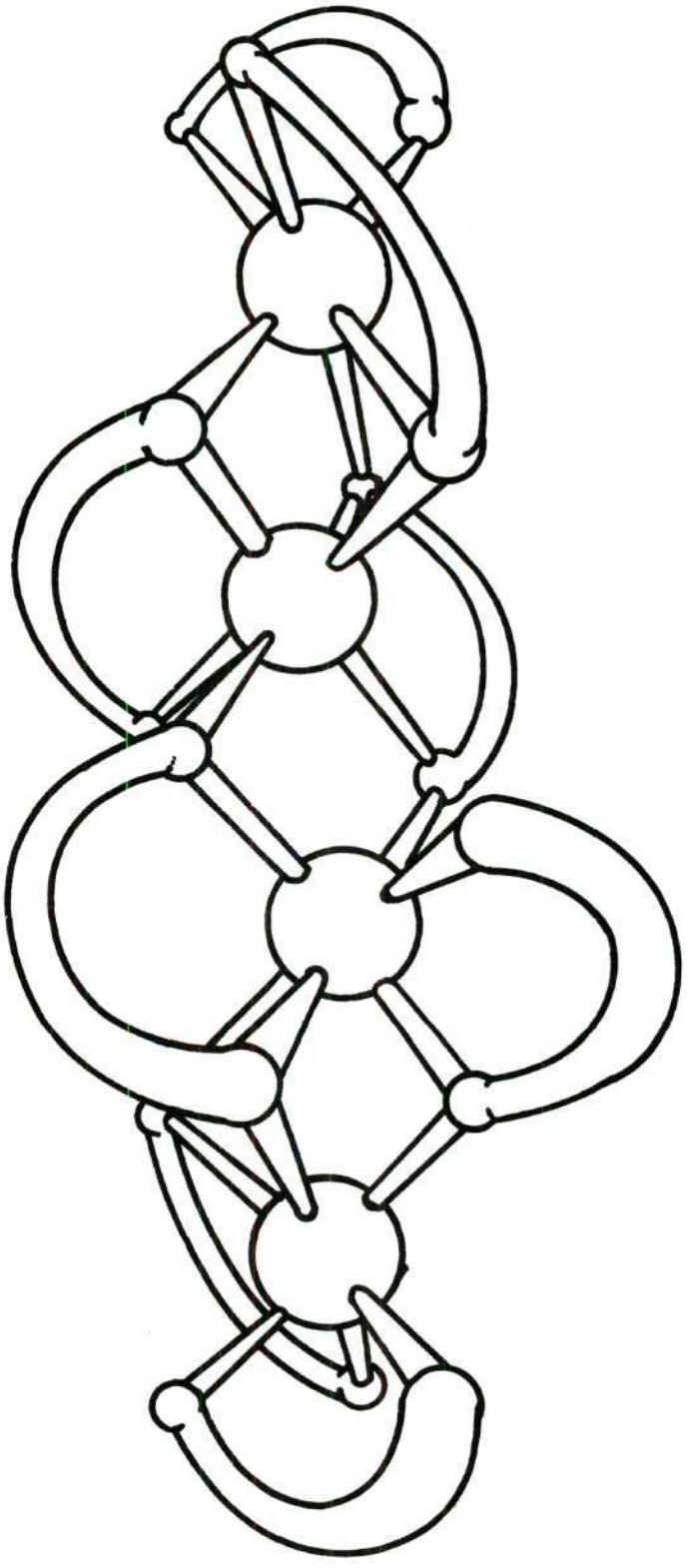

Figure 5. A Schematic Diagram of the Structure of $[Co(II)A_2^2]_4$. The O-C-C-C-O rings are indicated by curved lines.

to the monomer takes place between 0.01 and 0.001M.

X-ray study of single crystal anhydrous nickel (II) acetylacetonate has shown that the structure is trimetric in form with the three nickel ions in a linear row. The oxygen ions form a distorted octahedron around each nickel ion (29). Molecular weight studies of $[Ni(II)A_2]_3$ in the non-coordinating solvents indicate that the trimetric units found in the solid state are preserved at room temperature and up to 80°C (29).

Kaplan (30) made molecular weight studies of $NiA(CH_3O)(CH_3OH)$, $MgA(CH_3O)(CH_3OH)$, $CuA(CH_3OH)$, $CoA(CH_3O)(CH_3OH)$, and $CoA(CH_3O)$ dissolved in chloroform at concentrations of 0.1000F, 0.500F, and 0.025F. The number of basic chemical formula units in each molecule, the association number, were found to be between four and eight for the cobalt, nickel, and magnesium compounds, with association decreasing with dilution for the cobalt and magnesium compounds. The copper complex showed an association of two that was constant on dilution. Kaplan proposed that the methoxide ion was acting as a bridging group in the copper compound and suggested the structure shown in Fig. 6.

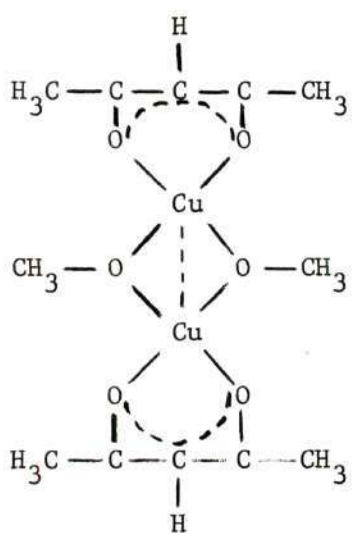

Figure 6. Structure of $CuA(CH_3O)$ in $CHCl_3$

Stability

When methoxo complexes, $MA(CH_3O)$, of the metal acetylacetonates, MA, are titrated with HCl (30), the complexes reacted to the acid in a two step procedure that can be stated as;

$$\text{Step 1} \quad MA(CH_3O) + H^+ \rightleftharpoons MA^+ + CH_3OH \qquad (8)$$

$$\text{Step 2} \quad MA^+ + H \rightleftharpoons M^{++} + HA \qquad (9)$$

Kaplan stated that the titration curves for the methoxo complexes seemed to show a stability order of Cu>Ni>Co>Mg. Calvin and Wilson (31) in measuring the formation constants of Cu(II) complexes with organic chelating ligands found that any group replacing $-CH_3$ on the acetylacetone ring and capable of participating in the ring resonance lowered the stability constant. It has been demonstrated (26) that the order of stability in divalent metal acetylacetonates is Cu>Ni>Co>Zn>Fe, Mn. No order of stability has yet been determined for the trivalent acetylacetonates.

CHAPTER III

INSTRUMENTATION AND EQUIPMENT

Magnet

The magnetic separations were made using a Carpco Model MWL-3465 laboratory, high-intensity, wet magnetic separator manufactured by Carpco Research and Engineering, Inc. of Jacksonville, Florida. The magnet was designed specifically for use in research of wet magnetic separations of weakly magnetic materials.

The magnet shown in Fig. 7 has a gap of 2.5 inches between the pole pieces. The pole pieces are made of low carbon steel five inches in diameter which taper down at the poles fo form rectangular pole faces three inches by four inches. The maximum magnetic flux produced in the gap in air is 3,800 gauss. This magnetic flux was constant throughout air space between the magnet poles. A metal box with outside dimensions of the air gap was placed between the poles and filled with 0.50 inch diameter low carbon steel spheres during separations. The spheres served as induced magnetic poles and created many points of high intensity flux. The regions of highest magnetic flux were produced at the point of contact of two spheres perpendicular to the pole faces. The maximum magnetic flux produced between the spheres was measured at various current settings using a Bell "240" Incremental Gaussmeter, manufactured by Bell, Inc., of Columbus, Ohio. Flux measurements were made for three different sphere sizes, 0.25, 0.50, and 0.75 inch diameter. The highest flux density

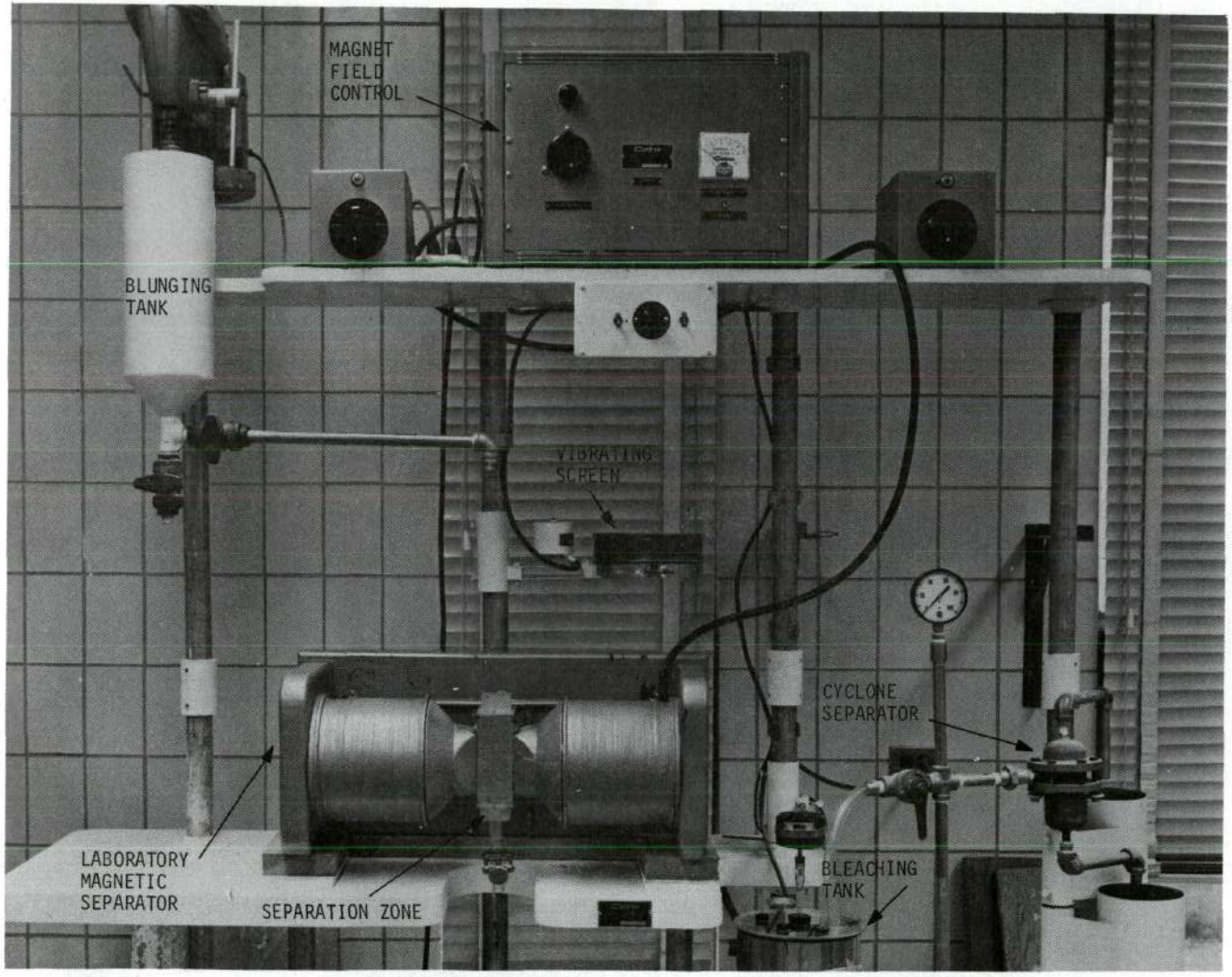

Figure 7. Laboratory Clay Processsing Plant Showing the High Intensity Wet Magnetic Separator.

recorded was 34,000 gauss at 5.4 amperes using the 0.75 inch diameter spheres. However, the 0.50 inch diameter spheres were used for all separations because they produced comparable flux densities and also created more points of high intensity flux. Maximum flux densities for the various current settings and sphere sizes were recorded in Appendix A.

In all separations a current setting of 5.0 amperes was used because this setting could be maintained after the magnet warmed up. Rather than placing the spheres randomly in the box, the spheres were arranged before each separation in the geometry shown in Fig. 8 to create many points of maximum flux density and to eliminate the positioning of the balls as a variable. The metal box was closed at the bottom with a plexiglass plate that had a 0.50 inch diameter hole in the center. A tygon tube was attached to the hole and by using a hose clamp, the rate of flow of suspension through the magnet could be controlled or completely stopped. In order to affect a separation in this magnet, the magnetic material must be attracted to the points of highest flux concentration and must be held there while the non-magnetic material passes through the separation zone.

Magnetic Susceptibility Apparatus

Magnetic susceptibility measurements were made using a Cahn RG electrobalance manufactured by Cahn Instrument Company, Paramount, California, a small electromagnet built for this work, a direct current power source, produced by Carpco Research and Engineering, Inc., of Jacksonville, Florida, capable of producing 220 volts with a maximum current of 10 amperes, and a Speedomax H, Model S, strip chart recorder, manufactured by Leeds and Northup Company, Philadelphia, Pennsylvania.

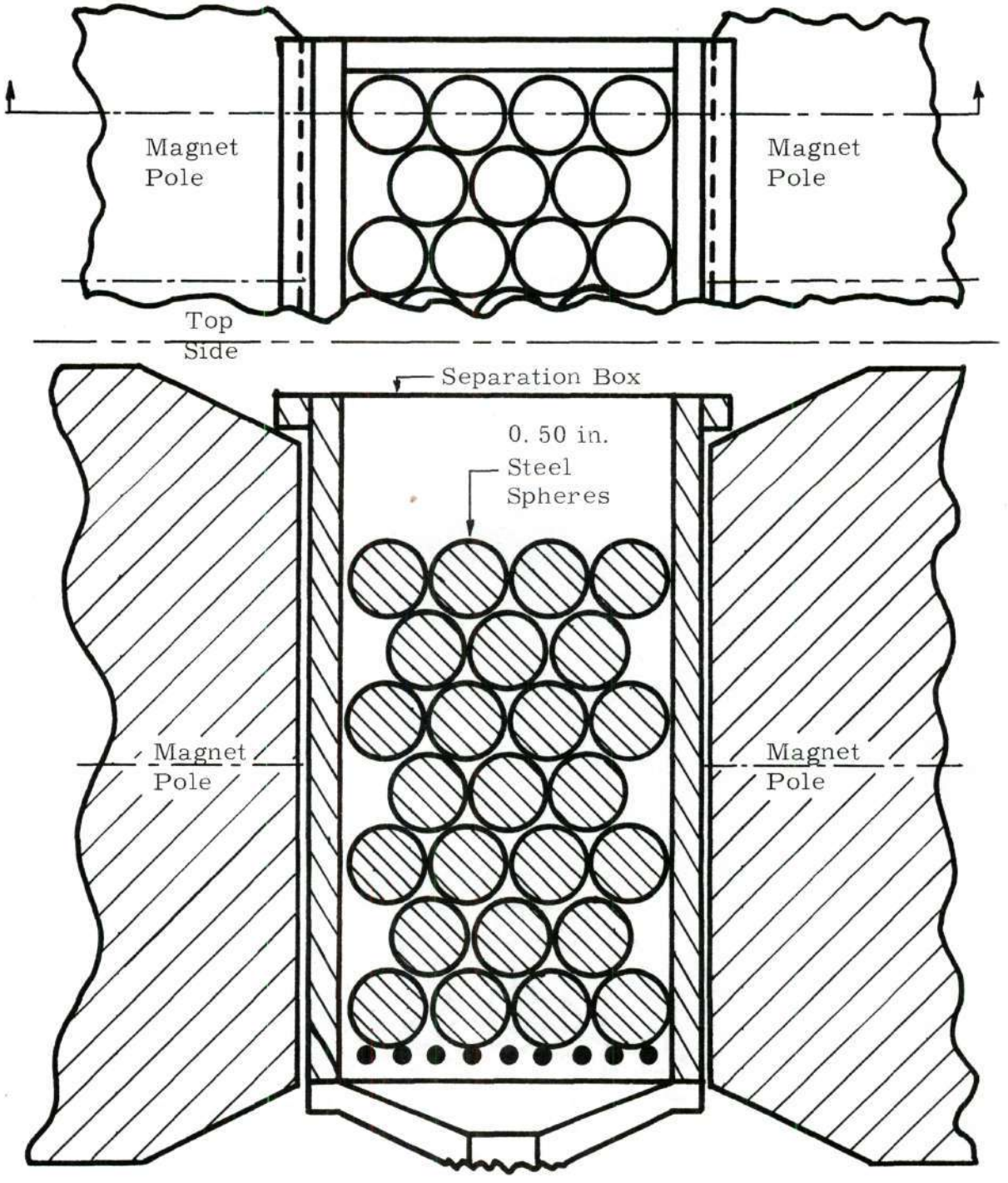

Figure 8. Arrangement of Spheres in Separation Zone of Magnet During Magnetic Separations.

The electromagnet was raised and lowered into position by a small screw jack and the current was monitored with a Triplett D. C. ampmeter. The equipment is shown in Fig. 9. The electromagnet consisted of a coil and two soft iron pole pieces. The coil was wound with 22 gauge magnet wire. The interior (refer to Fig. 10) of the coil was an inverted truncated cone that tapered down to a cylinder at the bottom. The bottom pole was a solid cylinder that was tapered on the top and flanged on the bottom. The top pole consisted of three separate pieces, an inverted truncated cone with a 0.75 inch hole in the center, a two inch washer that had a 0.75 inch hole through the center and a cylinder, flanged at the top with 7/32 inch hole through the center, and a 0.10 inch slot that cut from outside to the center of the cylinder.

The samples were inserted 0.25 inches below the center cylinder of the top pole by removing the center cylinder of the top pole and raising the magnet around the samples with a small jack until the samples were in position. Then the center cylinder was placed in position in the top pole by slipping the fiber, from which the sample hung, through the slot of the cylinder. Positioning of the sample was accomplished by a clip on the hang down fiber and a plexiglass cylinder which had two parallel lines cut in it. The plexiglass cylinder rested on the top pole and the magnet was raised until the clip on the fiber was between the two lines on the plexiglass cylinder.

X-ray Diffractometer

All X-ray diffraction analysis were made with a Norelco diffractometer. A copper target X-ray tube was used with a nickel filter. An angular aperture of 1° and a receiving slit of 0.003 inches was used to

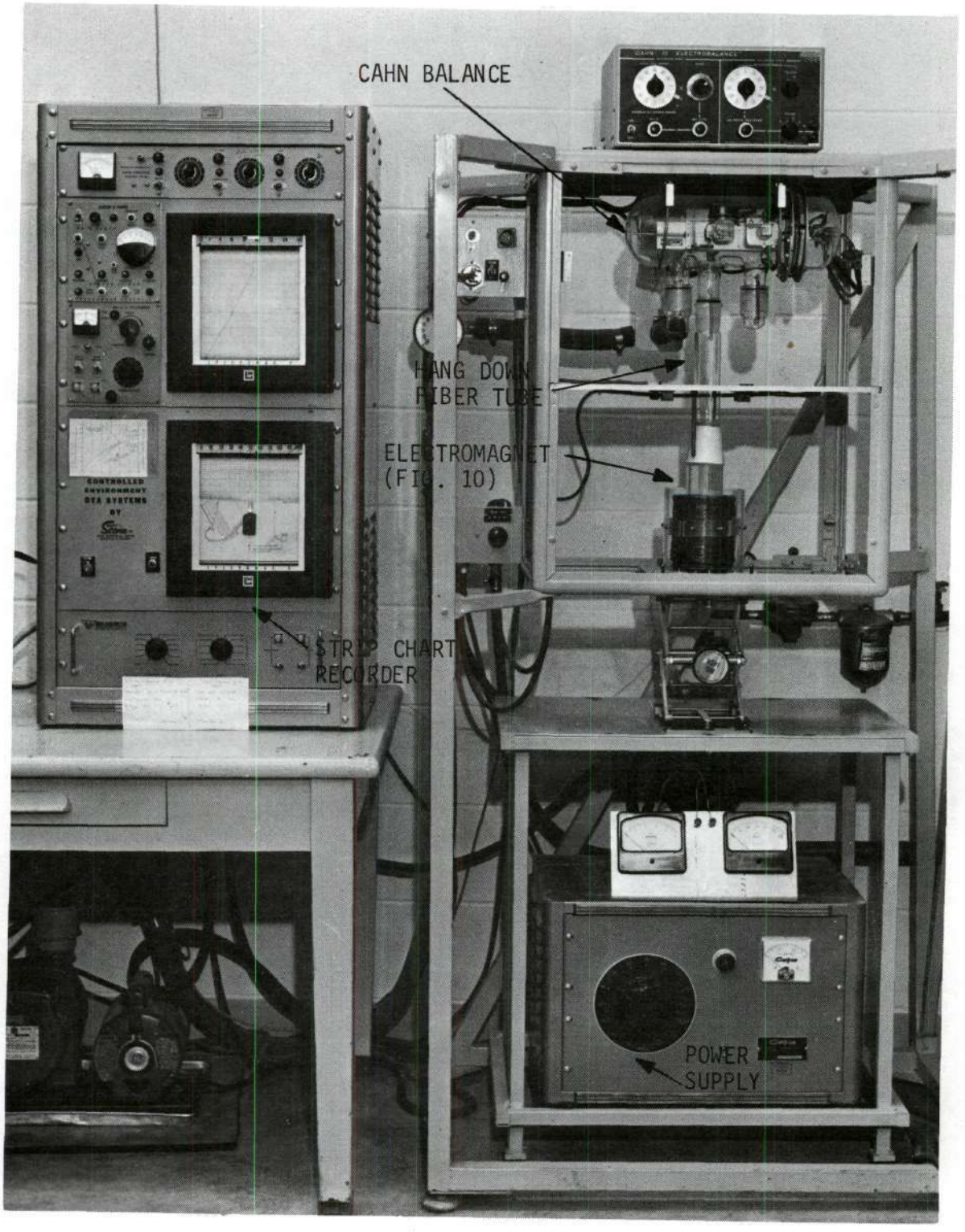

Figure 9. Magnetic Susceptibility Apparatus.

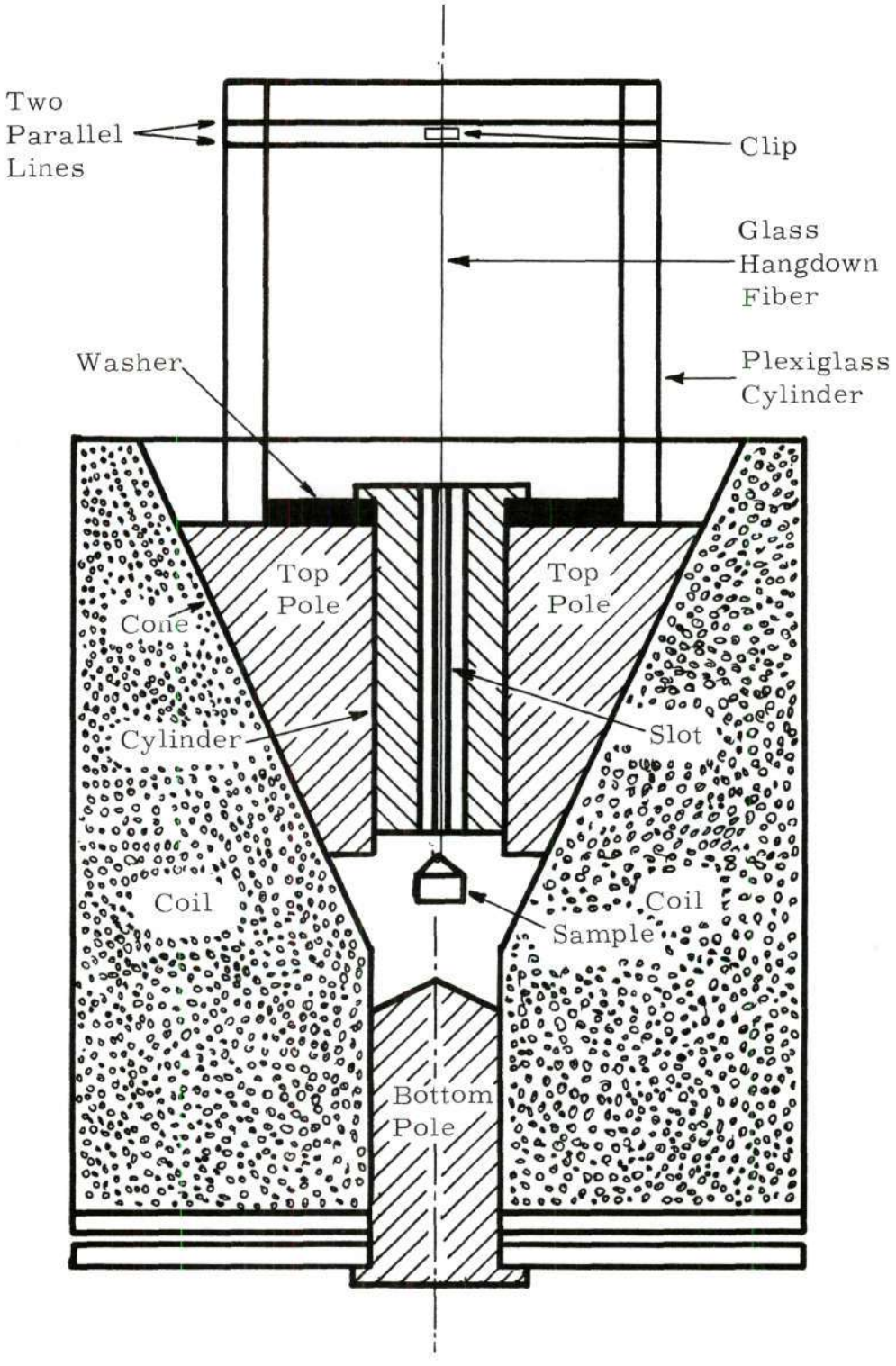

Figure 10. Electromagnet Used in Magnetic Susceptibility Measurements. Shown is Actual Size.

limit the primary X-ray beam and to limit the height of diffracted X-ray beam respectively. The X-ray detector was a sealed proportional counter.

X-ray Spectrograph

Iron analysis was made with a Norelco Universal Vacuum X-ray spectrograph. A tungsten target tube and a lithium fluoride analyzing crystal (cut parallel to the (200) plane) were used. The reflected fluorescent radiation was detected with a scintallation counter. Soller slits, entrance of 0.025 inches and exit of 0.040 inches, were used to collimate the radiation. The spectrograph was run at a vacuum of 60 to 40 microns of mercury.

Miscellaneous Equipment

pH Meter

A Beckman Zeromatic pH Meter with a Beckman Fiber Junction Electrode and a Beckman Glass Electrode was used for all pH determinations. The pH meter was calibrated before each titration at pH 4.0 and 7.0 with standard solutions.

Viscometer

All viscosity measurements were made with a Brookfield model LVF Viscometer, using a no. 1 spindel and a speed of 60 RPM. The viscometer was not calibrated for absolute values as it was desired only to know when minimum viscosity was reached.

Electrodialysis Apparatus

Electrodialysis of 1000 grams of Pioneer Kaolin was performed in a Mattson type cell. The cell consisted of three compartments in which a copper cathode and platinum anode were placed in the two outside

compartments and separated from the middle compartment by parchment paper. A 20 per cent suspension of Pioneer Kaolin and distilled water was placed in the center compartment. The cell was operated for 30 hours at a DC potential of 140 volts until the current flow dropped to a constant value. At this time it was assumed that the majority of the exchangable cations had been removed from the clay and had been replaced by hydrogen ions, creating what is referred to as a hydrogen clay.

CHAPTER IV

PROCEDURE

Preparation of Suspensions and Magnetic Separation

Air-floated Pioneer Kaolin from the Georgia Kaolin Company, Dry Branch, Georgia was used in all separations. All separations were made using a five per cent solids suspension of Pioneer Kaolin and water. Data for the clay, as reported by Georgia Kaolin Co., are shown in Appendix B.

Four basic separations were made. They were kaolin suspensions defloculated with (1) tetrasodium pyrophosphate (TSPP), (2) sodium hexametaphosphate and an addition of $FeCl_3$, (3) sodium hexametaphosphate (Calgon), and (4) sodium hydroxide and additions of seven different metal acetylacetonates dissolved in ethanol. The separations will be referred to respectively as (1) the TSPP separation, (2) the $FeCl_3$ separation, (3) the Calgon separation, and (4) the M(X)A separations, where M represents a metal cation, (X) its valence, and A represents acetylacetonate.

(1) TSPP Separation

A suspension of 200 grams of air-floated Pioneer Kaolin and 2000 milliliters of distilled water was blunged for 15 minutes on a drill press mixer at 2,025 RPM. The suspension was passed through a 325 mesh screen and diluted with 1,800 milliliters of distilled water, making a five per cent weight suspension. The weight of the clay remaining on the screen was 0.2 grams or less.

The clay suspension was defloculated by titrating with a five per

cent weight solution of TSPP until minimum viscosity was reached. The results of the titration are shown in Table 1.

Table 1. Defloculation of TSPP Suspension

Five Per Cent TSPP (milliliters)	Viscosity (centipoises)
0.0	5.0
0.1	4.5
0.2	3.6
0.5	3.4
1.0	3.4
1.5	3.4

It was found that 250 milliliters of liquid would just cover the spheres in the magnet gap. Therefore, six allotments were removed by siphoning 250 milliliters into a graduated cylinder while the suspension was being blunged, so as to eliminate settling during sampling. The six 250 ml allotments were placed in 500 ml flasks and stoppered. Five of the 250 ml allotments were placed in the magnet, one at a time, and held for 0, 5, 10, 15, 20 and 25 minutes at a current of 5.0 amperes and maximum field strength of 29,000 gauss. After the assigned time had elasped, the hose clamp on the tygon tube was released with the magnetic field still applied, and the suspension was allowed to slowly drain off so that as little turbulence as possible was created. The drained off portions were placed in their original flasks and labeled as the nonmagnetic portion of the separations. The nonmagnetic portions for the various times

were labeled 0-NM, 5-NM, 15-NM, 20-NM, and 25-NM, with 0, 5, 10, 15, 20 and 25 designation the number of minutes the suspension was in the magnetic field and NM representing the nonmagnetic portion of the separation.

Once the nonmagnetic portion of the separation had been drained off leaving the magnetic portion attached to the spheres, the magnetic field was turned off and the separation box was removed from the magnet. The box containing the spheres and the magnetic portion of the separation was placed in a degaussing coil to remove any residual magnetic forces. The spheres and the magnetic material were then emptied into a plastic container and the box was rinsed with approximately 200 ml of water to remove any remaining material. The plastic container was covered and shaken to give a slight scrubbing action to remove all the magnetic material from the spheres. The magnetic material was then poured into 500 ml flasks and the spheres were rinsed twice with 100 ml of water. The magnetic portions were labeled as 0-M, 5-M, 10-M, 15-M, 20-M, and 25-M, with 0, 5, 10, 15, 20, and 25 designating the number of minutes the suspension was in the magnetic field and M representing the magnetic portion of the separation.

The sixth allotment was used as an original sample and except for not being passed through the magnet, it received the same treatment as the rest of the samples.

All the samples were floculated with hydrochloric acid and filtered on preweighed filter paper. The samples were washed three times with distilled water and dried at 140°F. The weights of the samples were determined. All samples were ground with a mortar and pestle until the entire sample passed through a 200 mesh screen.

The per cent montmorillonite, magnetic susceptibility, and the per

cent iron was determined for all the samples.

(2) $FeCl_3$ Separation

A suspension of 100 grams of electrodialized Pioneer Kaolin and 1500 milliliters of distilled water was blunged for 15 minutes. Thirty milliequivalents of $FeCl_3$ were added to the suspension by adding 30 ml of 1.0 N $FeCl_3$ solution. A five per cent solids content was created by adding 370 ml of distilled water to the suspension. The suspension was blunged for 15 additional minutes. These conditions floculated the clay.

After 24 hours the clay was defloculated to minimum viscosity by titrating with a ten per cent weight solution of Calgon. Attempts to defloculate with TSPP were not successful. The results of the titration are shown in Table 2.

Table 2. Defloculation of $FeCl_3$ Suspension

Ten Per Cent Calgon (milliliters)	Apparent Viscosity (centipoises)	pH
0	5.2	3.2
1	5.2	3.0
2	5.2	3.0
3	5.0	3.3
5	5.5	3.1
8	5.1	3.1
11	5.3	3.1
15	4.7	3.0
20	3.6	2.9
22	3.6	2.9
25	3.7	2.9
30	3.5	2.9

The suspension was divided into six 250 ml portions as was done in the TSPP separation. The magnetic separation was performed exactly as described for the TSPP separation.

The samples were labeled according to time in minutes and magnetic portion; 0-NM, 5-NM, 10-NM, 15-NM, 20-NM, and 25-NM for the nonmagnetic portions. The sixth suspension was the original. The weight, magnetic susceptibility, weight per cent montmorillonite, and weight per cent iron were determined for each sample.

(3) Calgon Separation

One gram of Calgon was added to 1000 ml of distilled water. The solution was stirred until the calgon dissolved. A 100 gram sample of Pioneer Kaolin was added to the calgon solution and the suspension was blunged at 2,025 RMP on a drill press mixer for 30 minutes, screened through a 325 mesh screen, and diluted with 900 ml of distilled water, making a five per cent solids content. The material that remained on the 325 mesh screen was 0.2 per cent by weight. The viscosity of the suspension was 3.4 centipoises.

From the above suspension a 250 ml sample was siphoned into a graduated cylinder. This sample was separated according to the procedure described in the TSPP separation. However, the sample was passed through the magnetic separator three times. On each pass the suspension was held for five minutes and the magnetic material was removed after each pass. The magnetic portions were labeled Calgon 1st pass-M, 2nd pass-M, and Calgon 3rd pass-M. A schematic diagram of the separation is shown in Fig. 11. Samples were not taken of the nonmagnetic material after each pass. The nonmagnetic material that was analyzed was the remainder from the

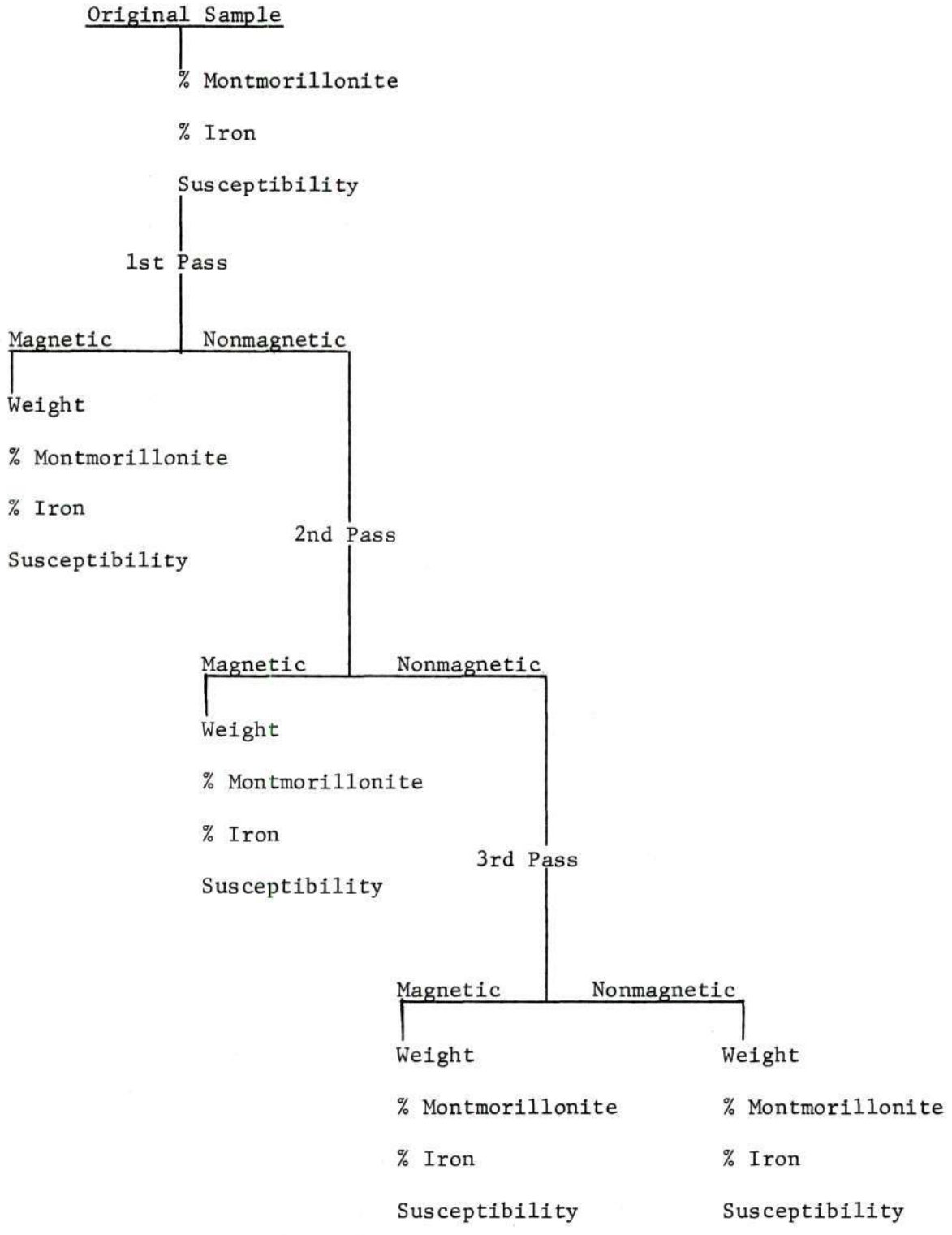

Figure 11. Schematic Diagram of Calgon Separation

passes and was labeled as Calgon-NM. A sample was drawn from the original suspension for analysis.

The weights of the various fractions were determined along with the magnetic susceptibility, per cent montmorillonite, and per cent iron, as shown in Fig. 11.

(4) M(X)A Separations

Twelve metal acetylacetonates were purchased from J.T. Baker Chemical Co., Philadelphia, N.J. They were Na(I)A, K(I)A, $Co(II)A_2$, $Cu(II)A_2$, $Mn(II)A_2$, $Ni(II)A_2$, $Zn(II)A_2$, $Al(III)A_3$, $Co(III)A_3$, $Cr(III)A_3$, $Fe(III)A_3$, and $Zr(IV)A_4$. The magnetic susceptibility of each compound was measured, and seven of the acetylacetonates were selected for addition to Pioneer Kaolin suspensions. They were $Co(II)A_2$, $Cu(II)A_2$, $Mn(II)A_2$, $Ni(II)A_2$, $Co(III)A_3$, $Cr(III)A_3$, and $Fe(III)A_3$.

A suspension was prepared by blunging 200 grams of electrodialized Pioneer Kaolin in 3500 ml of distilled water for 30 minutes. The suspension was defloculated by titrating with 0.1N NaOH. The apparent viscosity and pH of the suspension were measured during titration and the results were recorded in Table 3.

At this point the defloculated clay was passed through a 325 mesh screen with 0.5 per cent by weight remaining on the screen. The suspension was diluted to a five per cent solids content by adding 210 ml of distilled water. The pH of the suspension was adjusted to 7.4 by adding 10 ml of 0.1N NaOH. Eight 250 ml allotments were extracted from the above suspensions, put into 500 ml flasks, and stoppered.

Solutions of the selected seven metal acetylacetonates were prepared by dissolving 0.2 grams of the following metal acetylacetonates in

Table 3. Defloculation of M(X)A Suspension

0.1N NaOH (ml.)	Apparent Viscosity (centipoises)	pH
0	7.1	4.3
2	4.2	4.6
4	4.3	4.9
10	4.2	5.6
20	4.3	6.0
30	4.2	6.3
50	4.2	6.6
70	4.4	6.8
90	4.5	7.0

100 ml of ethanol, (1) $Mn(II)A_2$, (2) $Ni(II)A_2$, (3) $Co(III)A_3$, (4) $Cr(III)A_3$, and (5) $Fe(III)A_3$. The $Co(II)A_2$ and $Cu(II)A_2$ compounds were less soluble, therefore, solutions of 0.1 gram per 100 ml ethanol were prepared for them.

It was calculated that there were 12.8 grams of Pioneer Kaolin in 250 ml of a five per cent weight suspension of the clay, on the basis of four per cent montmorillonite in clay. Assuming the montmorillonite had a base exchange capacity of 100 meq per 100 grams, it was calculated that it would be necessary to add 0.51 meq of the metal acetylacetonates to satisfy the base exchange capacity of the montmorillonite in each 250 ml sample of above suspension.

To satisfy the base exchange capacity requirement of the montmorillonite, the volumes shown in Table 4 of the selected seven metal acetylacetonate solutions were added to seven of the eight 250 ml suspensions. These seven suspensions were labeled according to the metal acetylacetonate

addition as the $Co(II)A_2$, $Cu(II)A_2$, $Mn(II)A_2$, $Ni(II)A_2$, $Co(III)A_3$, $Cr(III)A_3$, and $Fe(III)A_3$ suspensions. The eighth 250 ml suspension of the clay was used as a standard and 30 ml of pure ethanol was added to it. This was labeled as the EtOH suspension. Before separation, 30 ml was extracted from each of the eight samples to be analyzed as the original sample before separation.

Table 4. Metal Acetylacetonate Additions

Metal Acetylacetonate	Weight/100 ml of Ethanol (grams)	Volume containing 0.51 Milliequivalents (milliliters)
$Co(II)A_2$	0.10	65.8
$Cu(II)A_2$	0.10	67.0
$Mn(II)A_2$	0.20	32.4
$Ni(II)A_2$	0.20	31.9
$Co(III)A_3$	0.20	30.1
$Cr(III)A_3$	0.20	30.7
$Fe(III)A_3$	0.20	30.2

The samples were then separated in the Carpco magnet for five minutes. Three passes were made through the magnet as in the Calgon separation. The procedure for each individual separation is described in the TSPP separation section.

The samples were labeled 0 for original, NM for nonmagnetic

portion, M for magnetic portion, 1, 2, or 3 for the 1st, 2nd, or 3rd pass through the magnet, and according to the metal acetylacetonate addition.

After separation the samples were put into preweighed breakers and dried at 140°F and the weight of each sample was determined. After drying and weighing each sample was ground to pass a 200 mesh screen. The per cent montmorillonite and magnetic susceptibility of each sample was determined.

Measurement of Magnetic Susceptibility

The Faraday method of measuring magnetic susceptibility was used in this thesis, and has been described adequately in the literature (1). In the Faraday method, a fairly constant nonhomogenous field with an axis of symmetry is needed. If a substance of susceptibility other than zero is placed in a region where the strength of the field changes with distance along the axis of symmetry, the substance will be subjected to a force along the axis according to Equation 2. Actually, when the magnetic field has no axis of symmetry Equation 2 becomes

$$F = m\chi H \left(\frac{dH}{dX} + \frac{dH}{dY} + \frac{dH}{dZ}\right) . \qquad (10)$$

By using the magnet shown in Fig. 10, the horizontal fields cancel at the center of rotation of the magnet, and therefore $\frac{dH}{dY}$ and $\frac{dH}{dZ}$ are 0, leaving only a verticle gradient or $\frac{dH}{dX}$. Equation 6, in this case, becomes Equation 2 or

$$F = m\chi H\frac{dH}{dX} . \qquad (2)$$

Using this equation the mass (m) of the sample is determined and then the force (F) placed on the sample by a magnetic field is determined. HdH/dX is measured using a substance of known magnetic susceptibility. Knowing the mass, the force placed on a substance by the magnetic field, and the product of field strength and field gradient, the magnetic susceptibility was calculated.

In the procedure that was followed for measuring magnetic susceptibility, a small glass bucket 0.25 inches in diameter and 0.14 inches deep was suspended on a quartz fiber from the B stirrup of the Cahn balance. The bucket was suspended approximately 0.25 inches from the top pole of the electromagnet. The bucket was positioned at the same point for each measurement by raising the coil until a metal clip on the fiber was between two lines cut on a plexiglass cylinder that rested on the top pole piece (Fig. 10).

Once the glass bucket was in position, the magnetic field was turned on and the force on the bucket due to the field was recorded in grams on a strip chart recorder.

The coil was then lowered and the bucket was filled with a sample. The bucket and sample were placed back in the coil and the weight of the sample was determined in grams. The magnetic field was turned on and the force on the bucket and sample was recorded. Thus, the force on the sample was equal to the force on the sample and bucket minus the force on the bucket. Since the force was in grams, it was multiplied by the acceleration of gravity, 980 cm/sec^2, to obtain the force in dynes.

The product of the magnetic field strength and field gradient was calibrated using Mohr's Salt, $FeSO_4 \cdot (NH_4)_2SO_4 \cdot 6H_2O$, which has a

susceptibility of $\frac{9500}{T + 1} \times 10^{-6}$ cgs units. The calibration was performed as described above using Mohr's Salt as the sample. Knowing the mass of the sample (m), the force on the sample (F) and the magnetic susceptibility of the sample (χ), the product of the field strength and field gradient ($H \frac{dH}{dX}$) was calculated using Equation 2. $H \frac{dH}{dX}$ for the magnet was calibrated at 1.5 and 2.0 amperes. The calibration is shown in Appendix C. The magnetic susceptibility of all samples was determined at the above two current settings. The data from the separation fraction was recorded in Appendix H.

Determination of Per Cent Montmorillonite

Each sample for montmorillonite determination was ground in a mortar and pestle to pass a 200 mesh screen and defloculated by adding 10 milliliters of a 0.0005 weight per cent solution of calgon to 0.50 grams of the sample. These suspensions were vibrated in an ultrasonic vibrator for 30 minutes to break down any particle aggregates. Then 1.5 milliliters of the suspensions were deposited on a glass slide 25 mm x 37 mm and air dried on an aluminum sheet that had been previously leveled. After drying, the glass slides were put in a desicator for 24 hours. The samples were removed from the desicator and X-ray diffraction trace was run from 2°2θ to 15°2θ. The samples were then put in an ethylene glycol vapor bath at 60°C for 60 minutes. An X-ray trace was run again on the samples from 2°2θ to 15°2θ.

The areas of the montmorillonite and kaolinite peaks were measured and the ratios of the montmorillonite peaks to kaolinite peaks were computed. The per cent montmorillonite was determined from the standard curves shown in Figure 23 in Appendix D. The X-ray setting shown in

Appendix D were used for all samples, both standards and magnetic separation samples. The data from the separation fractions was recorded in Appendix G.

Determination of Per Cent Iron

After the samples had been dried and ground to pass a 200 mesh screen, the samples were placed in the X-ray spectrograph sample holders which had previously been covered with a 0.25 mil milar film. The samples were placed in the sample holder as a loose powder and the sample holder was tapped gently until the powder packed to a smooth surface. Two standards containing 0.375 per cent iron and 0.709 per cent iron were placed in the spectrograph with two separation samples. Spectrograph traces were run from 55°2θ to 59°2θ using a LiF analyzing crystal. This range was sufficient to record the characteristic $K\alpha$ iron radiation. The areas of the $K\alpha$ iron peaks were measured with a plainmeter. The per cent was then determined from the standard curves shown in Fig. 24 of Appendix E. The X-ray spectrograph settings used for all iron measurements are recorded in Appendix E. The data from the separation fractions was recorded in Appendix I.

CHAPTER V

DISCUSSION OF RESULTS

1. Selection of Clay

Airfloated Pioneer Kaolin was selected to be used in the separations because it was typical of many clays whose montmorillonite content is slightly above the three per cent limit required for low viscosity clays. It was hoped that through magnetic separation, the montmorillonite content of the clay could be lowered to the extent that the clay would be desirable to be used as a paper coating clay, and therefore, it would be possible to open similar clay deposits to paper clay use.

X-ray analysis of the portion of the clay that was greater than 44 microns showed a slight amount of sericite mica, but the weight per cent greater than 44 microns constituted only 0.02 weight per cent of the clay. X-ray analysis of the whole clay failed to detect the mica and since the portion greater than 44 microns was removed before each separation, it was decided that the mica content was negligible. The only other mineral constituents detectable by X-ray analysis were montmorillonite, 3.1 ± 0.25 per cent, and kaolinite.

2. TSPP, $FeCl_3$, and Calgon Separations

A. Effect of Time on TSPP and $FeCl_3$ Separations

Calculations, Appendix F, showed that the velocity of weakly magnetic particles in a magnetic field decreases drastically as the size decreases. Therefore, time was made a factor in the TSPP and $FeCl_3$

separations of montmorillonite.

Fig. 12 shows the effect of holding the TSPP and $FeCl_3$ suspensions in the separation zone of the magnet for up to 25 minutes. Besides allowing time for the montmorillonite particles to migrate to points of highest flux concentration, stopping the suspension eliminated water currents which would keep the montmorillonite from reaching the points of maximum field strength. From Fig. 12 it is seen that the per cent montmorillonite in the magnetic portions of both separations increased to a maximum at five minutes and then decreased from 5 minutes to 25 minutes.

The per cent montmorillonite in the magnetic portion of the TSPP separations was greater for all measurements than the per cent montmorillonite in the magnetic portion of the $FeCl_3$ separations. However, Fig. 12 shows that per cent montmorillonite in the $FeCl_3$ nonmagnetic material was lower than in the TSPP nonmagnetic material. This is explained by Fig. 13, which shows that the weight per cent of the clay that was removed in the magnetic portion was greater for the $FeCl_3$ separation than for the TSPP separation. This would mean that although the per cent montmorillonite removed in the magnetic portion of the $FeCl_3$ separation was less than in the TSPP separation, the weight per cent of the total magnetic sample removed was so much greater for the $FeCl_3$ magnetic portion that a higher percentage of the total montmorillonite was removed by the $FeCl_3$ separation. This is shown in Fig. 14, where the per cent montmorillonite distribution is plotted vs. time for the TSPP and $FeCl_3$ separations.

Before discussing Fig. 15 where the "efficiency ratio" is plotted against time, it is necessary to define the "efficiency ratio." The "efficiency ratio" is the ratio of the per cent montmorillonite distribution

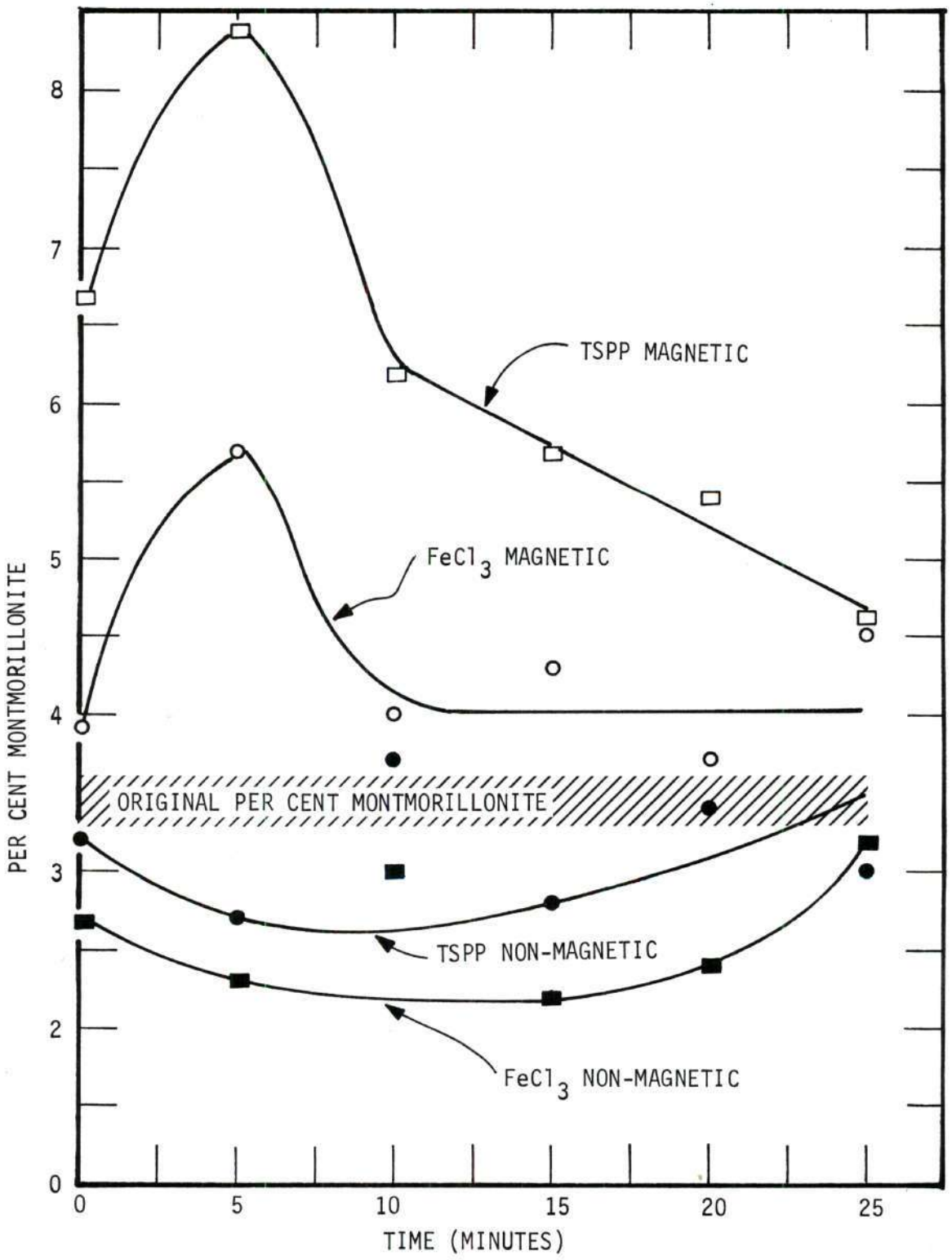

Figure 12. Per Cent Montomorillonite Versus Magnetic Separation Time for TSPP and $FeCl_3$ Separations.

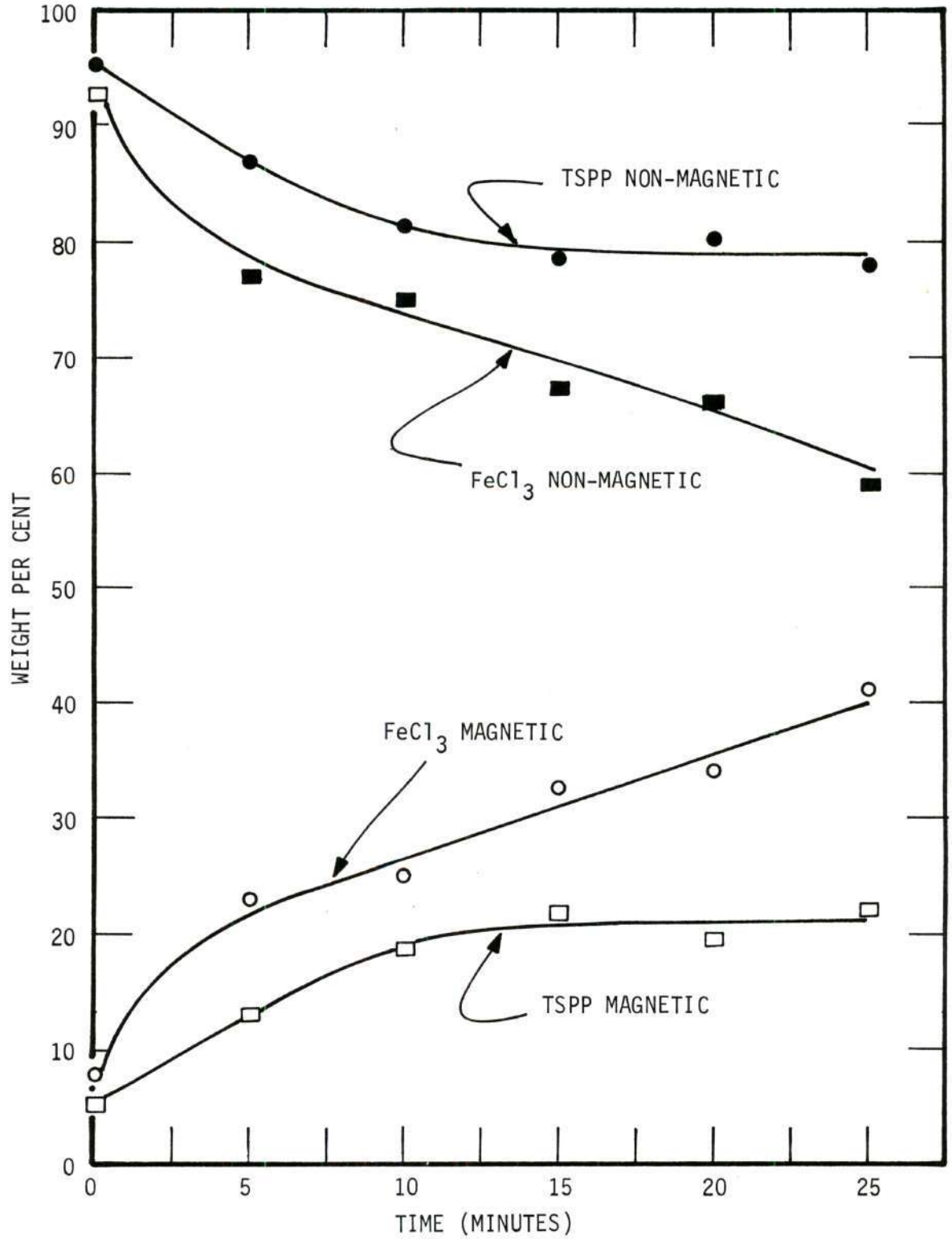

Figure 13. Weight Distribution Versus Separation Time for TSPP and $FeCl_3$ Separations.

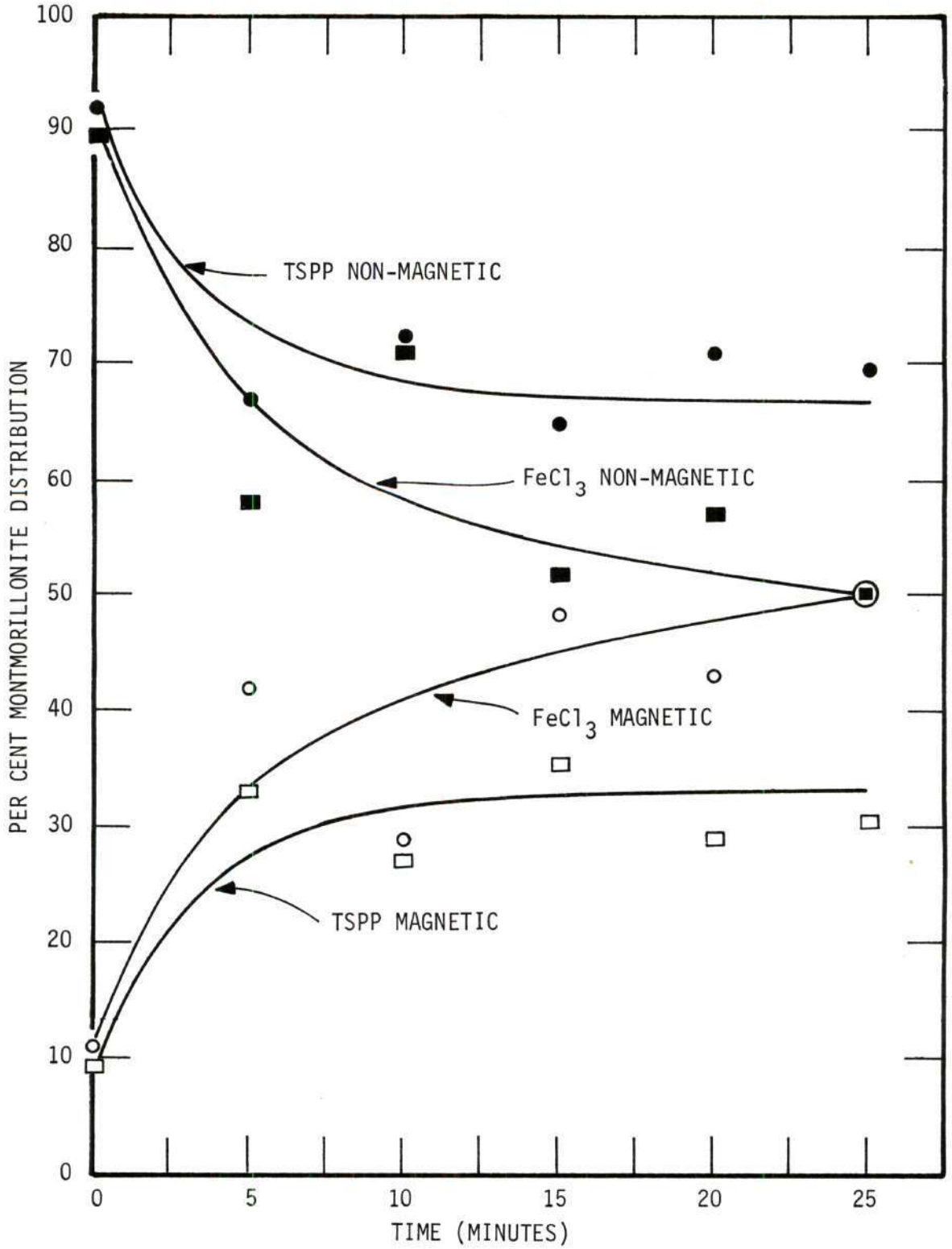

Figure 14. Per Cent Montmorillonite Distribution Versus Time for TSPP and $FeCl_3$ Separations.

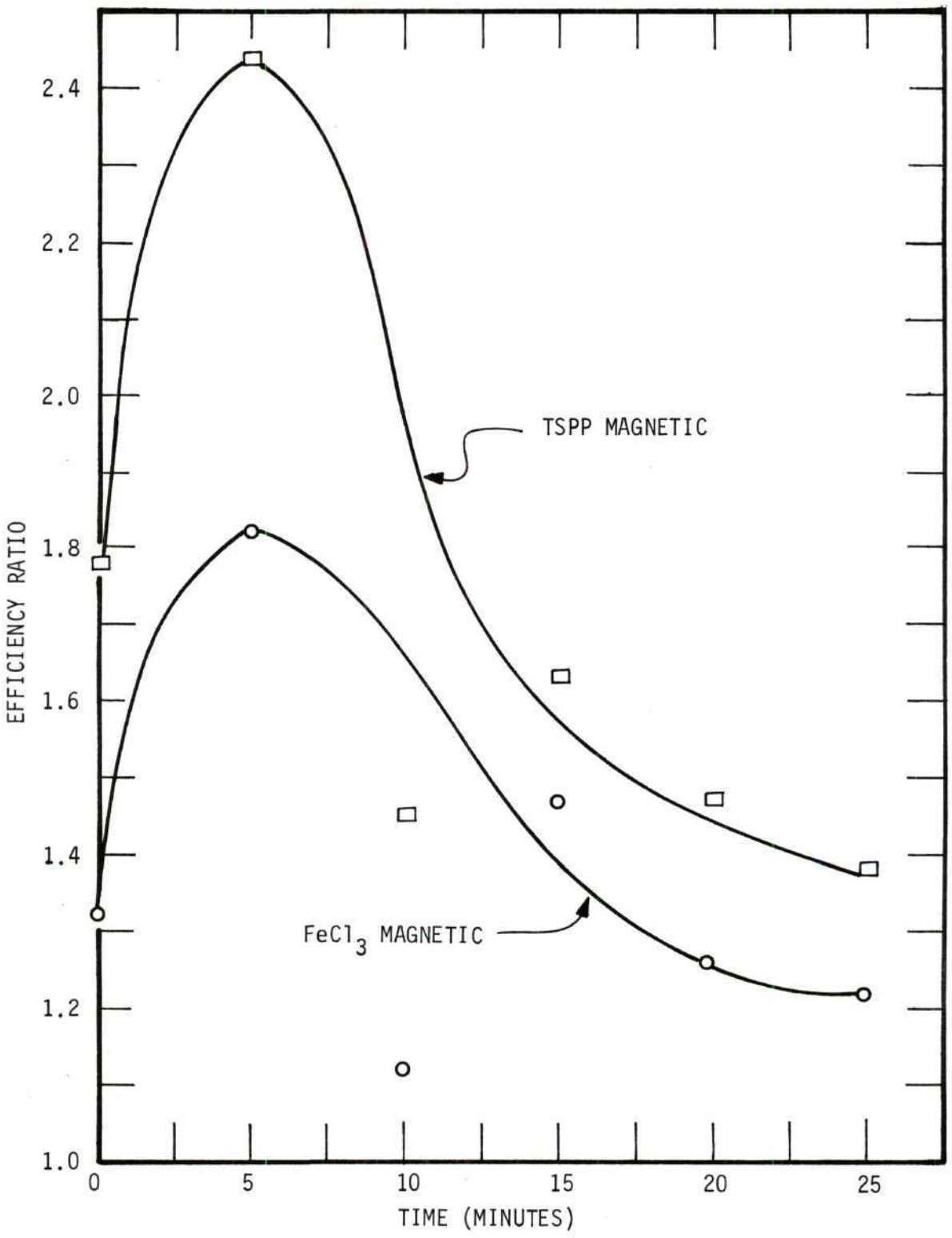

Figure 15. Efficiency Ratio Versus Time for Magnetic Portion of TSPP and $FeCl_3$ Separations.

to the per cent weight distribution for the magnetic fraction. This can be expressed as

$$\text{Efficiency Ratio} = \frac{\left[\dfrac{W_M/W_T \times \%\text{Mont}_M \times 100}{(W_M/W_T \times \%\text{Mont}_M) + (W_{NM}/W_T \times \%\text{Mont}_{NM})}\right]}{W_M/W_T \times 100} \qquad (11)$$

which will reduce to

$$\text{Efficiency Ratio} = \frac{W_T \times \%\text{Mont}_M}{(W_M \times \%\text{Mont}_M) + (W_{NM} \times \%\text{Mont}_{NM})} \qquad (12)$$

where W is the weight of a particular fraction, M represents magnetic fraction, NM represents nonmagnetic fraction, T represents the total or sum of the magnetic and nonmagnetic fractions, and Mont represents montmorillonite. If the ratio was equal to one, it would show that the montmorillonite was not being separated magnetically. An "efficiency ratio" greater than one for the magnetic portion would indicate that a separation was being made. For instance, an efficiency ratio of 2.00 would mean that if 10 per cent of the total weight was removed in the magnetic portion, then 20 per cent of the total montmorillonite had been removed in the magnetic portion. Fig. 15 shows that, for both separations, the efficiency ratio increases to a peak at five minutes, and then decreased for the next twenty minutes, and that the efficiency of the TSPP separation was greater than that of the $FeCl_3$ separation.

B. Correlation of Per Cent Montmorillonite, Magnetic Susceptibility, and Per Cent Iron for the TSPP Separations.

An excellent linear correlation is shown in Fig. 16 between magnetic susceptibility and per cent montmorillonite for the TSPP separations. The least squares line for the data was

$$\chi = [0.284\ (\%\ \text{Montmorillonite}) - 0.981] \times 10^{-6}\ \text{gm}^{-1} \qquad (13)$$

with a correlation coefficient of 0.90. A correlation coefficient of 0.90 with 16 variables means that the probability that the correlation was wrong was less than 5 out of 10,000. Equation 13, when extrapolated to 0 and 100 per cent montmorillonite, gives a value of $-0.98 \times 10^{-6}\ \text{gm}^{-1}$, for the magnetic susceptibility of the kaolinite in Pioneer Kaolin and a value of $27.42 \times 10^{-6}\ \text{gm}^{-1}$ for the montmorillonite. These values compare favorably with literature values, although the value for kaolinite is slightly low and that for montmorillonite is slightly higher than that given in the Review of Literature.

Although the correlation for magnetic susceptibility vs. per cent montmorillonite is excellent, there are several factors that must be examined before accepting the correlation. Three data points were omitted in the above correlation. They were the O-M, 15-M, and 10-NM samples. O-M and 15-M were omitted because the values for magnetic susceptibility for these two points at different field strengths were significantly different, and therefore, they were thought to contain ferromagnetic impurities. The point for 10-NM was omitted because its measured per cent montmorillonite was unreasonably high.

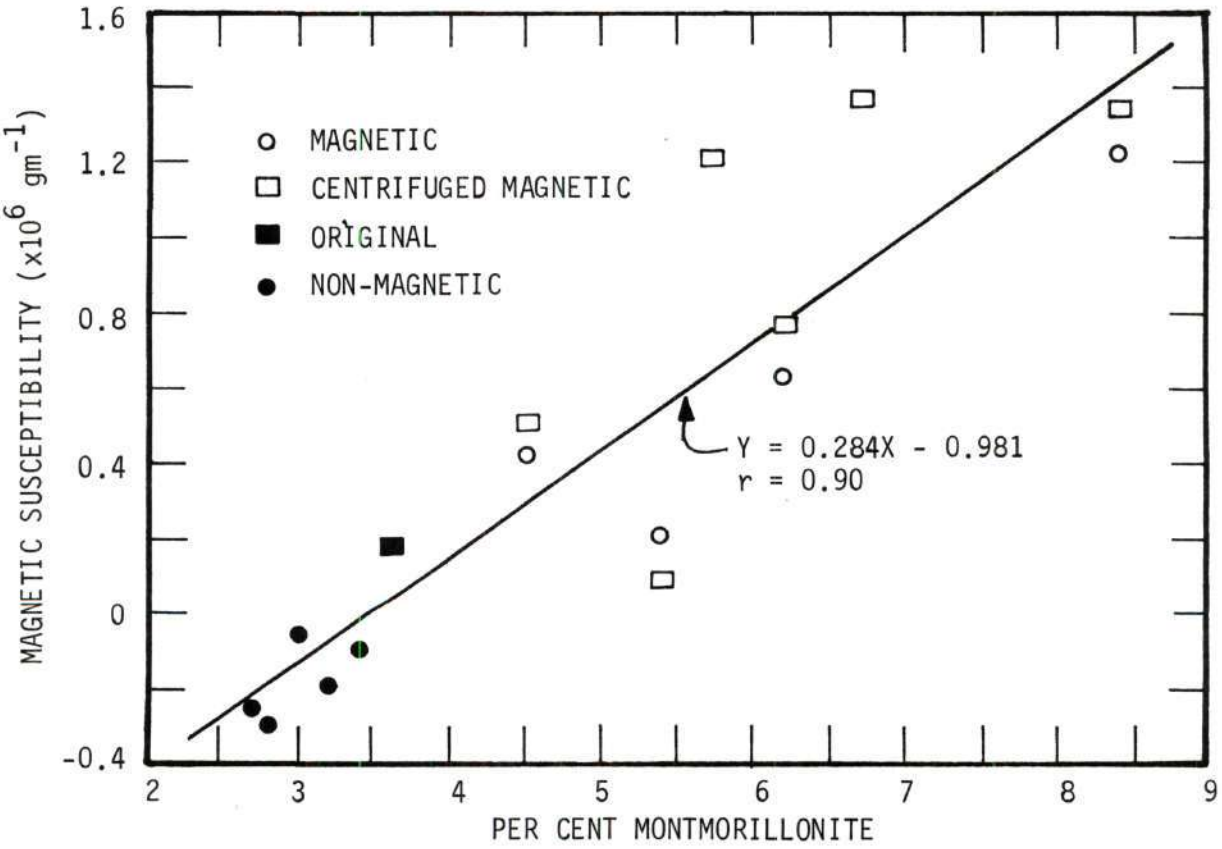

Figure 16. Correlation of Magnetic Susceptibility and Per Cent Montmorillonite for TSPP Separations.

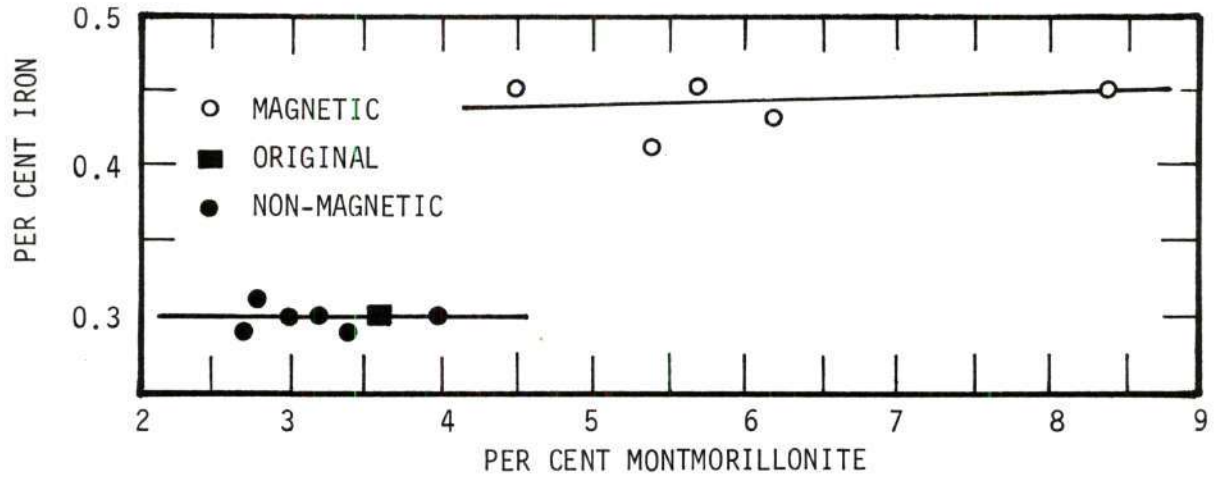

Figure 17. Correlation of Per Cent Iron and Per Cent Montmorillonite for TSPP Separations.

Because samples O-M and 15-M contained ferromagnetic impurities, all the samples from the magnetic portions were centrifuged in tetrabromoethane which has a density of 2.95 gm cm^{-3}. The magnetic susceptibilities of the samples were then remeasured. The centrifuging removed a very minor amount of black material from all the magnetic samples, with the most coming from O-M. The black material was thought to be some type of iron bearing mineral. The magnetic susceptibilities for all the samples, except O-M and 15-M were within experimental error of the measurements before centrifuging. The values found for O-M and 15-M were lowered significantly and were within experimental error at different field strengths. Therefore, all of the data for the centrifuged magnetic samples were included in the correlation between per cent montmorillonite and magnetic susceptibility. The centrifuged samples were too small to recheck for per cent iron and the data was not used in any correlation involving per cent iron.

The major uncertainty in the magnetic susceptibility-montmorillonite correlation is thought to be due to iron impurities in the magnetic portions of the separations. The iron impurities are shown, (see Fig. 17), by the fact that the original and nonmagnetic portions of the separations contain the same percentage of iron, whereas the magnetic portions contain higher percentages of iron. The iron impurity may have been introduced into the magnetic portions during the scrubbing procedure for removing the magnetic portions of the separations from the iron spheres in the magnetic separator. If no iron impurities had been introduced into the magnetic portions, then either the per cent iron in the nonmagnetic portion would be lower than the per cent iron in the original sample, or the

magnetic portions would contain the same amount of iron as the original and nonmagnetic portions. There is the possibility that a few iron bearing particles such as illemanite, etc. could be easily removed from the original sample and give the magnetic fraction a high iron content without appreciably affecting the iron content of the original and nonmagnetic fractions. As a consequence, there was no definite correlation between per cent iron and per cent montmorillonite as shown in Fig. 17. However, in general the greater amounts of iron were associated with the large percentages of montmorillonite. It appears from Fig. 18 that there was, also, no specific correlation between per cent iron and magnetic susceptibility. In general, the higher susceptibilities were associated with the higher percentages of iron. Although the data at this point was insufficient to establish a definite correlation between per cent iron and magnetic susceptibility, a correlation was established later in this thesis which shows that there is good reason to believe that a positive correlation did exist, and that iron in the montmorillonite was the controlling factor for the magnetic susceptibility of the kaolin clay. The Review of Literature shows that good correlations have been established between the magnetic susceptibility of other minerals and the per cent iron content. This would mean that if the greatest amounts of iron were associated with the montmorillonite then a correlation would exist as shown in Fig. 16. There are reasons to believe that such a correlation should exist, for the montmorillonite was certainly separated magnetically during the separations. The magnetic susceptibilities of many compounds are additive, therefore, it would be reasonable to expect a linear correlation between magnetic susceptibility of the kaolin clay and per cent montmorillonite.

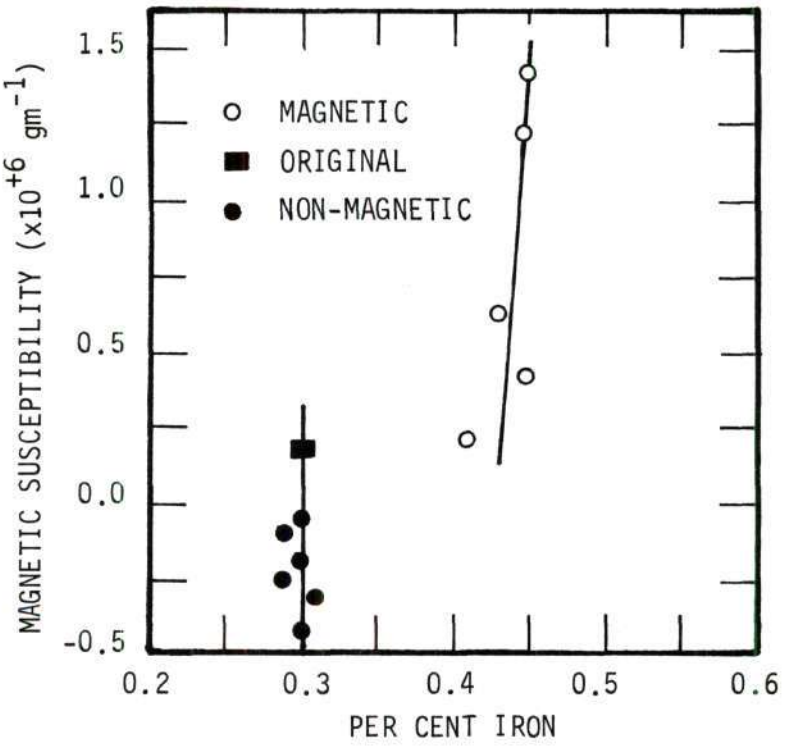

Figure 18. Correlation of Magnetic Susceptibility and Per Cent Iron for TSPP Separation.

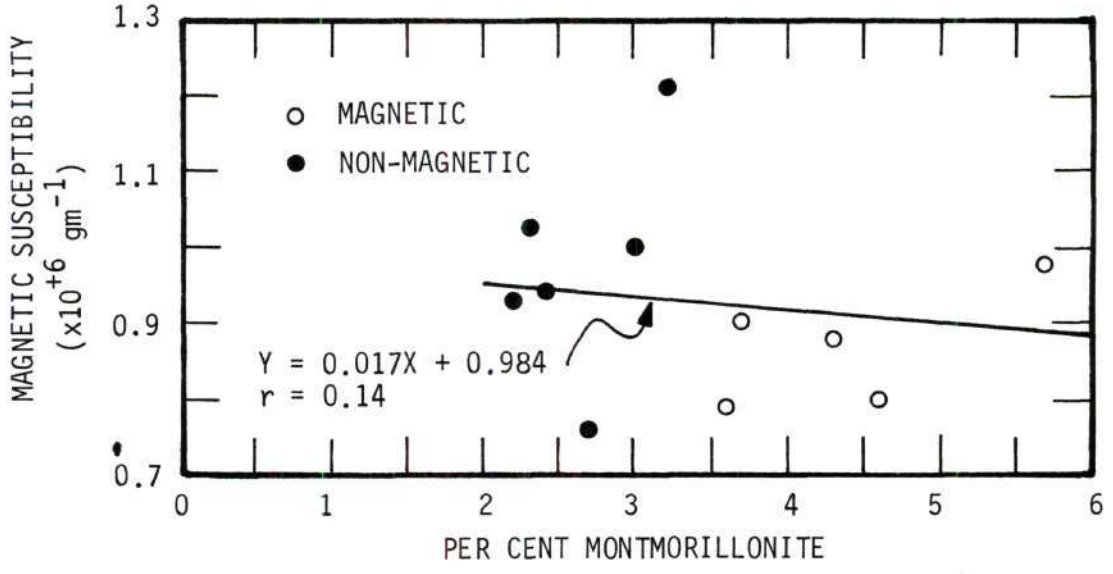

Figure 19. Correlation of Magnetic Susceptibility and Per Cent Montmorillonite for $FeCl_3$ Separation.

On the basis of the above arguments, it was thought that a correlation between magnetic susceptibilities and per cent montmorillonite similar to the one shown by Fig. 16 did exist, but due to iron impurities the true correlation was obscured and the slope of the line in Equation 13 was too large. There is no doubt that magnetic materials were removed during the separation, because all of the susceptibilities of the nonmagnetic portions were diamagnetic, while the original sample was paramagnetic. Whether this drop in susceptibility was due entirely to the removal of montmorillonite or to the removal of some other magnetic impurity is not known, but at least a portion of the drop in susceptibility must be due to the removal of montmorillonite. This also is indicated by the relative high magnetic susceptibility of samples where the high specific gravity minerals were removed by means of heavy liquids.

C. Correlation of Per Cent Montmorillonite, Magnetic Susceptibility, and Per Cent Iron in the $FeCl_3$ Separation

A doubtful correlation was established between magnetic susceptibility and per cent montmorillonite for the $FeCl_3$ separations. A plot of the data shown in Fig. 19. The least squares line for magnetic susceptibility, χ, vs. per cent montmorillonite was

$$\chi = [-0.017 \text{ (\% Montmorillonite)} + 0.984] \times 10^{-6} gm^{-1} \qquad (14)$$

with a correlation coefficient, r, of -0.14. This indicates that there was very little linear correlation, and a slight negative trend is shown.

Figs. 20 and 21 offer an explanation for the slight negative trend between per cent montmorillonite and magnetic susceptibility. A negative

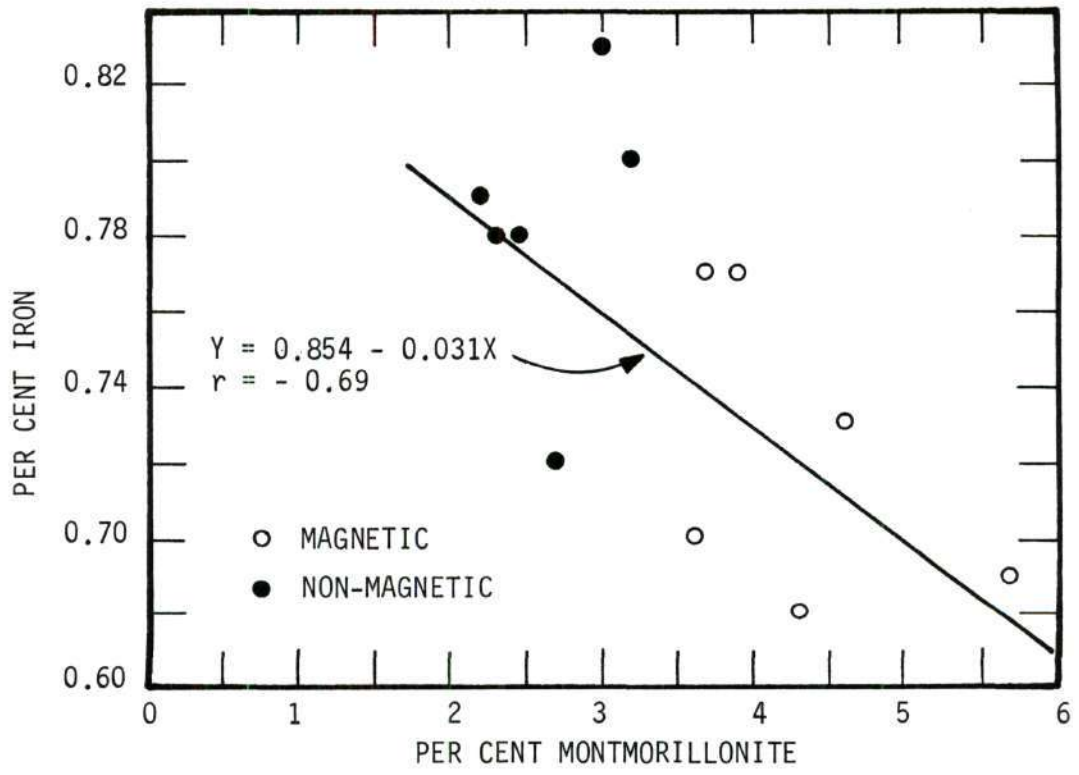

Figure 20. Correlation of Per Cent Iron and Per Cent Montmorillonite for $FeCl_3$ Separation.

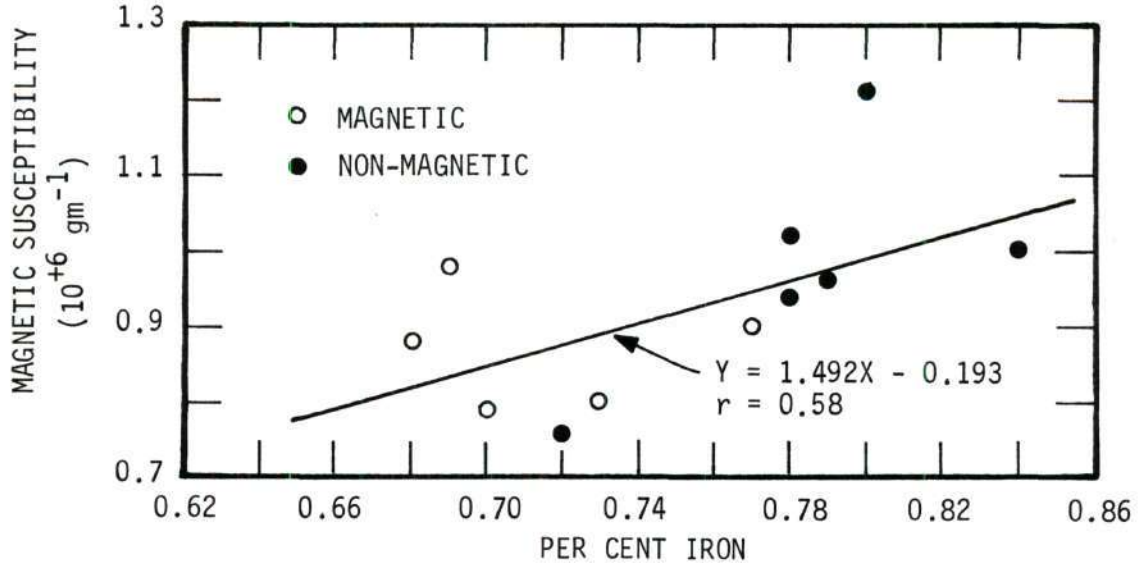

Figure 21. Correlation of Per Cent Iron and Magnetic Susceptibility for $FeCl_3$ Separation.

correlation was established between per cent iron and per cent montmorillonite. The least squares line for the data was

$$\% \text{ Fe} = -0.031 \ (\% \text{ Montmorillonite}) + 0.854 \qquad (15)$$

with a correlation coefficient r of -0.69. A correlation coefficient of 0.69 with 11 variables means that the probability that the correlation is wrong is less than 1 out of 100. The negative trend shown by Fig. 20 was thought to be due to particle size separation during separation rather than to an association of the iron with any particle mineral species. The larger montmorillonite and kaolinite particles would end up in the magnetic portions due to settling and magnetic attraction, while the finer particles would remain in suspension and would be drained off with the nonmagnetic portions of the separation. Because the per cent montmorillonite is at most 5.7 per cent in any one fraction, the particle size distribution will be controlled by the kaolinite, and due to settling the larger kaolinite particle size distribution will be in the magnetic fractions. Since the base exchange capacity of both minerals increases as the particle size decreases, a larger percentage of iron would be associated with the finer particles and the nonmagnetic fractions would contain the smaller particle size distribution. These circumstances lead to the negative trend shown in Fig. 20.

Fig. 21 shows that the magnetic susceptibility of the various portions of the $FeCl_3$ separations was dependent on the per cent iron they contained. The least squares line to the data was,

$$\chi = [1.492\ (\%\ Fe) - 0.193] \times 10^{-6}\ gm^{-1} \qquad (16)$$

with a correlation coefficient of 0.58, which in this case means that the probability that the correlation is wrong is less than 3 out of 100.

Because the magnetic susceptibility was dependent on the per cent iron in the sample, and because the per cent iron was higher in the samples containing the lower per cent montmorillonite due to the particle size separation, the slight negative trend was established between magnetic susceptibility and per cent montmorillonite for the $FeCl_3$ separations.

The data from the original sample was omitted from the correlation shown for the $FeCl_3$ separations because it was found to contain 0.23 per cent iron. This value was unreasonably lower than that of the other samples which ranged between 0.67 and 0.83 per cent iron. It was not thought that the magnetic and nonmagnetic portions were contaminated by iron in the magnet because enough $FeCl_3$ had been added to increase the per cent iron in the clay to 1.60 per cent. The per cent increase in the $FeCl_3$ separation samples over that of the TSPP original was between 0.37 and 0.53 per cent iron. This shows that between 7 and 10 meq of iron/100 grams clay was exchanged onto the clay. Filtering and washing out of the iron may be the reason for the low iron value of the $FeCl_3$ original sample.

D. Calgon Separation

It was determined from the TSPP and $FeCl_3$ separations that the optimum time for the magnetic separation of montmorillonite from kaolinite was five minutes under the conditions previously set forth. Therefore, in the calgon separation three separations were made on the nonmagnetic

portion using the optimum five minute separation time. The results found are summarized in Table 5.

Table 5. Results of Calgon Separation

Sample	Per Cent Weight Distribution	Per Cent Montmoril-lonite	Per Cent Iron	Magnetic Susceptibility (x 10^6 gm^{-1})
Original	---	2.9	0.25	-0.20
1st pass M	15.2	3.9	0.40	0.76
2nd pass M	9.1	3.2	0.35	0.59
3rd pass M	7.4	3.4	0.30	0.43
NM	68.2	2.9	0.25	-0.38

An analysis of the correlations between per cent montmorillonite, per cent iron, and magnetic susceptibility indicate the same trends shown by the TSPP separations. In general, the higher magnetic susceptibility values were associated with the higher percentages of montmorillonite, the higher percentages of iron were associated with the higher percentages of montmorillonite and the higher magnetic susceptibility values were associated with the higher percentages of iron. Once again as in the TSPP separation the per cent iron was the same in the original and nonmagnetic samples, while the magnetic samples contained higher percentages of iron. This indicates iron contamination of the magnetic samples from the separator or separation of small amounts of iron bearing minerals. But once

again the nonmagnetic sample showed a substantial decrease in magnetic susceptibility over that found in the original, indicating that some magnetic component has been removed. By the same reasoning given in the discussion for the TSPP separation, some of the decrease in susceptibility of the nonmagnetic sample and increase in the magnetic sample should be due to montmorillonite separation.

A comparison of the effectiveness of the calgon separations with the TSPP and $FeCl_3$ separations is given by the Calgon 1st-pass magnetic sample. The calgon sample contained 3.9 per cent montmorillonite as compared to 8.4 per cent for the TSPP sample and 5.7 per cent for the $FeCl_3$ sample at the same time interval. This indicates that the Calgon addition did not disperse the suspension as well as did the TSPP addition or either it did not reduce the attractive forces between the montmorillonite and kaolinite particles as effectively to allow free migration of the particles.

An analysis of the second and third passes show that they accomplished very little. The increase in per cent montmorillonite in the magnetic portions of the second and third passes was so small that the effect on the nonmagnetic portions was almost negligible.

E. Combined Correlation of Per Cent Montmorillonite, Magnetic Susceptibility, and Per Cent Iron for the TSPP, $FeCl_3$, and Calgon Separations

Data from the TSPP, $FeCl_3$ and Calgon separations were combined in an attempt to establish more positive correlations between magnetic susceptibility, per cent montmorillonite and per cent iron. There seemed to be no correlation at all between magnetic susceptibility and per cent montmorillonite or between per cent iron and per cent montmorillonite.

However, a calculation of the least square line for the magnetic susceptibility of all the samples vs. the per cent iron in them gave the equation

$$\chi = [2.166\ (\%\ Fe) - 0.592] \times 10^{-6} gm^{-1} \qquad (17)$$

with a correlation coefficient of 0.80. A further calculation of the square of the magnetic susceptibility vs. per cent iron gave an even better correlation coefficient of 0.94. This means that the probability is less than 5 in 10,000 that the correlation is wrong. The equation found for the correlation between the square of the magnetic susceptibility and the per cent iron was

$$\chi^2 = [1.992\ (\%\ Fe) - 0.598] \times 10^{-12} gm^{-2} \qquad (18)$$

This relationship is shown in Fig. 22. A relationship for the square of magnetic susceptibility with increasing iron content was also found for sphalerites as pointed out in the Review of Literature.

The above relationship would indicate that the magnetic susceptibility of the separation sample was dependent to a large extent on the per cent iron in them. If the iron was associated with the montmorillonite then there should be some correlation between per cent montmorillonite and magnetic susceptibility. This was believed to be the case for the correlation found between magnetic susceptibility and per cent montmorillonite in the TSPP separations. Extrapolating Equation 18 to zero per cent iron gives a value for the magnetic susceptibility of iron free Pioneer Kaolin of $-0.77 \times 10^{-6} gm^{-1}$. This compares favorably with the

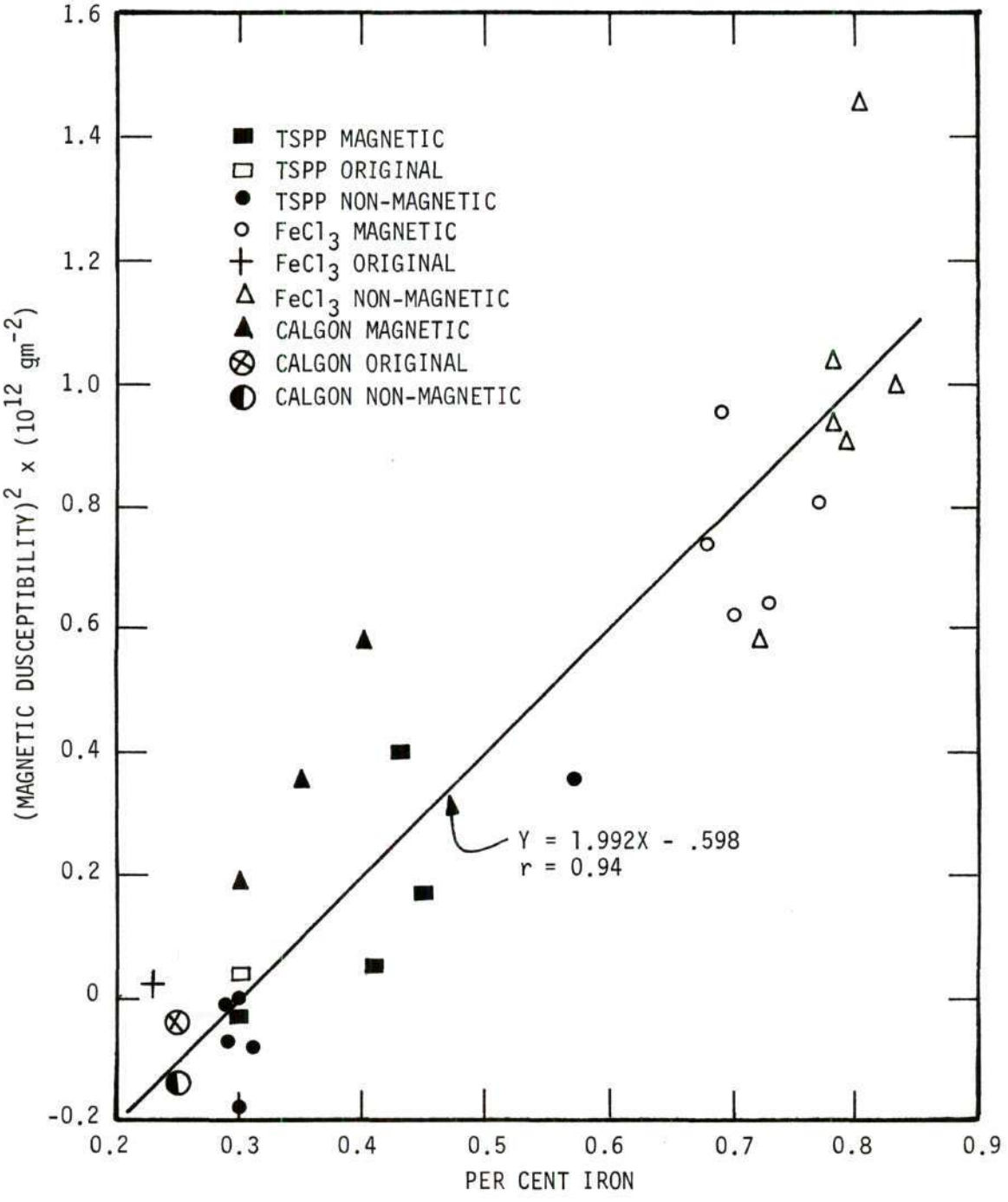

Figure 22. Correlation of Magnetic Susceptibility and Per Cent Iron for Combined Data from TSPP, $FeCl_3$ and Calgon Separations.

value of $-0.98 \times 10^{-6} gm^{-1}$ found using Equation 11 for montmorillonite free Pioneer Kaolin. This strongly indicates the majority of the iron in the TSPP separation was associated with the montmorillonite.

F. Discussion of Results of TSPP, $FeCl_3$, and Calgon Additions

1. TSPP. The purpose of adding TSPP to the clay suspension was to defloculate the clay so that the montmorillonite particles could migrate freely in the magnetic field with as little interaction with the kaolinite particles as possible, and also to keep the larger kaolinite particles in suspension to prevent them from settling on the low carbon steel spheres in the separation zone of the magnetic separator. However, the problem of settling was only partically prevented, because from Fig. 12 it is thought that two processes were occurring simultaneously. The first was montmorillonite particles being attracted magnetically, to the points of contact between the spheres, and the second was kaolinite, due to its large particle size (compared to that of montmorillonite), settling out of suspension onto the spheres. Due to the small particle size of montmorillonite it is highly improbable that the increased concentrations of montmorillonite in the magnetic portion of the separations were due to montmorillinite settling, because in the absence of a magnetic field the montmorillinite would remain in suspension and would be concentrated in the fine fraction. (Settling clay suspensions is a method commonly used to concentrate montmorillonite in the fine fractions.) Therefore, settling would produce an effect opposite to that found. In other words, it would concentrate the montmorillonite in the nonmagnetic portions rather than the magnetic portions. To demonstrate this, a separation was made without the magnetic field. Everything was identical to the five-minute TSPP

separation except the magnetic field was not turned on. It was found that the per cent montmorillonite was 3.2 for the original fraction, 1.6 for the magnetic fraction, and 3.6 for the nonmagnetic fraction, which shows that the montmorillonite was concentrated in the nonmagnetic fraction instead of the magnetic fraction in the absence of a magnetic field.

During the first five minutes when the per cent montmorillonite was increasing in the magnetic portion (refer to Fig. 12), the large montmorillonite particles were being separated magnetically at a faster rate than the kaolinite was settling, but once the larger montmorillonite particles were removed, the rate of settling of the kaolinite became greater than the magnetic separation of the montmorillonite. Therefore, the per cent montmorillonite in the magnetic portion decreased after the initial five minutes of separation.

From theoretical calculations made in Appendix F it is thought that only the larger montmorillonite particles were acted on magnetically due to the short time allowed for separation before settling became the dominant factor. Unfortunately, it was impossible to make an accurate comparison of the effect of time on the separation with the theoretical calculations made in Appendix F because of the two above processes occurring simultaneously.

It can be seen from Fig. 13 that after ten minutes the weight per cent distribution became constant or increased only slightly in the TSPP magnetic portions. This indicates that the large kaolinite particles had settled and the magnetic particles had been attracted to the steel spheres causing the system to reach an equilibrium condition. This can also be seen in Fig. 14 where after ten minutes the montmorillonite distribution

levels off in the TSPP magnetic portion.

2. $FeCl_3$. Fe^{+++} ions in the form of $FeCl_3$ were added to the electrodialized suspensions of Pioneer Kaolin to take advantage of the larger difference in base exchange capacity between montmorillonite and kaolinite to increase the magnetic susceptibility of montmorillonite to a greater extent than that of kaolinite. The ferric chloride was added to an electrodialized sample of the clay because it was thought that electrodializing the clay would free exchange sites to allow more adsorption of the Fe^{+++} ions than if the clay had not been electrodialized. The $FeCl_3$ was added before the suspension was defloculated with calgon to prevent the calgon from blocking any exchange positions. Enough Fe^{+++} ions had to be added to satisfy the exchange capacity of the kaolinite because its completed exchange reaction is faster than the completed exchange reaction of montmorillonite. Therefore, 30 meq of $FeCl_3$ per 100 grams of Pioneer Kaolin was added to satisfy both the exchange capacity of montmorillonite and kaolinite. This was obviously too much since, as was pointed out earlier, a maximum of 10 meq per 100 grams of clay was adsorbed. This means that 20 meq remained in solution.

It is apparent from Fig. 15 that $FeCl_3$ separation was much less efficient than the TSPP separation. There are thought to be three possible explanations for this. The first is that adsorption of the iron by the kaolinite caused it to become paramagnetic, whereas before it had been diamagnetic. This would cause the kaolinite to be magnetically attracted along with the montmorillonite to the points of highest flux density, whereas in the TSPP separation the kaolinite had not been attracted magnetically. The second explanation is the excess Fe^{+++} ion in solution

caused particle aggregation since Fe^{+++} ions act as a good floculent. Particle aggregation would cause a higher settling rate for the kaolinite and montmorillonite which would retard the efficiency of the separation. The third possible reason for a less efficient separation is that calgon did not disperse the suspension as well as did TSPP. This would also cause more particle aggregation and higher settling rate. In all probability, the reduced efficient was caused by a combination of the above factors. These explanations are substantiated by Fig. 13 where after five minutes the weight distribution of the $FeCl_3$ magnetic portions increase linear with time whereas the TSPP magnetic portions become almost constant. The only possible explanation is that the kaolinite as well as the montmorillonite is being attracted magnetically and/or the rate of settling is greater.

Perhaps of major importance is the fact that although the efficiency of the $FeCl_3$ separation was less than that of the TSPP separation, due to the larger weight distribution of the $FeCl_3$ magnetic portions, the per cent montmorillonite in the nonmagnetic portion of the $FeCl_3$ separation was approximately 0.5 per cent less than that in the TSPP separation. But this was accomplished at the expense of removing almost twice as much clay in the magnetic portions.

3. Calgon. As stated earlier the calgon separation was much poorer than either the $FeCl_3$ or TSPP separations. Thus defloculating the $FeCl_3$ separation with calgon rather than TSPP could have been the major cause for a decrease in separation efficiency from the TSPP separation to the $FeCl_3$ separation. However, the possibilities mentioned above for the drop in efficiency between the TSPP and $FeCl_3$ separations must still be

considered for it is impossible with the data obtained to make a proper evaluation.

3. Metal Acetylacetonate Separations

Paramagnetic metal acetylacetonates were added to the clay suspensions with the hope that the acetylacetonates would be absorbed by the montmorillonite, as other organic compounds are. This would cause a preferred adsorption of the magnetic material by the montmorillonite without affecting the magnetic properties of the kaolinite since kaolinite does not adsorb organic compounds. The purpose of dissolving the metalic-organic compounds in ethanol before adding the complex to the suspensions was two fold. First, metal acetylacetonates are insoluble in water and therefore they had to be dissolved in a liquid that was missible with water. (The metal acetylacetonates solutions were added to distilled water and to water containing NaOH to see if any precipitation occurred. No precipitation was visible and the mixtures appeared completely missible.) Second, it is known that in coordinating solvents, such as ethanol, the metal acetylacetonates exist as polymers and it was hoped that the ethanol would "prop open" the montmorillonite lattice to allow the large paramagnetic metal acetylacetonate polymers to enter. Montmorillonite absorbs polar molecules but unfortunately no information could be found on the polarity of metal acetylacetonate molecules in solution.

The metal acetylacetonates were added in quantities approximately equal to the base exchange capacity of montmorillonite since it is known that montmorillonite adsorbs many metalic-organic compounds in quantities equal to its base exchange capacity for inorganic ions. The pH of the M(X)A suspensions was adjusted to pH 7.4 to prevent the M(X)A compounds

from breaking down.

A. Selection of M(X)A Compounds

The magnetic susceptibilities of the twelve M(X)A compounds were measured as received. The values are given in Table 6. The values in Table 6 are the average of two values taken at two different field strengths.

Six of the metal acetylacetonates were found to be paramagnetic and because the magnetic susceptibility measurements were found to be constant with field strength it was determined that the samples contained no ferromagnetic impurities.

Table 6. Magnetic Susceptibility of M(X)A Compounds

Compounds	χ 25°C ($gm^{-1} \times 10^{6}$)
Na(I)A	-0.63
K(I)A	-0.91
$Co(II)A_2$	37.63
$Cu(II)A_2$	4.11
$Mn(II)A_2$	53.91
$Ni(II)A_2$	14.98
$Zn(II)A_2$	-0.93
$Al(III)A_3$	-1.03
$Co(III)A_3$	-0.69
$Cr(III)A_3$	16.78
$Fe(III)A_3$	40.76
$Zr(IV)A_4$	-1.03

The six paramagnetic compounds, $Co(II)A_2$, $Cu(II)A_2$, $Mn(II)A_2$, $Ni(II)A_2$, $Cr(III)A_3$, and $Fe(III)A_3$ were selected for additions to the clay suspensions. $Co(III)A_3$ was also selected as an addition since Co(III) is paramagnetic in other valence states.

B. Results of M(X)A Separations

Table 7 presents a summary of the data from the M(X)A separations. A comparison can be made between the five-minute magnetic fraction of the TSPP and $FeCl_3$ separations and the first pass magnetic fractions of the M(X)A separations. It is evident that in all cases the per cent montmorillonite in the first pass magnetic fraction of the M(X)A separations is less than that in either the $FeCl_3$ or TSPP separations.

The additions of the metal acetylacetonates had no positive effect on the magnetic separations because the per cent montmorillonite in the EtOH reference separation was as high in the magnetic fraction as either the $Co(II)A_2$ separation or the $Mn(II)A_2$ separation and higher than the rest. A good indication of the relative importance of the separation was the efficiency ratio. The efficiency ratio for the M(X)A separation was calculated by a summation of the data from the three magnetic fractions. A comparison of the efficiency ratio for the various M(X)A separations shows again that the EtOH standard separation was as good as any of the separations to which metal acetylacetonates were added.

The efficiency ratio also indicates a large difference in the separations between the II valence and III valence acetylacetonates. The II valence M(X)A separations had an efficiency ratio close to that of the EtOH separation, but the III valence M(X)A separations had an efficiency ratio that was close to 1.00 which means that there was no separation for

Table 7. Summary of Data From M(X)A Separations

Sample	Per Cent Montmorillonite	Magnetic Susceptibility (x $10^6 gm^{-1}$)	Weight Per Cent Of Original	Efficiency Ratio for Total Magnetics
EtOH-0	3.2	0.23	-	
EtOH-NM	2.0	-0.22	63.7	
EtOH-1M	4.2	8.6*	14.0	1.43
EtOH-2M	3.8	4.71*	12.9	
EtOH-3M	3.0	3.38*	9.3	
$Co(II)A_2$-0	3.0	0.09	-	
$Co(II)A_2$-NM	1.9	0.06	67.2	
$Co(II)A_2$-1M	4.3	1.99	14.5	1.48
$Co(II)A_2$-2M	3.3	1.78	10.2	
$Co(II)A_2$-3M	3.1	1.92	9.3	
$Cu(II)A_2$-0	2.6	-0.04	-	
$Cu(II)A_2$-NM	2.6	-0.14	66.6	
$Cu(II)A_2$-1M	3.8	1.35	13.6	1.23
$Cu(II)A_2$-2M	3.6	1.32	11.7	
$Cu(II)A_2$-3M	3.3	1.70	8.1	
$Mn(II)A_2$-0	2.9	0.14	-	
$Mn(II)A_2$-NM	2.5	0.09	64.3	
$Mn(II)A_2$-1M	3.8	1.50	16.0	1.20
$Mn(II)A_2$-2M	3.2	0.78	11.3	
$Mn(II)A_2$-3M	2.8	0.86	8.3	

Table 7. Summary of Data From M(X)A Separations (Continued)

Sample	Per Cent Montmorillonite	Magnetic Susceptibility ($\times 10^6$ gm^{-1})	Weight Per Cent Of Original	Efficiency Ratio for Total Magnetics
$Ni(II)A_2$-O	3.3	0.00	-	
$Ni(II)A_2$-NM	2.4	-0.08	64.4	
$Ni(II)A_2$-1M	4.3	0.86	15.5	1.34
$Ni(II)A_2$-2M	4.2	1.03	11.8	
$Ni(II)A_2$-3M	2.8	1.27	8.2	
$Co(III)A_3$-O	3.2	-0.05	-	
$Co(III)A_3$-NM	2.5	0.10	72.8	
$Co(III)A_3$-1M	2.9	0.93	12.4	1.14
$Co(III)A_3$-2M	3.2	1.04	8.3	
$Co(III)A_3$-3M	2.9	4.72*	6.5	
$Cr(III)A_3$-O	3.1	0.02	-	
$Cr(III)A_3$-NM	2.7	-0.19	70.9	
$Cr(III)A_3$-1M	3.1	1.53	12.4	0.99
$Cr(III)A_3$-2M	2.8	1.45	9.3	
$Cr(III)A_3$-3M	1.7	1.22	7.4	
$Fe(III)A_3$-O	3.0	0.09	-	
$Fe(III)A_3$-NM	2.7	-0.08	67.6	
$Fe(III)A_3$-1M	2.9	0.88	13.5	1.06
$Fe(III)A_3$-2M	2.8	1.08	10.6	
$Fe(III)A_3$-3M	3.2	0.81	8.3	

*These samples contained ferromagnetic impurities.

the III valence compound but just random settling.

From this the only conclusion that can be drawn are that, the II valence acetylacetonate compounds had very little if any effect on the magnetic separation and the III valence compounds were detrimental, when compared to the EtOH reference, to the point that no separation was made.

It is thought that possibly the III valence compounds were less stable then the II valence compounds, and that they broke down in the suspension freeing the III valence metal ions. This may have caused particle-particle interaction in the III valence separations, thereby preventing separation. However, the most probable answer is, that, due to polymerization of the acetylacetonates in the ethanol, the metalic-organic compounds were just too large to expand the montmorillonite lattice.

There was no indication from the 001 montmorillonite d spacings upon X-ray analysis that any of the metal acetylacetonates had expanded the lattice. Apparently, either the compounds were too large to be adsorbed or they were not polar enough.

No correlation was found between the per cent montmorillonite and the magnetic susceptibilities of the various fractions. However, as in other separations, the greater susceptibilities were found in the magnetic portions and the nonmagnetic had susceptibilities below that of the original sample. This shows that some magnetic material was being removed but it was not known if the difference in susceptibility was due only to the montmorillonite.

CHAPTER VI

CONCLUSIONS AND RECOMMENDATIONS

Conclusions

1. In magnetically separating weakly magnetic materials in the micron and submicron particle size range, time must be made a controlling factor to achieve the most efficient separation.

2. The most efficient magnetic separation of montmorillonite from kaolinite was achieved by defloculating with TSPP.

3. A correlation between magnetic susceptibility and per cent montmorillonite was determined for the kaolinite-montmorillonite system found in Pioneer Kaolin when defloculated with TSPP. The least squares line for the correlation was

$$\chi = (0.284\ \%\ \text{Montmorillonite} - 0.981) \times 10^{-6}\ \text{gm}^{-1}. \qquad (19)$$

From equation 19, the magnetic susceptibility of the kaolinite in Pioneer Kaolin was found to be $-0.98 \times 10^{-6}\ \text{gm}^{-1}$, and that for the montmorillonite was found to be $27.42 \times 10^{-6}\ \text{gm}^{-1}$.

4. A correlation between magnetic susceptibility and per cent iron was found for Pioneer Kaolin in the TSPP, $FeCl_3$ and Calgon Separations. The least squares line for the correlation was

$$\chi^2 = (1.992\ \%\ \text{Fe} - 0.598) \times 10^{-12}\ \text{gm}^{-2}. \qquad (20)$$

The magnetic susceptibility of iron free Pioneer Kaolin, from equation 20, was $-0.77 \times 10^{-6} gm^{-1}$.

5. Addition of $FeCl_3$ to a Pioneer Kaolin suspension produced a magnetic separation of montmorillonite from kaolinite that was less efficient than that produced with additions of TSPP.

6. Defloculation of Pioneer Kaolin with Calgon produced a separation that was less efficient than either the TSPP or $FeCl_3$ separation.

7. The optimum separation of montmorillonite from kaolinite in the TSPP and $FeCl_3$ separation occurred when the clay suspensions had been held stationary in the magnetic separator for a period of five minutes.

8. Additions of divalent, paramagnetic metal acetylacetonates in ethanol, (copper, cobalt, manganese, and nickle), to Pioneer Kaolin water suspensions had little if any effect on the magnetic separation of montmorillonite from kaolinite.

9. Addition of trivalent, paramagnetic metal acetylacetonates in ethanol, (cobalt, chromium, and iron), to Pioneer Kaolin water suspensions were detrimental, when compared with ethanol only, to the magnetic separation of montmorillonite from kaolinite to the extent that no detectable separation was made.

Recommendations

Although the results of the separations involving the metalic-organic additions were disappointing, it is felt that a paramagnetic, metalic-organic compound can be found that will be stable and will expand the montmorillonite lattice. Once this is accomplished a more efficient magnetic separation of montmorillonite from kaolinite will be possible.

It is recommended that, if ways are not found to increase the magnetic susceptibility of weakly magnetic material by either chemical or physical treatment, either (1) higher magnetic fields and/or field gradients will have to be produced, (2) magnetic separators will have to be designed so that flow through the separation may be controlled or completely stopped, or (3) the distance that particles have to travel in order to be separated will have to be minimized.

APPENDIX A

DETERMINATION OF THE FIELD STRENGTH OF A CARPCO LABORATORY MAGNETIC SEPARATOR

The magnetic field strength of a Carpco laboratory magnetic separator was measured using a Bell "240" gaussmeter. The gaussmeter was calibrated using 1,000 gauss and zero gauss standards.

The magnet was equipped with spheres of low carbon steel, 0.75, 0.50, and 0.25 inches in diameter. In order to insert the gaussmeter probe between the spheres, two spheres of equal diameter were spaced 0.025 inches apart and two strips of T-316 stainless steel were silver soldered on opposite sides of the spheres to maintain the 0.025 inch gap while the balls were in the magnetic field. This procedure was performed on all three sphere sizes.

Spheres were then placed in the separation zone and one of the spaced pair was placed so that it was surrounded by other spheres, all of equal size. The spaced spheres were positioned perpendicular to the magnet pole faces and a small opening was left above the gap so the gaussmeter probe could be inserted. The maximum field strength between the spaced spheres was measured at various current settings from 1.0 to 5.2 amperes.

The values of field strength vs. current were recorded in Table 8 for the three different sphere sizes.

Table 8. Magnetic Field Strength for Carpco Laboratory Magnetic Separator*

Amperes	Field Strength 0.75 in. balls (Kilogauss)	Field Strength 0.50 in. balls (Kilogauss)	Field Strength 0.25 in. balls (Kilogauss)
5.2	33.8	29.2	21.2
5.0	33.5	29.0	21.1
4.5	33.2	28.6	20.7
4.0	32.9	28.0	20.3
3.5	32.5	27.5	19.8
3.0	31.9	26.7	18.8
2.5	30.6	25.3	17.4
2.0	28.9	23.1	15.2
1.5	26.5	20.1	12.5
1.0	22.0	15.3	9.2

*Measurements were made using a 0.025 inch gap.

APPENDIX B

DATA ON AIR FLOATED PIONEER KAOLIN

The data present in Tables 9 and 10 are typical values for Pioneer Kaolin reported by the Georgia Kaolin Company, Dry Branch, Georgia. Table 9 is a chemical analysis and Table 10 is a particle size analysis for the Pioneer Kaolin.

Table 9. Chemical Analysis of Pioneer Kaolin

Oxide	Per Cent
SiO_2	45.68
Al_2O_3	38.51
Fe_2O_3	0.44
TiO_2	1.43
CaO	0.24
MgO	0.14
Na_2O	0.04
K_2O	0.14
H_2O	13.51

Table 10. Particle Size Distribution of Pioneer Kaolin

Particle Size (microns)	Cumulative Weight Per Cent Under
10	86
5	73
2	54
1	38
0.5	22
0.2	6

A particle size analysis was made on the Pioneer Kaolin used for the experiments in this thesis using the centrifuge-pipette method. The results agreed within two per cent of the values reported by Georgia Kaolin Company for particle size distribution. A mineralogical analysis showed there to be 3.1 + 0.25 per cent montmorillonite in the Pioneer Kaolin.

APPENDIX C

CALIBRATION OF HdH/dX FOR MAGNETIC SUSCEPTIBILITY MEASUREMENTS

Mohr's Salt, which has a magnetic susceptibility of $9500/(T + 1) \times 10^{-6} gm^{-1}$, was used for measuring HdH/X. The susceptibility of all samples was measured at 25°C. Therefore, χ for Mohr's Salt at 25°C is $31.77 \times 10^{-6} gm^{-1}$. Substituting into Equation 2 for χ gives,

$$F_g \, 980 = m. \, 31.77 \times 10^{-6} \, HdH/dX. \tag{21}$$

The equation that was used for calculating HdH/dX was

$$HdH/dX = \frac{F_g}{m} \, (30.85 \times 10^6), \tag{22}$$

where F_g was the force on Mohr's Salt in milligrams and m was the mass of Mohr's Salt in milligrams.

HdH/dX was measured at 1.50 amperes and 2.00 amperes. During the magnetic susceptibility measurements, the glass fiber from which the sample bucket was suspended was broken twice. Therefore, three separate determinations of HdH/dX were required. HdH/dX was measured periodically during the susceptibility measurements of the separation samples to check for instrument variation and sample placement variation.

The HdH/dX measurements are shown in Tables 11, 12, and 13. Table 11 shows that HdH/dX for the TSPP separation measurements was 2.323 x 10^6 gm cm sec^{-2} at 1.50 amps. with a standard deviation 3.5 per cent and 4.173 x 10^6gm cm sec^{-2} at 2.00 amps. with a standard deviation of 4.3 per cent. For the $FeCl_3$ separations, Calgon separations, original and nonmagnetic fractions of M(X)A separations, and the metal acetylacetonates, HdH/dX was, as shown in Table 12, 2.218 x 10^6gm cm sec^{-2} at 1.50 amps. with a standard deviation of 1.4 per cent and 3.941 x 10^6gm cm sec^{-2} at 2.0 amps. with a standard deviation of 1.4 per cent. The magnetic susceptibility measurements for the magnetic fractions of the M(X)A separations were made, as shown in Table 13, with a HdH/dX of 2.258 gm cm sec^{-2} at 1.50 amps. with a standard deviation of 1.4 per cent and 4.032 x 10^6gm cm sec^{-2} at 2.0 amps. with a standard deviation of 2.0 per cent. The equations given at the bottom of Tables 11, 12, and 13 were used to calculate magnetic magnetic susceptibility, where they applied.

Table 11. Calibration of HdH/dX for Determination of Magnetic Susceptibility of TSPP Separation Fractions

Sample	Weight of Sample (mg)	1.50 Amperes: Force on Bucket (mg)	Force on Bucket +Sample (mg)	Force on Sample (mg)	HdH/dX gm cm sec^{-2} x 10^6	2.00 Amperes: Force on Bucket (mg)	Force on Bucket +Sample (mg)	Force on Sample (mg)	HdH/dX gm cm sec^{-2} x 10^6
Mohr's Salt	23.800	-0.083	1.785	1.868	2.421	-0.158	3.310	3.468	4.494
Mohr's Salt	23.680	-0.083	1.710	1.793	2.335	-0.158	3.025	3.183	4.145
Mohr's Salt	23.015	-0.080	1.665	1.745	2.339	-0.154	2.025	3.079	4.126
Mohr's Salt	20.725	-0.080	1.395	1.475	2.195	-0.154	2.485	2.639	3.927
		Average			2.323	Average			4.173
		Standard Deviation			0.081	Standard Deviation			0.178
		%Standard Deviation			3.5%	%Standard Deviation			4.3%

$$\chi_{1.5} = \frac{F_g}{m} \; 419.34 \times 10^{-6} gm^{-1}$$

$$\chi_{2.0} = \frac{F_g}{m} \; 236.94 \times 10^{-6} gm^{-1}$$

Table 12. Calibration of HdH/dX for Determination of Magnetic Susceptibility of $FeCl_3$ Separation Fractions, Calgon Separation Fractions, Original and Nonmagnetic Fractions of M(X)A Separations, and the Metal Acetylacetonates

Sample	Weight of Sample (mg)	1.50 Amperes				2.00 Amperes			
		Force on Bucket (mg)	Force on Bucket +Sample (mg)	Force on Sample (mg)	HdH/dX gm cm sec^{-2} x 10^6	Force on Bucket (mg)	Force on Bucket +Sample (mg)	Force on Sample (mg)	HdH/dX gm cm sec^{-2} x 10^6
Mohr's Salt	25.590	-0.060	1.800	1.860	2.24	-0.120	3.200	3.320	4.00
Mohr's Salt	26.975	-0.060	1.900	1.960	2.24	-0.120	3.325	3.445	3.94
Mohr's Salt	15.625	-0.064	1.050	1.114	2.20	-0.130	1.900	2.030	4.01
Mohr's Salt	20.245	-0.068	1.375	1.443	2.20	-0.132	2.425	2.557	3.90
Mohr's Salt	18.385	-0.072	1.277	1.349	2.26	-0.141	2.229	2.370	3.98
Mohr's Salt	28.245	-0.056	1.980	2.036	2.22	-0.120	3.490	3.610	3.94
Mohr's Salt	26.050	-0.070	1.746	1.816	2.15	-0.143	3.085	3.228	3.82
Mohr's Salt	27.350	-0.071	1.905	1.976	2.23	-0.137	3.360	3.497	3.94
		Average			2.218	Average			3.941
		Standard Deviation			0.031	Standard Deviation			0.057
		%Standard Deviation			1.4%	%Standard Deviation			1.4%

$$\chi_{1.5} = \frac{F_g}{m} \; 441.84 \times 10^{-6} gm^{-1} \qquad \chi_{2.0} = \frac{F_g}{m} \; 248.67 \times 10^{-6} gm^{-1}$$

Table 13. Calibration of HdH/dX for Determination of Magnetic Susceptibility of Magnetic Fraction of M(X)A Separations

Sample	Weight of Sample (mg)	1.50 Amperes: Force on Bucket +Sample (mg)	Force on Bucket (mg)	Force on Sample (mg)	HdH/dX gm cm sec^{-2} x 10^6	2.00 Amperes: Force on Bucket (mg)	Force on Bucket +Sample (mg)	Force on Sample (mg)	HdH/dX gm cm sec^{-2} x 10^6
Mohr's Salt	26.735	-0.081	1.914	1.995	2.302	-0.147	3.310	3.457	3.989
Mohr's Salt	27.695	-0.081	1.935	2.016	2.246	-0.155	3.440	3.695	4.116
Mohr's Salt	23.915	-0.081	1.674	1.755	2.264	-0.154	3.000	3.154	4.068
Mohr's Salt	20.525	-0.084	2.040	2.124	2.219	-0.158	3.625	3.783	3.953
		Average			2.258	Average			4.032
		Standard Deviation			0.030	Standard Deviation			0.080
		%Standard Deviation			1.3%	%Standard Deviation			2.0%

$$\chi_{1.5} = \frac{F_g}{m} \; 434.01 \times 10^{-6} gm^{-1} \qquad \chi_{2.0} = \frac{F_g}{m} \; 243.06 \times 10^{-6} gm^{-1}$$

APPENDIX D

STANDARDS FOR DETERMINING PER CENT MONTMORILLONITE IN KAOLINITE

Two clays from Freeport Kaolin Company of Georgia, were selected to be used for preparing standards. The two clays were Freeport #27 and Freeport #6 Tile clay.

X-ray analysis of Freeport #27 clay showed nothing detectable by X-ray diffraction other than kaolinite. Freeport #6 Tile clay was reported to contain 28 per cent montmorillonite. A very minor amount of mica was detected by X-ray analysis, but other than the mica only montmorillonite and kaolinite was shown to be present.

The two clays were dried for 24 hours at 140°C. 25 grams samples were then prepared by mixing the two above clays so that the final samples contained 0, 1, 2, 3, 4, 5, 7, 10, 15, 25 and 28 per cent montmorillonite.

The 25 gram samples were blunged on a drill press blunger at 2050 RPM for five hours with 500 ml. of distilled water containing 0.25 grams of Calgon. 1.5 ml. of each standard suspension was deposited on a 25 mm x 37 mm glass slide and air dried. After air drying the samples were put in a desicator for 24 hours.

Immediately upon removing the samples from the desicator, an X-ray diffractometer trace was run on the samples from 2°2θ to 15°2θ. The only peaks that were recorded were the 001 peaks of montmorillonite and kaolinite. The montmorillonite lattice was then expanded by placing the

standard in an ethylene glycol vapor both for one hour at 60°C. This was sufficient to expand the 001 plane of montmorillonite to 17.0Å.

The areas of the 001 montmorillonite and kaolinite peaks were measured with a plainmeter and recorded in Table 15. The ratio of the montmorillonite peak area to kaolinite peak area was calculated and recorded in Table 15 for both the untreated and glycolated standards. From these ratios, two standard curves, untreated and glycolated standards, were drawn from 0 to 28 per cent montmorillonite.

The X-ray settings and instrumentation are recorded in Table 14 below.

Table 14. X-ray Diffractometer Settings for Montmorillonite-Kaolinite Standards and Separation Samples

Killivolts	25
Milliamperes	10
Time Constant	2
Scale Factor	2×10^3
PHA	95%
Chart Speed	0.5 inch/min.
Scan Speed	1°2θ/min.
Radiation	Copper Kα
Filter	Nickel

Table 15. Peak Areas and Ratios for Kaolinite-Montmorillonite Standards

A. Untreated Montmorillonite.

Per Cent M*	Area M (in^2)	Area K** (in^2)	Area M/Area K
0	0.00	-	0.000
1	0.01	1.10	0.009
2	0.03	1.09	0.029
3	0.06	1.03	0.058
4	0.09	.96	0.094
5	0.13	.96	0.136
7	0.19	.93	0.204
10	0.30	1.09	0.275
15	0.47	1.10	0.427
25	1.13	1.23	0.919
28	1.17	1.05	1.114

B. Montmorillonite Lattice Expanded With Ethylene Glycol.

Per Cent M	Area M (in^2)	Area K (in^2)	Area M/Area K
0	0.000	-	0.000
1	0.04	1.17	0.034
2	0.08	1.32	0.061
3	0.11	1.13	0.097
4	0.14	1.09	0.129
5	0.20	1.11	0.180
7	0.34	1.10	0.309
10	0.54	1.16	0.465
15	0.65	0.99	0.657
25	1.35	1.04	1.298
28	1.48	0.94	1.489

* -- M represents montmorillonite.

** -- K represents Kaolinite.

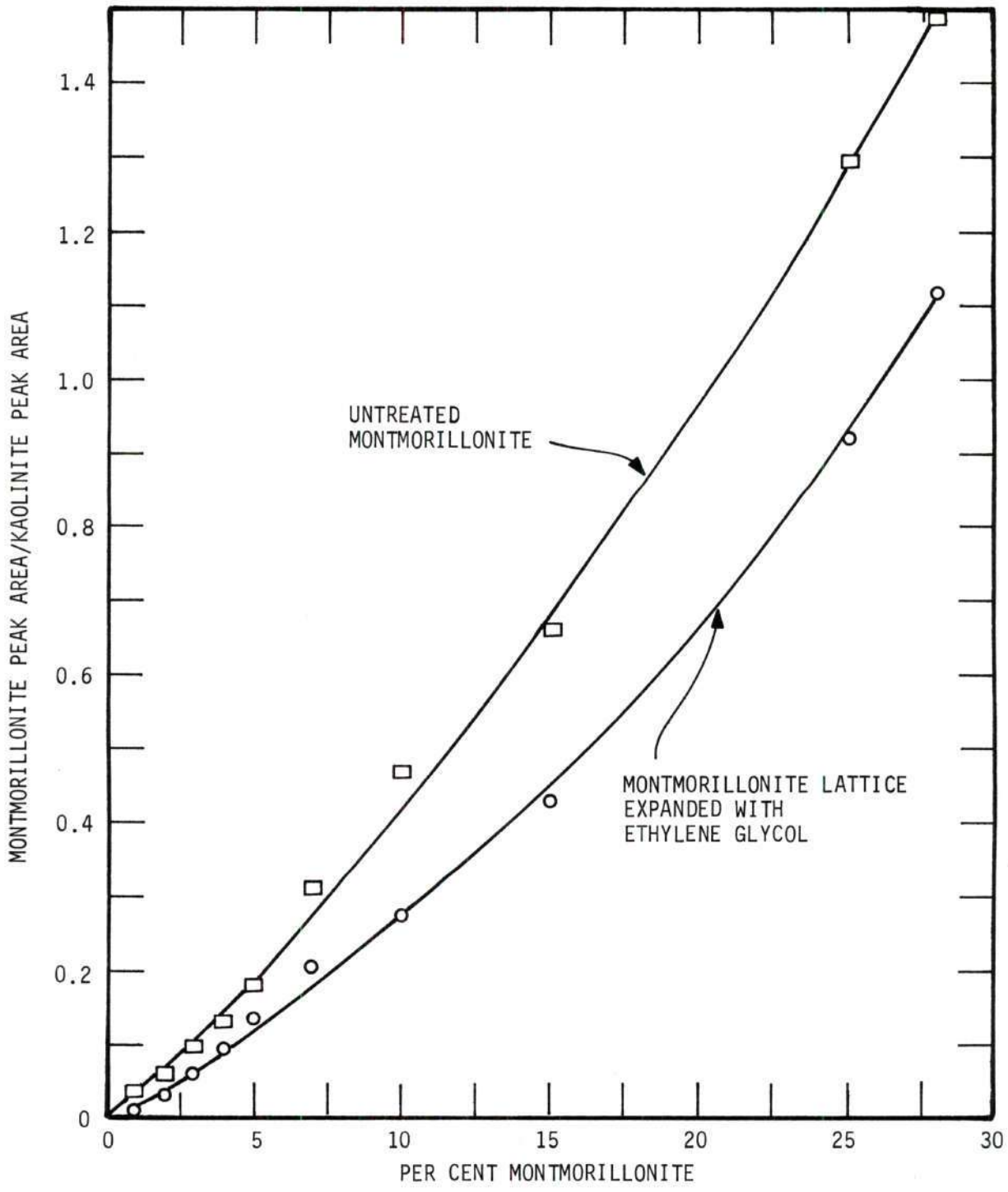

Figure 23. Standard Curves for Determining Per Cent Montmorillonite in Kaolinite.

APPENDIX E

STANDARDS FOR DETERMINING PER CENT IRON IN KAOLINITE

A mixture of minus 325 mesh Al_2O_3 and S_1O_2 was weighed in the molar ratio found in Kaolinite, $Al_2O_3 \cdot 2S_1O_2$. Two five gram samples were prepared as standards containing the above $Al_2O_3 \cdot 2S_1O_2$ mixture and additions of 0.333 per cent and 0.667 per cent iron in the form of reagent grade Fe_2O_3.

The per cent iron in the $Al_2O_3 \cdot 2S_1O_2$ matrix was determined by the formulas,

$$\frac{I_x}{I_{x + 0.333}} = \frac{X}{X + 0.333} \tag{23}$$

and

$$\frac{I_x}{I_{x + 0.667}} = \frac{X}{X + 0.667} \tag{24}$$

where I represents the integrated intensity of the Kα iron peaks and X is the per cent iron in the original $Al_2O_3 \cdot 2S_1O_2$ matrix. The integrated intensity was determined by measuring the area under the Kα iron peaks with a plainmeter. Both determinations of the original per cent iron showed that there was 0.042 per cent iron in the $Al_2O_3 \cdot 2S_1O_2$ matrix. Therefore, the two standards contained 0.375 per cent iron and 0.709 per cent iron.

The two standards were run each time the per cent iron was determined in the separation fractions to avoid error from instrument variation. The standard curves shown in Fig. 24 are the areas under the standard iron peaks plotted against per cent iron. The per cent iron in the separation fractions was determined using these curves. The accuracy of the data was ±0.01 per cent iron.

The X-ray spectrograph settings used for all iron measurements are given in Table 16 below.

Table 16. X-ray Spectrograph Settings for Iron Determinations

Analyzing Crystal	Lithium Fluoride
Killovolts	22
Milliamperes	25
Time Constant	2
Scale Factor	5×10^4
PHA	90 per cent
Chart Speed	0.5 inch/min.
Scan Speed	1°2θ/min.
2θ Angle	55°-59°

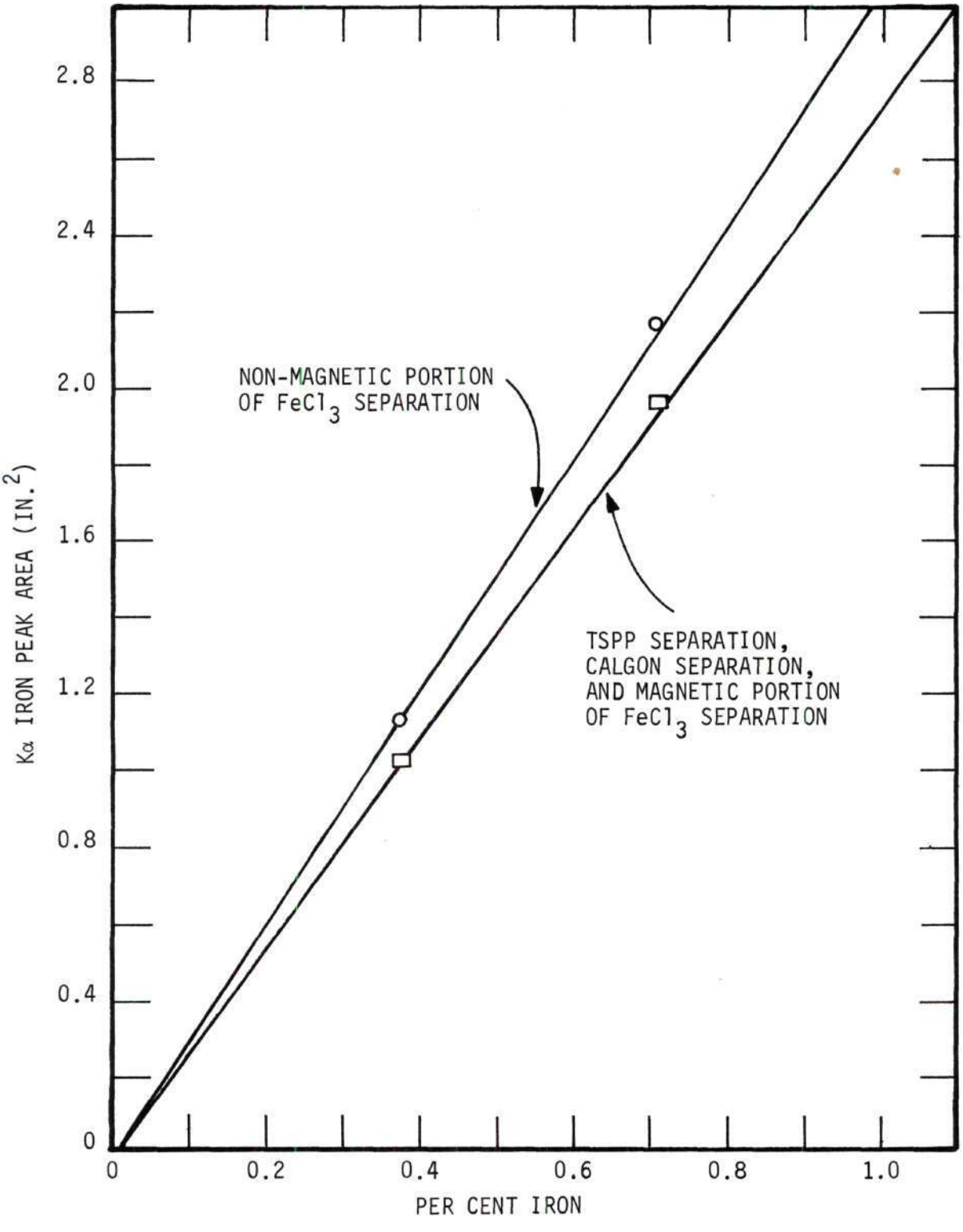

Figure 24. Standard for Determining Per Cent Iron.

APPENDIX F

THE RELATION OF TIME AND PARTICLE SIZE TO THE MAGNETIC SEPARATION OF WEAKLY MAGNETIC PARTICLES IN THE MICRON AND SUBMICRON PARTICLE SIZE RANGE

Theoretical Considerations

The purpose of this section is to make a theoretical approach to the wet magnetic separation of weakly magnetic particles in the micron and submicron particle size range. Specifically, the relationship between particle size and the time required for moving a particle a certain distance in water and in a magnetic force field will be considered. The motion of a single particle will be considered so as to avoid the complications of forces due to particle-particle interaction.

The forces that act on a particle in water in a nonhomogenous magnetic field are given by the equation,

$$F_{particle} = F_{magnetic} - F_{gravity} - F_{friction} - F_{\substack{\text{kinetic motion from} \\ \text{moving medium}}} \qquad (25)$$

where the magnetic field must move a particle against the force of gravity, as was the case in the separations presented in this thesis. Also, the forces due to the initial motion imparted by a moving medium will not be considered, as the separations made in this thesis were made in a stationary medium. Equation 25 is the result of combining Equation 2, the force on a particle in a homogenous magnetic field, and Equation 3, the forces on a particle in water and the earth's gravitational field. It

should be noted that in Equation 25 the forces due to gravity is negative since the magnetic field must oppose gravity to hold a particle in the magnet.

Substitution of the various force equations from Equation 2 and Equation 3 in the Review of Literature into Equation 25 yields,

$$\underbrace{m\frac{d^2X}{dt^2}}_{\text{Total Force}} = \underbrace{m\chi H\frac{dH}{dX}}_{\text{Magnetic Force}} - \underbrace{m'g}_{\text{Gravitational Force}} - \underbrace{3\pi\mu d\frac{dX}{dt}}_{\text{Frictional Force}} \qquad (26)$$

where: m = the mass of the particle in gm,

X = the distance the particle must travel in cm,

$\frac{d^2X}{dt^2}$ = the acceleration of the particle in cm/sec^2,

t = the time for a particle to travel the distance X,

χ = the magnetic susceptibility of the particle in cgs units,

H = the magnetic field strength in gauss,

$\frac{dH}{dX}$ = the magnetic field gradient in gauss per cm,

m' = the mass of the particle minus the mass of the fluid displaced by the particle in gm,

g = the acceleration of gravity in cm/sec^2,

μ = the viscosity of the suspending medium in poises,

$\frac{dX}{dt}$ = the velocity of the particle in cm/sec,

and d = the equivalent spherical diameter of the particle in cm.

Further substitution of $\frac{\pi d^3}{6}\rho$ for m and $\frac{\pi d^3}{6}(\rho-\rho_o)$ for m' gives,

$$\frac{\pi d^3}{6} \rho \frac{d^2X}{dt^2} = \frac{\pi d^3}{6} \rho \chi H \frac{dH}{dX} - \frac{\pi d^3}{6} (\rho-\rho_o)g - 3\pi \mu d \frac{dX}{dt} \qquad (27)$$

where ρ is the density of the particle and ρ_o is the density of the suspending medium, both in gm/cm^3.

Dividing both sides by $\frac{\pi d^3}{6} \rho$ and rearranging terms produces,

$$\frac{d^2X}{dt^2} + \frac{18}{\rho d^2} \frac{dX}{dt} = \chi H \frac{dH}{dX} - \frac{(\rho-\rho_o)}{\rho} g \qquad (28)$$

Let $$A = \frac{18\mu}{\rho d^2} \qquad (29)$$

and $$B = \chi H \frac{dH}{dX} - \frac{(\rho-\rho_o)}{\rho} g \qquad (30)$$

since they are both constants under a given set of conditions.

Substitution of Equations 29 and 30 in Equation 28 gives,

$$\frac{d^2X}{dt^2} + A \frac{dX}{dt} = B \qquad (31)$$

Integrating Equation 31 with respect to time gives,

$$\frac{dX}{dt} = \frac{1}{A} B + C e^{-tA} \qquad (32)$$

The initial conditions are $\frac{dX}{dt} = 0$ when $t = 0$. From this, it follows that,

$$C = -\frac{1}{A} B \tag{33}$$

and

$$\frac{dX}{dt} = \frac{1}{A} B (1 - e^{-tA}) \tag{34}$$

Substituting Equations 29 and 30 for A and B in Equation 34 yields,

$$\frac{dX}{dt} = \left(\frac{\rho d^2}{18 \mu}\right)\left[\chi H \frac{dH}{dX} - \frac{(\rho-\rho_o)}{\rho} g\right]\left(1 - e^{\frac{-t\ 18\mu}{\rho d^2}}\right) \tag{35}$$

Under the following conditions, it will be shown that the exponentional term of Equation 35 approaches 0 in a fraction of a second.

Assume that the suspending medium is water at 24°C. Then, viscosity, μ, equals 0.00914 gm $cm^{-1} sec^{-1}$. Also assume that the particle that is being acted upon is montmorillonite that has a density of 2.60 gm cm^{-3}. (Reported values for the density of montmorillonite range from 2.20 to 2.70[11].) Substituting these values into the exponential term gives $e^{-t0.063d^{-2}}$. The particle size, d, will be limited to 10^{-3} cms or 10 microns and below, as this is the particle size range of most clay minerals. Under these limits, $e^{-t0.063d^{-2}}$ would go to a value of 0.44×10^{-27} in one thousandth of a second. As the particle size decreases, the exponential term would become even smaller. Therefore, it can be assumed that the exponential term is 0. This means that a particle of 10 microns

or below reaches terminal velocity in a fraction of a second and that its acceleration is 0.

Under the above conditions, Equation 35 becomes

$$\frac{dX}{dt} = \left(\frac{\rho d^2}{18\mu}\right)\left[\chi H \frac{dH}{dX} - \frac{(\rho-\rho_o)}{\rho} g\right] \tag{36}$$

Integration with respect to time yields,

$$X = \left(\frac{\rho d^2}{18\mu}\right)\left[\chi H \frac{dH}{dX} - \frac{(\rho-\rho_o)}{\rho} g\right] t \tag{37}$$

Equation 37 shows that for a particle in the micron and submicron particle size range, the time required for a particle to move a certain distance X through water under the forces of gravity and a nonhomogeneous magnetic field is inversely proportional to the square of the particle size, or,

$$t \propto \frac{1}{d^2} . \tag{38}$$

Practical Application

The following is a calculation of the maximum time it would take a particle of montmorillonite of a certain particle size to travel from the point of lowest flux concentration to the point of highest flux concentration against gravity and under the conditions found in the separations described in this thesis.

Substituting the above values for the viscosity of water and the density of montmorillonite, 980 cm sec^{-2} for the acceleration of gravity, and 1.00 gm cm^{-3} for the density of water into Equation 37 gives,

$$X = \left(\frac{d^2}{0.063}\right)\left(\chi H \frac{dH}{dX} - 603\right) t \qquad (39)$$

The magnetic susceptibility of the montmorillonite in Pioneer Kaolin given by Equation 13 was found to be 27.42 x 10^{-6} gm^{-1}.

The field strength that was used was the maximum field strength plus the minimum field strength divided by two. The maximum field strength as shown in Appendix A for the 0.50 inch spheres at 5.0 amperes was 29,000 gauss, and the minimum field strength that could be measured was 6,000 gauss. Using these values, an average field strength of 17,500 gauss was obtained.

The value that was used for the field gradient was also the average. This was assumed to be the maximum field strength minus the minimum field strength divided by the maximum distance a particle would have to travel to reach the point of highest flux concentration at the point where the spheres touched perpendicular to the pole faces. This distance was 0.465 cm, and the value for dH/dX was 49,462 gauss cm^{-1}.

This maximum distance the particle would have to travel is explained by referring to Fig. 25. Fig. 25 shows the arrangement of the spheres in relation to the magnet poles during the separations described. (Also refer to Fig. 8). The point of minimum flux concentration is probably near the center of the space between the spheres near point 5. However, the

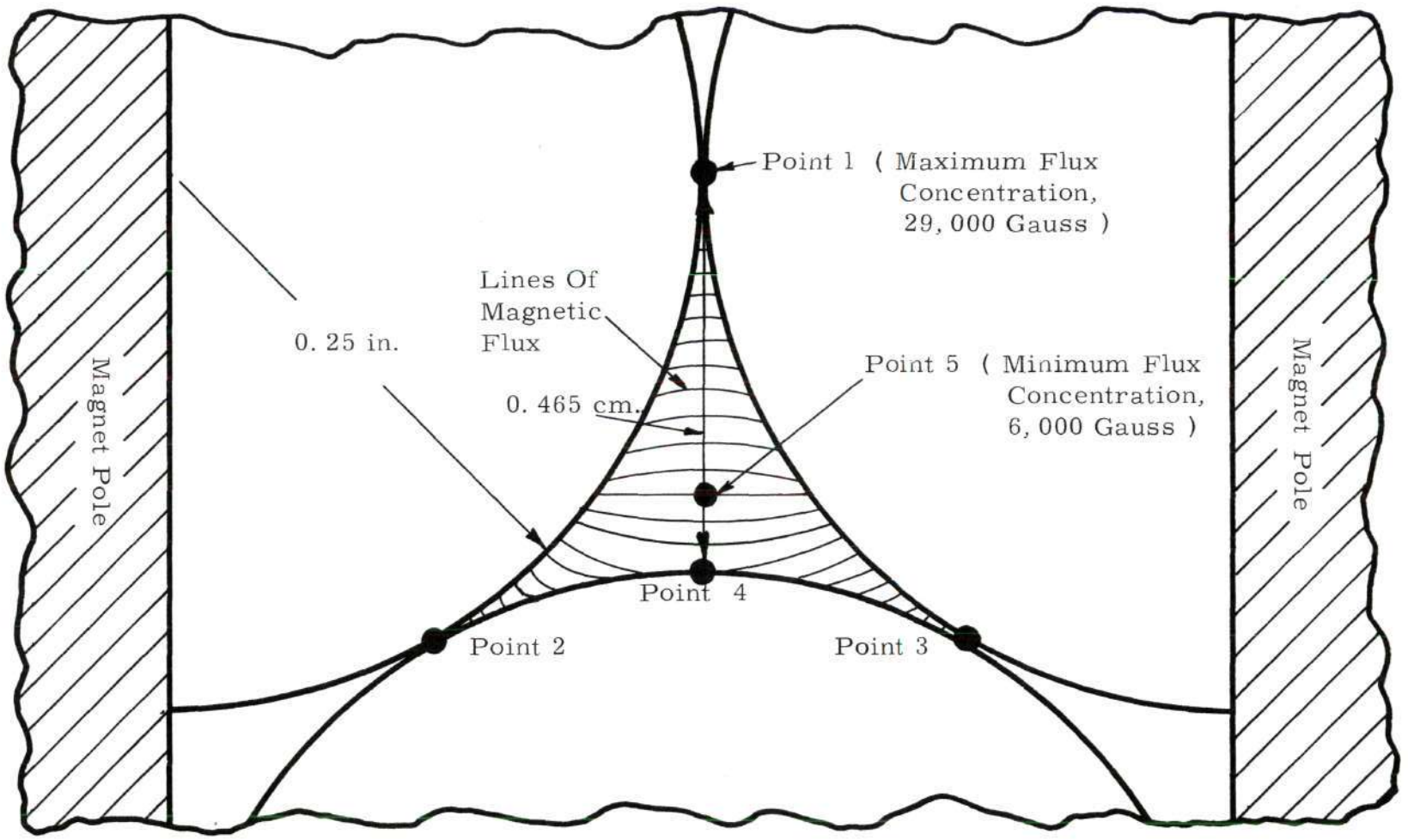

Figure 25. Diagram of Maximum Path a Magnetic Particle Must Travel to Reach the Point of Maximum Flux Concentration.

gaussmeter probe was too large to map the magnetic field between the spheres, and only a maximum and minimum field strength could be obtained. Since these calculations were for the maximum time of travel, the maximum distance that a particle would have to travel was taken to be the distance from point 4 to point 1 in Fig. 25 instead of from point 5 to point 1. The maximum field strength was at point 1 and the minimum field strength was measured with the gaussmeter probe as close to point 4 as possible. There will be a flux concentration at points 2 and 3, but the flux concentrations at points 2 and 3 will be much less than at point 1. If the particle were any further from point 1 than 4, it would be pulled in the directions of points 2 or 3 due to the field gradients in those directions.

Substituting the above values for χ, HdH/dx and X into Equation 39 yields

$$.465 = \frac{d^2}{0.063} (23{,}056 - 603)t \qquad (40)$$

(These calculations are for a particle traveling upward against gravity, but Equation 40 shows that the gravity component is so small compared to the magnetic component that the direction from which the particle starts makes little difference.)

Combining terms in Equation 40 yields

$$t = \frac{1.305 \times 10^{-6}}{d^2} \qquad (41)$$

where t is time in seconds and d is particle size in centimeters.

The range of particle size for montmorillonite is 0.2 to 0.02 microns. Therefore, as shown in Fig. 26, it would take from 54.4 to 5,440 minutes, respectively, for a particle of montmorillonite to travel from the point of lowest flux concentration to the point of highest flux concentration under the conditions stated above.

Evaluations of Assumptions

Probably the largest source of error was the assumption that the maximum field strength was 29,000 gauss because the field strength was measured with the spheres spaced 0.025 inches. The maximum field strength would be higher with the spheres touching as was the case under actual conditions. This would cause an increase both in H and dH/dX and a decrease in time.

Assuming an average value for H and dH/dX was also in error, H would be much higher nearer point 1 than at point 4, and due to the geometry of the spheres dH/dX would be higher at point 4 than at point 1. These two factors might combine to produce a constant HdH/dX but it is extremely improbable.

Although the calculations were made for a particle traveling the maximum distance, it should be noted that for actual separations, the majority of the particles would start closer to point 1. This would also decrease the time of separation.

The calculations were made for a single particle and thereby eliminated the necessity of dealing with forces due to particle-particle interaction as are found in clay suspensions. By separating suspensions of

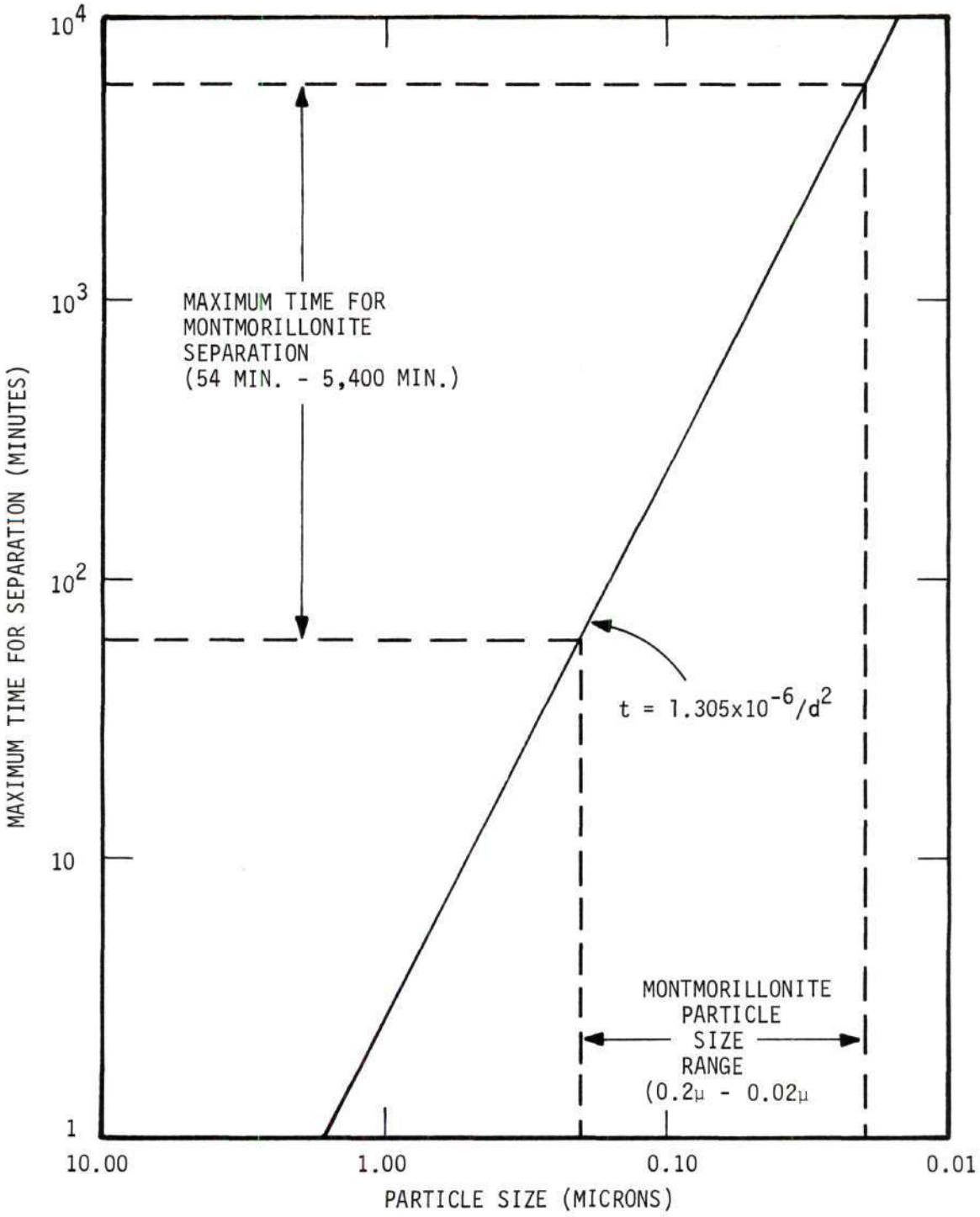

Figure 26. Maximum Time of Separation Versus Particle Size (From Equation F-41).

low solids content, particle-particle interaction might be avoided, but for suspensions of higher solids content, magnetic particles would have to move around nonmagnetic particles as they were pulled by magnetic forces, assuming the suspension was defloculated. This would result in an increase in the distance traveled and therefore an increase in time.

Conclusions

The absolute accuracy of Equation 41, due to some of the assumptions made, leaves much to question, but it does show the importance of time in the wet magnetic separation of weakly magnetic particles in the micron and submicron particle size range.

According to Equation 41, a particle of 100 microns would take only 2.18×10^{-4} minutes to travel the maximum distance required for separation under the above specified conditions, and even a particle of 10 microns would take only 2.18×10^{-2} minutes. This would indicate that for a particle greater than ten microns, time would not be important, and it would only be necessary to pass the suspension through the separation zone of the magnet to affect a separation. However, as shown by Fig. 26, below 10 microns, the length of time that weakly magnetic particles remain in the separation zone of the magnet will effect the degree of separation tremendously.

From this, it is concluded that in order to magnetically separate weakly magnetic materials in the micron and submicron particle size range, either (1) higher magnetic fields and/or field gradients will have to be produced, (2) magnets will have to be designed so that the flow through the separation zone can be controlled or completely stopped, (3) the distance that particles have to travel in order to be separated will have to

be minimized, (4) the magnetic susceptibility, χ, of the material being separated will have to be increased by chemical or physical treatment, or (5) two or more combinations of the above will have to be used.

APPENDIX G

PER CENT MONTMORILLONITE DATA

Reproducibility and Accuracy

The reproducibility of the montmorillonite percentages was determined using the average values from the original samples of the 11 different separations. The average per cent montmorillonite from the 11 original samples was 3.1 per cent with a standard deviation of 0.25 per cent. This corresponds to a per cent standard deviation of 8.1 per cent.

The absolute accuracy of the montmorillonite percentages could not be determined because there is much variation in the structure and chemical content of montmorillonite from different localities. Both of these would affect the montmorillonite peak intensities and therefore, the per cent of montmorillonite determined in this thesis. It is hoped that because the clays used to prepare the standards and the clay used in the separations came from the same general area that the montmorillonites were similar.

The data for the per cent montmorillonite found in the various separation fractions is presented in Tables 17, 18, 19, and 20.

Table 17. Per Cent Montmorillonite in TSPP Separation Fractions

Sample	Montmorillonite Lattice Unexpanded				Montmorillonite Lattice Expanded				Average Per Cent M
	Area M (in^2)	Area K (in^2)	Area M / Area K	Per Cent M	Area M (in^2)	Area K (in^2)	Area M / Area K	Per Cent M	
Original	0.16	1.80	0.089	3.8	0.19	1.61	0.118	3.4	3.6
0-M	0.22	1.17	0.188	7.0	0.28	1.21	0.231	6.3	6.7
5-M	0.28	1.24	0.226	8.1	0.37	1.13	0.327	8.7	8.4
10-M	0.22	1.38	0.159	6.0	0.34	1.45	0.234	6.3	6.2
15-M	0.20	1.42	0.155	5.9	0.29	1.46	0.199	5.5	5.7
20-M	0.20	1.47	0.136	5.3	0.27	1.38	0.196	5.4	5.4
25-M	0.16	1.47	0.109	4.4	0.26	1.56	0.167	4.6	4.5
0-NM	0.12	1.79	0.067	3.1	0.18	1.55	0.116	3.3	3.2
5-NM	0.11	1.87	0.059	2.8	0.15	1.72	0.087	2.6	2.7
10-NM	0.15	1.88	0.080	3.5	0.25	1.51	0.165	4.5	4.0
15-NM	0.12	2.02	0.059	2.8	0.16	1.67	0.096	2.8	2.8
20-NM	0.15	1.85	0.081	3.5	0.19	1.60	0.119	3.4	3.4
25-NM	0.12	1.80	0.067	3.1	0.16	1.54	0.104	3.0	3.0

Table 18. Per Cent Montmorillonite in $FeCl_3$ Separation Fractions

Sample	Montmorillonite Lattice Unexpanded				Montmorillonite Lattice Expanded				Average Per Cent M
	Area M (in^2)	Area K (in^2)	Area M / Area K	Per Cent M	Area M (in^2)	Area K (in^2)	Area M / Area K	Per Cent M	
Original	.10	1.39	.072	3.2	.23	1.96	.117	3.4	3.3
0-M	.14	1.33	.105	4.3	.15	1.27	.118	3.4	3.9
5-M	.22	1.38	.159	6.0	.26	1.36	.191	5.3	5.7
10-M	.12	1.28	.094	3.9	.16	1.32	.121	3.5	3.7
15-M	.21	1.72	.122	4.8	.26	1.92	.135	3.8	4.3
20-M	.13	1.59	.082	3.6	.20	1.61	.124	3.6	3.6
25-M	.21	1.75	.120	4.7	.28	1.80	.156	4.4	4.6
0-NM	.12	1.77	.068	3.1	.09	1.26	.071	2.2	2.7
5-NM	.11	1.86	.059	2.8	.10	1.89	.053	1.8	2.3
10-NM	.10	1.66	.060	2.8	.21	1.93	.109	3.2	3.0
15-NM	.08	1.52	.053	2.6	.09	1.85	.049	1.7	2.2
20-NM	.10	1.71	.058	2.8	.10	1.72	.058	1.9	2.4
25-NM	.11	1.63	.067	3.1	.23	1.93	.119	3.4	3.2

Table 19. Per Cent Montmorillonite in Calgon Separations

Sample	Montmorillonite Lattice Unexpanded				Montmorillonite Lattice Expanded				Average Per Cent M
	Area M (in^2)	Area K (in^2)	$\frac{\text{Area M}}{\text{Area K}}$	Per Cent M	Area M (in^2)	Area K (in^2)	$\frac{\text{Area M}}{\text{Area K}}$	Per Cent M	
Original	0.10	1.45	0.069	3.1	0.17	1.92	0.089	2.7	2.9
NM	0.12	1.74	0.069	3.1	0.18	2.04	0.088	2.7	2.9
1-M	0.11	1.04	0.106	4.3	0.18	1.53	0.118	3.4	3.9
2-M	0.09	1.19	0.076	3.4	0.16	1.61	0.099	2.9	3.2
3-M	0.11	1.27	0.086	3.7	0.17	1.65	0.103	3.0	3.4

Table 20. Per Cent Montmorillonite in M(X)A Separation Fractions

Sample	Montmorillonite Lattice Unexpanded				Montmorillonite Lattice Expanded				Average Per Cent M
	Area M (in^2)	Area K (in^2)	Area M / Area K	Per Cent M	Area M (in^2)	Area K (in^2)	Area M / Area K	Per Cent M	
EtOH-O	0.12	1.82	0.066	3.0	0.18	1.57	0.115	3.3	3.2
EtOH-NM	0.09	1.90	0.047	2.4	0.08	1.75	0.046	1.6	2.0
EtOH-1M	0.18	1.62	0.111	4.4	0.22	1.56	0.141	4.0	4.2
EtOH-2M	0.20	2.07	0.096	4.0	0.22	1.75	0.126	3.6	3.8
EtOH-3M	0.14	1.86	0.075	3.4	0.12	1.47	0.082	2.5	3.0
$Co(II)A_2$-O	0.10	1.65	0.061	2.9	0.17	1.60	0.106	3.1	3.0
$Co(II)A_2$-NM	0.05	1.60	0.031	1.9	0.09	1.65	0.055	1.8	1.9
$Co(II)A_2$-1M	0.12	1.46	0.082	3.6	0.32	1.79	0.179	5.0	4.3
$Co(II)A_2$-2M	0.13	1.85	0.070	3.2	0.20	1.73	0.116	3.3	3.3
$Co(II)A_2$-3M	0.09	1.38	0.065	3.0	0.12	1.15	0.104	3.1	3.1
$Cu(II)A_2$-O	0.12	1.73	0.069	3.1	0.11	1.70	0.065	2.1	2.6
$Cu(II)A_2$-NM	0.11	1.88	0.059	2.8	0.10	1.35	0.074	2.3	2.6
$Cu(II)A_2$-1M	0.14	1.61	0.087	3.7	0.19	1.42	0.134	3.8	3.8
$Cu(II)A_2$-2M	0.20	1.88	0.106	4.3	0.17	1.71	0.099	2.9	3.6

Table 20. Per Cent Montmorillonite in M(X)A Separation Fractions (Continued)

Sample	Montmorillonite Lattice Unexpanded				Montmorillonite Lattice Expanded				Average Per Cent M
	Area M (in^2)	Area K (in^2)	Area M / Area K	Per Cent M	Area M (in^2)	Area K (in^2)	Area M / Area K	Per Cent M	
Cu(II)A_2-3M	0.13	1.65	0.079	3.5	0.15	1.44	0.104	3.1	3.3
Mn(II)A_2-0	0.12	1.80	0.067	3.1	0.15	1.74	0.086	2.6	2.9
Mn(II)A_2-NM	0.10	1.92	0.052	2.6	0.13	1.77	0.073	2.3	2.5
Mn(II)A_2-1M	0.15	1.53	0.098	4.1	0.19	1.58	0.120	3.4	3.8
Mn(II)A_2-2M	0.12	1.74	0.069	3.1	0.19	1.66	0.114	3.3	3.2
Mn(II)A_2-3M	0.07	1.42	0.049	2.5	0.13	1.22	0.107	3.1	2.8
Ni(II)A_2-0	0.12	1.65	0.073	3.3	0.19	1.69	0.112	3.2	3.3
Ni(II)A_2-NM	0.10	1.91	0.052	2.6	0.11	1.71	0.064	2.1	2.4
Ni(II)A_2-1M	0.19	1.53	0.124	4.9	0.20	1.54	0.130	3.7	4.3
Ni(II)A_2-2M	0.20	1.81	0.110	4.4	0.21	1.52	0.138	3.9	4.2
Ni(II)A_2-3M	0.10	1.49	0.067	3.1	0.11	1.42	0.077	2.4	2.8
Co(III)A_3-0	0.11	1.73	0.064	3.0	0.19	1.60	0.119	3.4	3.2
Co(III)A_3-NM	0.11	1.83	0.060	2.8	0.11	1.65	0.067	2.1	2.5
Co(III)A_3-1M	0.10	1.57	0.063	3.0	0.13	1.38	0.094	2.8	2.9

Table 20. Per Cent Montmorillonite in M(X)A Separation Fractions (Continued)

Sample	Montmorillonite Lattice Unexpanded				Montmorillonite Lattice Expanded				Average Per Cent M
	Area M (in^2)	Area K (in^2)	Area M / Area K	Per Cent M	Area M (in^2)	Area K (in^2)	Area M / Area K	Per Cent M	
$Co(III)A_3$-2M	0.120	1.58	0.076	3.4	0.15	1.43	0.105	3.1	3.2
$Co(III)A_3$-3M	0.11	1.55	0.071	3.2	0.12	1.44	0.083	2.5	2.9
$Cr(III)A_3$-0	0.10	1.48	0.068	3.1	0.14	1.31	0.107	3.1	3.1
$Cr(III)A_3$-NM	0.08	1.84	0.043	2.3	0.15	1.45	0.103	3.0	2.7
$Cr(III)A_3$-1M	0.11	1.43	0.077	3.4	0.15	1.71	0.088	2.7	3.1
$Cr(III)A_3$-2M	0.10	1.41	0.071	3.3	0.10	1.35	0.074	2.3	2.8
$Cr(III)A_3$-3M	-	-	-	-	0.10	0.78	0.056	-	-
$Fe(III)A_3$-0	0.12	1.68	0.072	3.2	0.15	1.64	0.091	2.7	3.0
$Fe(III)A_3$-NM	0.10	1.79	0.056	2.7	0.14	1.58	0.089	2.7	2.7
$Fe(III)A_3$-1M	0.12	1.60	0.075	3.4	0.09	1.18	0.076	2.3	2.9
$Fe(III)A_3$-2M	0.10	1.41	0.071	3.3	0.10	1.35	0.074	2.3	2.8
$Fe(III)A_3$-3M	0.16	1.82	0.088	3.8	0.13	1.54	0.084	2.5	3.2

APPENDIX H

MAGNETIC SUSCEPTIBILITY DATA

Accuracy and Reproducibility

The accuracy of the magnetic susceptibility data was the limit of reproducibility of HdH/dX since HdH/dX was calibrated with chemically pure Mohr's Salt, and also it was limited by the sensitivity of the Cahn balance. The limit of sensitivity in reading the recorder was ±0.005 on a minimum scale factor of 0.375 mg. Using a minimum sample weight of 15 mg and a minimum HdH/dX of 2.20×10^{6} gm cm sec^{-2}, the limit of sensitivity for a magnetic susceptibility measurement was calculated to be $\pm 0.06 \times 10^{-6} gm^{-1}$.

Therefore, the accuracy of the magnetic susceptibility measurements for all cases except the TSPP separations was ±2.0 per cent of the total value or $\pm 0.06 \times 10^{-6} gm^{-1}$, which ever one was greater. For the TSPP separations, the accuracy was ±4.3 per cent of the total value or $\pm 0.06 \times 10^{-6} gm^{-1}$, which ever one was greater.

Table 21. Magnetic Susceptibility of TSPP Separation Fractions

Sample	Weight of Sample (mg)	1.50 Amperes				2.00 Amperes				Average $\chi_{25°C}$ (gm^{-1} x 10^6)
		Force on Bucket (mg)	Force on Bucket +Sample (mg)	Force on Sample (mg)	$\chi_{25°C}$ (gm^{-1} x 10^6)	Force on Bucket (mg)	Force on Bucket +Sample (mg)	Force on Sample (mg)	$\chi_{25°C}$ (gm^{-1} x 10^6)	
Original	20.870	-0.080	-0.071	0.009	0.18	-0.154	0.139	0.015	0.17	0.18
0-M	20.940	-0.080	0.098	0.178	3.56	-0.154	0.116	0.270	3.05	3.31*
5-M	22.525	-0.080	-0.011	0.069	1.28	-0.154	-0.045	0.109	1.14	1.22
10-M	31.610	-0.080	-0.030	0.050	0.66	-0.154	-0.075	0.079	0.59	0.63
15-M	24.285	-0.080	0.008	0.088	1.52	-0.154	0.019	0.135	1.32	1.42*
20-M	27.935	-0.080	0.068	0.012	0.18	-0.154	-0.124	0.030	0.25	0.21
25-M	28.415	-0.080	0.053	0.027	0.40	-0.154	-0.101	0.053	0.44	0.42
0-NM	21.945	-0.080	-0.090	-0.010	-0.19	-0.154	-0.171	-0.017	-0.18	-0.19
5-NM	19.915	-0.080	-0.094	-0.014	-0.29	-0.154	-0.173	-0.019	-0.23	-0.26
10-NM	21.195	-0.080	-0.105	-0.025	-0.49	-0.154	-0.188	-0.034	-0.38	-0.43
15-NM	23.130	-0.080	-0.098	-0.018	-0.32	-0.159	-0.173	-0.029	-0.30	-0.31
20-NM	24.015	-0.080	-0.086	-0.006	0.10	-0.154	-0.165	-0.011	-0.11	-0.10
25-NM	19.095	-0.080	-0.083	-0.003	0.06	-0.154	-0.158	-0.004	-0.05	-0.05

Table 21. Magnetic Susceptibility of TSPP Separation Fractions (Continued)

Sample	Weight of Sample (mg)	1.50 Amperes				2.00 Amperes				Average $\chi_{25°C}$ (gm^{-1} x 10^6)
		Force on Bucket (mg)	Force on Bucket +Sample (mg)	Force on Sample (mg)	$\chi_{25°C}$ (gm^{-1} x 10^6)	Force on Bucket (mg)	Force on Bucket +Sample (mg)	Force on Sample (mg)	$\chi_{25°C}$ (gm^{-1} x 10^6)	
0-M**	21.930	-0.076	0.002	0.078	1.39	-0.144	-0.017	0.127	1.32	1.36
5-M**	22.655	-0.076	0.004	0.080	1.38	-0.144	-0.015	0.129	1.30	1.34
10-M**	23.060	-0.076	-0.030	0.046	0.78	-0.144	-0.068	0.076	0.75	0.77
15-M**	20.190	-0.076	-0.011	0.065	1.26	-0.144	-0.041	0.103	1.16	1.21
20-M**	21.080	-0.076	-0.071	0.005	0.09	-0.144	-0.135	0.009	0.10	0.10
25-M**	23.375	-0.076	-0.047	0.029	0.49	-0.144	-0.090	0.054	0.53	0.51

* -- Samples contained ferromagnetic impurities.

** -- Measurement made after sample was centrifuged in tetrabromoethane with a density of 2.95 gm cm^{-3}.

Table 22. Magnetic Susceptibilities of $FeCl_3$ Separation Fractions

Sample	Weight of Sample (mg)	1.50 Amperes				2.00 Amperes				Average $\chi_{25°C}$ (gm^{-1} x 10^6)
		Force on Bucket (mg)	Force on Bucket +Sample (mg)	Force on Sample (mg)	$\chi_{25°C}$ (gm^{-1} x 10^6)	Force on Bucket (mg)	Force on Bucket +Sample (mg)	Force on Sample (mg)	$\chi_{25°C}$ (gm^{-1} x 10^6)	
Original	20.945	-0.071	-0.071	0.000	0.00	-0.142	-0.139	0.003	0.03	0.02
0-M	15.310	-0.071	-0.015	0.056	1.61	-0.142	-0.138	0.104	1.69	1.65
5-M	18.090	-0.071	-0.032	0.039	0.95	-0.142	-0.068	0.073	1.00	0.98
10-M	22.530	-0.071	-0.029	0.042	0.82	-0.142	-0.053	0.089	0.98	0.90
15-M	22.515	-0.071	-0.030	0.043	0.84	-0.142	-0.059	0.083	0.92	0.88
20-M	20.550	-0.071	-0.034	0.037	0.72	-0.142	-0.071	0.071	0.86	0.79
25-M	16.805	-0.071	-0.042	0.029	0.76	-0.142	-0.086	0.056	0.83	0.80
0-NM	21.150	-0.071	-0.030	0.041	0.62	-0.139	-0.062	0.077	0.96	0.76
5-NM	18.110	-0.071	-0.030	0.041	1.00	-0.139	-0.064	0.075	1.03	1.00
10-NM	21.510	-0.071	-0.024	0.047	0.96	-0.139	-0.049	0.090	1.04	1.00
15-NM	18.395	-0.071	-0.034	0.037	0.89	-0.139	-0.068	0.071	0.96	0.93
20-NM	19.200	-0.071	-0.032	0.039	0.90	-0.139	-0.066	0.076	0.98	0.94
25-NM	15.430	-0.071	-0.029	0.042	1.20	-0.139	-0.063	0.076	1.22	1.21

Table 23. Magnetic Susceptibility of Calgon Separation Fractions

Sample	Weight of Sample (mg)	1.50 Amperes				2.00 Amperes				Average $\chi_{25°C}$ (gm^{-1} x 10^6)
		Force on Bucket (mg)	Force on Bucket +Sample (mg)	Force on Sample (mg)	$\chi_{25°C}$ (gm^{-1} x 10^6)	Force on Bucket (mg)	Force on Bucket +Sample (mg)	Force on Sample (mg)	$\chi_{25°C}$ (gm^{-1} x 10^6)	
Original	21.630	-0.071	-0.082	-0.011	-0.22	-0.141	-0.156	-0.015	-0.17	-0.20
NM	19.130	-0.071	-0.089	-0.027	-0.41	-0.141	-0.168	-0.027	-0.35	-0.38
1-M	19.265	-0.071	-0.036	-0.035	0.80	-0.141	-0.085	0.056	0.72	0.76
2-M	23.505	-0.071	-0.038	0.033	0.62	-0.141	-0.088	-0.053	0.56	0.59
3-M	18.255	-0.071	-0.057	0.036	0.34	-0.141	-0.105	-0.036	0.56	0.43

Table 24. Magnetic Susceptibilities of Metal Acetylacetonates

Sample	Weight of Sample (mg)	1.50 Amperes				2.00 Amperes				Average $\chi_{25°C}$ (gm^{-1} x 10^6)
		Force on Bucket (mg)	Force on Bucket +Sample (mg)	Force on Sample (mg)	$\chi_{25°C}$ (gm^{-1} x 10^6)	Force on Bucket (mg)	Force on Bucket +Sample (mg)	Force on Sample (mg)	$\chi_{25°C}$ (gm^{-1} x 10^6)	
Na(I)A	-0.068	-0.084	-0.016	11.090	-0.64	-0.132	-0.160	-0.028	-0.63	-0.63
K(I)A	-0.068	-0.104	-0.036	15.780	-1.01	-0.132	-0.184	-0.052	-0.82	-0.91
$Co(II)A_2$	-0.060	1.125	1.185	13.880	37.72	-0.120	1.975	2.095	37.53	37.63
$Cu(II)A_2$	-0.060	0.000	0.060	6.560	4.04	-0.120	-0.010	0.110	4.17	4.11
$Mn(II)A_2$	-0.064	2.000	2.064	16.830	54.18	-0.130	3.500	3.630	53.63	53.91
$Ni(II)A_2$	-0.060	0.330	0.390	11.445	15.05	-0.120	0.566	0.686	14.90	14.98
$Zn(II)A_2$	-0.064	-0.090	-0.026	10.930	-1.05	-0.130	-0.166	-0.036	-0.82	-0.93
$Al(III)A_3$	-0.068	-0.090	-0.022	9.280	-1.05	-0.132	-0.170	-0.038	-1.02	-1.03
$Co(III)A_3$	-0.060	-0.090	-0.030	18.570	-0.71	-0.120	-0.170	-0.050	-0.67	-0.69
$Cr(III)A_3$	-0.060	-0.320	0.380	10.560	15.90	-0.120	0.630	0.750	17.66	16.78
$Fe(III)A_3$	-0.060	1.100	1.160	12.600	40.67	-0.120	1.950	2.070	40.85	40.76
$Zr(IV)A_4$	-0.064	-0.090	-0.026	10.375	-1.10	-0.130	-0.170	-0.040	-0.96	-1.03

Table 25. Magnetic Susceptibility of M(X)A Separation Fractions

Sample	Weight of Sample (mg)	1.50 Amperes				2.00 Amperes				Average $\chi_{25°C}$ (gm^{-1} x 10^6)
		Force on Bucket (mg)	Force on Bucket +Sample (mg)	Force on Sample (mg)	$\chi_{25°C}$ (gm^{-1} x 10^6)	Force on Bucket (mg)	Force on Bucket (mg)	Force on Sample (mg)	$\chi_{25°C}$ (gm^{-1} x 10^6)	
EtOH-O	17.760	-0.071	-0.062	0.009	0.22	-0.139	-0.122	0.017	0.24	0.23
EtOH-NM	20.710	-0.071	-0.083	-0.012	-0.25	-0.137	-0.154	-0.017	-0.20	-0.22
EtOH-1M	19.805	-0.080	0.396	0.476	10.43	-0.154	0.566	0.710	6.82	8.63*
EtOH-2M	16.705	-0.081	0.115	0.196	5.09	-0.154	0.141	0.295	4.29	4.71*
EtOH-3M	19.600	-0.084	0.045	0.129	3.65	-0.158	0.092	0.250	3.10	3.38*
$Co(II)A_2$-O	18.520	-0.071	-0.069	0.002	0.05	-0.139	-0.129	0.010	0.13	0.09
$Co(II)A_2$-NM	20.355	-0.071	-0.069	0.002	0.04	-0.137	-0.131	0.006	0.07	0.06
$Co(II)A_2$-1M	27.330	-0.080	0.053	0.133	2.11	-0.154	0.056	0.210	1.87	1.99
$Co(II)A_2$-2M	23.055	-0.081	0.020	0.101	1.90	-0.154	0.004	0.158	1.66	1.78
$Co(II)A_2$-3M	27.475	-0.084	0.045	0.129	2.04	-0.158	0.045	0.203	1.79	1.92
$Cu(II)A_2$-O	20.995	-0.071	-0.075	-0.004	-1.08	-0.139	-0.139	-0.000	0.00	-0.04
$Cu(II)A_2$-NM	24.420	-0.071	-0.080	-0.009	-0.16	-0.137	-0.149	-0.012	-0.12	-0.14
$Cu(II)A_2$-1M	18.660	-0.080	0.060	0.060	1.39	-0.154	-0.054	0.100	1.30	1.35

Table 25. Magnetic Susceptibility of M(X)A Separation Fractions (Continued)

Sample	Weight of Sample (mg)	1.50 Amperes				2.00 Amperes				Average $\chi_{25°C}$ (gm^{-1} x 10^6)
		Force on Bucket (mg)	Force on Bucket +Sample (mg)	Force on Sample (mg)	$\chi_{25°C}$ (gm^{-1} x 10^6)	Force on Bucket (mg)	Force on Bucket +Sample (mg)	Force on Sample (mg)	$\chi_{25°C}$ (gm^{-1} x 10^6)	
$Cu(II)A_2$-2M	18.280	-0.081	-0.023	0.058	1.38	-0.154	-0.060	0.094	1.25	1.32
$Cu(II)A_2$-3M	20.915	-0.084	0.002	0.002	1.78	-0.158	-0.019	0.139	1.61	1.70
$Mn(II)A_2$-O	21.795	-0.071	-0.064	0.007	0.14	-0.139	-0.126	0.013	0.15	0.15
$Mn(II)A_2$-NM	20.860	-0.071	-0.067	0.004	0.08	-0.137	-0.128	0.009	0.11	0.10
$Mn(II)A_2$-1M	18.255	-0.080	-0.013	0.067	1.59	-0.154	-0.049	0.105	1.40	1.50
$Mn(II)A_2$-2M	21.830	-0.081	-0.041	0.040	0.79	-0.154	-0.086	0.068	0.76	0.78
$Mn(II)A_2$-3M	24.240	-0.084	-0.034	0.050	0.89	-0.158	-0.075	0.083	0.83	0.86
$Ni(II)A_2$-O	20.780	-0.071	0.071	0.000	0.00	-0.139	-0.139	0.000	0.00	0.00
$Ni(II)A_2$-NM	20.110	-0.071	-0.075	-0.004	-0.08	-0.137	-0.143	-0.006	-0.07	-0.07
$Ni(II)A_2$-1M	18.000	-0.080	-0.044	0.036	0.87	-0.154	-0.092	0.062	0.84	0.86
$Ni(II)A_2$-2M	31.320	-0.081	-0.004	0.077	1.06	-0.154	-0.026	0.128	0.99	1.03
$Ni(II)A_2$-3M	22.255	-0.083	-0.014	0.069	1.30	-0.158	-0.041	0.117	1.24	1.27

Table 25. Magnetic Susceptibility of M(X)A Separation Fractions (Continued)

Sample	Weight of Sample (mg)	1.50 Amperes				2.00 Amperes				Average $\chi_{25°C}$ (gm^{-1} x 10^6)
		Force on Bucket (mg)	Force on Bucket +Sample (mg)	Force on Sample (mg)	$\chi_{25°C}$ (gm^{-1} x 10^6)	Force on Bucket (mg)	Force on Bucket +Sample (mg)	Force on Sample (mg)	$\chi_{25°C}$ (gm^{-1} x 10^6)	
$Co(III)A_3$-O	24.670	-0.071	-0.074	-0.003	-0.05	-0.139	-0.144	-0.005	-0.05	-0.05
$Co(III)A_3$-NM	21.325	-0.071	-0.066	0.005	0.10	-0.137	-0.128	0.009	0.10	0.10
$Co(III)A_3$-1M	21.045	-0.080	0.034	0.046	0.95	-0.154	-0.075	0.079	0.91	0.93
$Co(III)A_3$-2M	19.205	-0.081	-0.034	0.047	1.06	-0.154	-0.073	0.081	1.02	1.04
$Co(III)A_3$-3M	25.545	-0.083	0.233	0.316	5.19	-0.158	0.300	0.458	4.25	4.72*
$Cr(III)A_3$-O	22.695	-0.071	-0.071	0.000	0.00	-0.139	-0.135	-0.004	0.04	0.02
$Cr(III)A_3$-NM	23.650	-0.071	-0.083	-0.012	-0.22	-0.137	-0.152	-0.015	-0.16	-0.19
$Cr(III)A_3$-1M	21.580	-0.080	0.000	0.080	1.61	-0.154	-0.026	0.128	1.44	1.53
$Cr(III)A_3$-2M	22.855	-0.081	-0.004	0.077	1.46	-0.154	-0.019	0.135	1.44	1.45
$Cr(III)A_3$-3M	17.330	-0.083	-0.030	0.053	1.28	-0.158	-0.074	0.084	1.15	1.22
$Fe(III)A_3$-O	18.505	-0.071	-0.067	0.004	0.09	-0.139	-0.132	0.007	0.09	0.09
$Fe(III)A_3$-NM	23.290	-0.071	-0.075	-0.004	-0.08	-0.137	-0.144	-0.007	-0.008	-0.08

Table 25. Magnetic Susceptibility of M(X)A Separation Fractions (Continued)

Sample	Weight of Sample (mg)	1.50 Amperes				2.00 Amperes				Average $\chi_{25°C}$ (gm^{-1} x 10^6)
		Force on Bucket (mg)	Force on Bucket +Sample (mg)	Force on Sample (mg)	$\chi_{25°C}$ (gm^{-1} x 10^6)	Force on Bucket (mg)	Force on Bucket +Sample (mg)	Force on Sample (mg)	$\chi_{25°C}$ (gm^{-1} x 10^6)	
$Fe(III)A_3$-1M	21.820	-0.080	-0.036	0.044	0.87	-0.154	-0.075	0.079	0.88	0.88
$Fe(III)A_3$-2M	18.290	-0.081	-0.034	0.047	1.11	-0.154	-0.075	0.079	1.05	1.08
$Fe(III)A_3$-3M	16.560	-0.083	-0.051	0.032	0.81	-0.154	-0.098	0.056	0.80	0.81

*Contain ferromagnetic impurities

APPENDIX I

PER CENT IRON DATA

Table 26. Per Cent Iron in TSPP, $FeCl_3$, and Calgon Separation Fractions

Sample	TSPP Separation		$FeCl_3$ Separation		Calgon Separation	
	Kα Iron Peak Area (in^2)	Per Cent Iron	Kα Iron Peak Area (in^2)	Per Cent Iron	Kα Iron Peak Area (in^2)	Per Cent Iron
Original	0.81	0.30	0.65	0.23	0.70	0.25
0-M	1.52	0.56	2.07	0.77	-	-
5-M	1.22	0.45	1.84	0.69	-	-
10-M	1.17	0.43	2.08	0.77	-	-
15-M	1.23	0.45	1.82	0.68	-	-
20-M	1.11	0.41	1.87	0.70	-	-
25-M	1.22	0.45	1.97	0.73	-	-
0-NM	0.82	0.30	2.19	0.72	-	-
5-NM	0.78	0.29	2.37	0.78	-	-
10-NM	0.82	0.30	2.50	0.83	-	-
15-NM	0.84	0.31	2.39	0.79	-	-
20-NM	0.79	0.29	2.35	0.78	-	-
25-NM	0.81	0.30	2.42	0.80	-	-
1-M	-	-	-	-	1.09	0.40
2-M	-	-	-	-	0.96	0.35
3-M	-	-	-	-	0.85	0.30
NM	-	-	-	-	0.70	0.25

Table 27. Weight Analysis of Montmorillonite in TSPP Separations

Sample	Weight (grams)	Per Cent Weight Distribution	Weight Fraction X Per Cent Montmorillonite	Calculated Original Per Cent Montmorillonite	Per Cent Montmorillonite Distribution	Efficiency Ratio
O-M	0.5506	5.1	0.3		9.1	1.78
				3.3		
O-NM	10.1671	94.9	3.0		90.9	
5-M	1.5283	13.3	1.1		32.4	2.44
				3.4		
5-NM	9.9574	86.7	2.3		67.6	
10-M	2.1896	18.8	1.2		27.2	1.45
				4.4		
10-NM	9.4495	81.2	3.2		72.7	
15-M	2.5340	21.7	1.2		35.3	1.63
				3.4		
15-NM	9.1378	78.3	2.2		64.7	
20-M	2.3203	19.6	1.1		28.9	1.47
				3.8		
20-NM	9.4882	80.4	2.7		71.1	
25-M	2.5620	21.9	1.0		30.3	1.38
				3.3		
25-NM	9.1324	78.1	2.3		69.7	

Table 28. Weight Analysis of Montmorillonite in $FeCl_3$ Separations

Sample	Weight (grams)	Per Cent Weight Distribution	Weight Fraction X Per Cent Montmorillonite	Calculated Original Per Cent Montmorillonite	Per Cent Montmorillonite Distribution	Efficiency Ratio
0-M	0.8844	7.7	0.3		10.7	1.32
				2.8		
0-NM	10.5490	92.3	2.5		89.3	
5-M	2.6528	23.0	1.3		41.9	1.82
				3.1		
5-NM	8.8735	77.0	1.8		58.1	
10-M	2.9279	25.0	0.9		28.1	1.12
				3.2		
10-NM	8.7655	75.0	2.3		71.9	
15-M	3.7612	32.8	1.4		48.3	1.47
				2.8		
15-NM	7.7177	67.2	1.5		51.7	
20-M	3.9143	34.0	1.2		42.9	1.26
				2.8		
20-NM	7.5887	66.0	1.6		57.1	
25-M	4.6199	41.0	1.9		50.0	1.22
				3.8		
25-NM	6.6432	59.0	1.9		50.0	

Table 29. Weight Analysis of Montmorillonite in Calgon and M(X)A Separations

Sample	Weight (grams)	Per Cent Weight Distribution	Weight Fraction X Per Cent Montmorillonite	Calculated Original Per Cent Montmorillonite	Per Cent Montmorillonite Distribution For NM and Total M	Efficiency Ratio for Total M
Calgon 1-M	1.7872	15.2	0.59			
Calgon 2-M	1.0634	9.1	0.29	3.1	36.3	1.15
Calgon 3-M	0.8723	7.4	0.25			
Calgon NM	7.9980	68.2	1.98		63.7	
EtOH 1-M	1.489	14.0	0.59			
EtOH 2-M	1.372	12.9	0.49	2.6	51.7	1.43
EtOH 3-M	0.990	9.3	0.28			
EtOH NM	6.750	63.7	1.27		48.3	
Co(II)$A_2$1-M	1.500	14.5	0.62			
Co(II)$A_2$2-M	1.059	10.2	0.34	2.5	48.6	1.48
Co(II)$A_2$3-M	0.839	8.1	0.25			
Co(II)A_2NM	6.950	67.2	1.28		51.4	

Table 29. Weight Analysis of Montmorillonite in Calgon and M(X)A Separations (Continued)

Sample	Weight (grams)	Per Cent Weight Distribution	Weight Fraction X Per Cent Montmorillonite	Calculated Original Per Cent Montmorillonite	Per Cent Montmorillonite Distribution for NM and Total M	Efficiency Ratio for Total
$Cu(II)A_2$1-M	1.347	13.6	0.52			
$Cu(II)A_2$2-M	1.159	11.7	0.42	2.9	41.2	1.23
$Cu(II)A_2$3-M	0.805	8.1	0.27			
$Cu(II)A_2$NM	6.60	66.6	1.73		58.8	
$Mn(II)A_2$1-M	1.633	16.0	0.61			
$Mn(II)A_2$2-M	1.154	11.3	0.36	2.8	42.7	1.20
$Mn(II)A_2$3-M	0.842	8.3	0.23			
$Mn(II)A_2$NM	6.55	64.3	1.61		57.3	
$Ni(II)A_2$1-M	1.527	15.5	0.67			
$Ni(II)A_2$2-M	1.153	11.8	0.50	3.0	47.5	1.34
$Ni(II)A_2$3-M	0.807	8.2	0.23			
$Ni(II)A_2$NM	6.32	64.4	1.55		52.5	

Table 29. Weight Analysis of Montmorillonite in Calgon and M(X)A Separations (Continued)

Sample	Weight (grams)	Per Cent Weight Distribution	Weight Fraction X Per Cent Montmorillonite	Calculated Original Per Cent Montmorillonite	Per Cent Montmorillonite Distribution for NM and Total M	Efficiency Ratio for Total
$Co(III)A_3$1-M	1.302	12.4	0.36			
$Co(III)A_3$2-M	0.871	8.3	0.27	2.6	31.1	1.14
$Co(III)A_3$3-M	0.680	6.5	0.19			
$Co(III)A_3$NM	7.65	72.8	1.82		68.9	
$Cr(III)A_3$1-M	1.262	12.4	0.38			
$Cr(III)A_3$2-M	0.941	9.3	0.26	2.7	28.7	0.99
$Cr(III)A_3$3-M	0.748	7.4	0.13			
$Cr(III)A_3$NM	7.20	70.9	1.91		71.3	
$Fe(III)A_3$1-M	1.389	13.5	0.39			
$Fe(III)A_3$2-M	1.095	10.6	0.30	2.8	34.4	1.06
$Fe(III)A_3$3-M	0.850	8.3	0.27			
$Fe(III)A_3$NM	6.95	67.6	1.83		65.6	

BIBLIOGRAPHY

1. Cooper, James D., "Clays," Mineral Facts and Problems, U.S. Government Printing Office, Bureau of Mines, Bulletin 630, Washington, D.C., 232, 1965.

2. Iannicelli, J. and Millman, N., "Relation of Viscosity of Kaolin-Water Suspensions to Montmorillonite Content of Certain Georgia Clays," Clays and Clay Minerals, Proc. 14th Conf., Pergamon Press, New York, 347, 1966.

3. Selwood, P.W., Magnetochemistry, Interscience Publishers, Inc., New York, 1956.

4. Stone, W.J.D., "Wet Magnetic Separation of Industrial Minerals," The Canadian Mining and Metallurgical Bulletin, 1288, (1964).

5. Spokes, Ernest M. and Mitchell, David R., "Relation of Magnetic Susceptibility to Mineral Composition," Mining Engineering, 373, (1958).

6. Orr, Clyde, Jr., and Dallavalle, J.M., Fine Particle Measurement, The MacMillan Company, New York, 1959.

7. Reno, Duane, and Taylor, Garvin L., "Magnetic Susceptibility," Analytical Data on Reference Clay Minerals, American Petroleum Institute, Project 49, Columbia University, New York, 125, 1950.

8. Nilakantan, P., Magnetic Anistropy and Pleochroism of Biotite Mica, The Indian Academy of Science, Bangalore, India, 1938.

9. Grim, Ralph E., Clay Mineralogy, McGraw-Hill, New York, 1953.

10. Brindly, G.W., "X-ray Identification and Structure of the Clay Minerals," Mineralogical Society of Great Britain Monograph, 32, 1951.

11. Hofmann, U., K. Endell, and D. Wilson, "Kristallstructur und Quellung von Montmorillonite," Z. Krist 86, 340, 1933.

12. Marshall, C.E., "Layer Lattices and Base-Exchange Clays," Z.Krist 91, 433, 1935.

13. Hendricks, S.B., "Lattice Structure of Clay Minerals and Some Properties of Clays," Journal of Geology 50, 276, 1942.

14. Hendricks, S.B. and Ross, "Lattice Limitations of Montmorillonite," Z. Krist C, 251, 1938.

15. Thomas, G.W., and Coleman, N.T., "The Fate of Exchangeable Iron in Acid Clay Systems," Soil Science 94, 229, 1964.

16. Lutz, J.F., "The Effect of Iron on Some Physico-Chemical Properties of Bentonite Suspensions," Soil Science Society Proceedings, 8, 1938.

17. Grim, Ralph E., "Modern Concepts of Clay Minerals," Journal of Geology L 3, 225, 1964.

18. Brindley, G.W., and Satyabrata, Ray, "Complexes of Ca-Montmorillonite with Primary Monohydric Alcohols (Clay-Organic Studies-VIII)," The American Mineralogist 49, 106, 1964.

19. Greenland, D.J., "Adsorption of Polyvinyl Alcohols by Montmorillonite," Journal of Colloid Science 18, 647, 1968.

20. Brindley, G.W. and Moll, William F., Jr., "Complexes of Natural and Synthetic Ca-Montmorillonites with Fatty Acids (Clay-Organic Studies - IX)," The American Mineralogist 50, 1355, 1965.

21. McAtee, James L., Jr., "Inorganic-Organic Cation Exchange on Montmorillonite," The American Mineralogist 44, 1230, 1959.

22. Roberts, A.L., Street, G.B., and White, D., "The Mechanism of Phenol Adsorption by Organo-Clay Derivatives," Journal of Applied Chemistry 14, 261, 1964.

23. Brunton, George, "Vapor Pressure Glycolation of Oriented Clay Minerals," Publication No. 43, Exploration and Production Research Division, Shell Development Co., Houston, Texas.

24. Street, G.B., and White, D., "The Adsorption of Phenol by Organo-Clay Derivatives," Journal of Applied Chemistry 13, 203, 1963.

25. Inorganic Syntheses, McGraw-Hill Book Company, New York, Vol. 2, pp. 14, 17, 25, 119, 121, 123; Vol 5, pp. 108, 109, 113, 130, 188; Vol 6, pp. 147, 164; Vol 7, pp. 50, 183; Vol 8, pp. 38, 125, 130, 153; Vol 9, p. 167.

26. Holm, R.H., and Cotton, F.A., "Spectral Investigations of Metal Complexes of B-Deketones. I. Nuclear Magnetic Resonance and Ultraviolet Spectra of Acetylacetonates," Journal of American Chemical Society 80, 5658, 1958.

27. Cotton, F.A., and Elder, R.C., "The Tetrameric Structure of Anhydrous, Crystalline Cobalt (II) Acetylacetonate," Journal of The American Chemical Society 86, 2294, 1967.

28. Cotton, F.A. and Soderberg, R.H., "A Spectroscopic Study of the Polymeric Nature of Bis (acetylacetonate) - cobalt (II)," Inorganic Chemistry 3, 1, 1964.

29. Fackler, J.P., Jr., and Cotton, F.A., "Molecular Association and Electronic Structures of Nickel (II) Chelates. II. Bis - (3-Phenyl-2,4 - pentanediono) - nickel (II) and High Temperature Studies of Nickel Acetylacetonate," Journal of American Chemical Society 83, 3775, 1967.

30. Kaplan, R.I., A Study of the Products Formed by the Reaction of Divalent Metal B- Dicarbonyl Compounds with the Methoxide Ion, Master's Thesis in Chemistry, Georgia Institute of Technology, Atlanta, Georgia, 38, 42, 49-51; September, 1965.

31. Calvin, M., and Wilson, K.W., "Stability of Chelate Compounds," Journal of American Ceramic Society 67, 2003, 1945.